Naval Research Reviews

Office of Naval Research
One / 1992
Vol XLIV

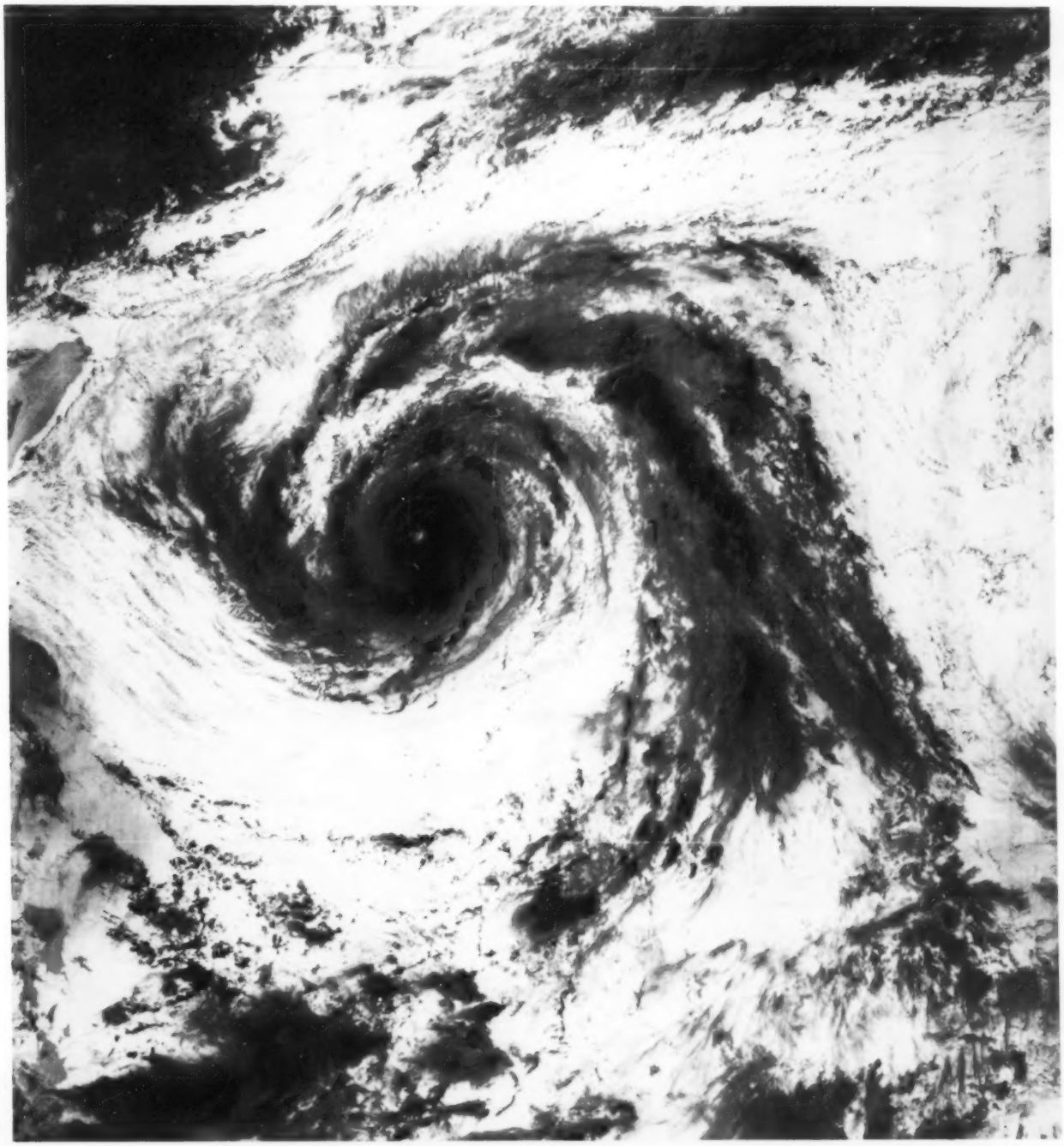

Naval Postgraduate School

The Naval Postgraduate School was created with an important mission in mind: to develop naval leaders who have both operational and analytical skills.

Today's Postgraduate School is a place where junior officers can acquire the fundamental skills and understanding necessary to bring new technologies to the fleet – to convert invention into combat readiness.

Secretary of Defense Richard Cheney states that, "The school is absolutely vital." Navy Secretary H. Lawrence Garrett III calls the Naval Postgraduate School "the front line for the future".

After his visit to the campus, Presidential Science Advisor D. Allan Bromley said, "What particularly impressed me was the unique mixture of outstanding fundamental science coupled to very clear, well-developed ideas as to how the science in question could be applied to specific Navy problems and applications."

Beginning as the School of Marine Engineering at Annapolis in 1909, with one program of study, the Navy's graduate institution now provides advanced programs in nearly 30 fields, ranging from the traditional engineering and physical sciences to the rapidly evolving space sciences.

The Naval Postgraduate School continues to be an important strategic investment for the nation – a flagship educational institution to build and enhance the United States' 21st century leadership and technological capability.

Naval Research Reviews

Office of Naval Research
One / 1992
Vol XLIV

Articles

2
Notes from the Superintendent and Provost

3
The NPS Research Program
Jeffrey B. Knorr

5
Tropical Cyclone Motion
Russell L. Elsberry

12
CAPS – A Tool for Real-Time System Development and Acquisition
Luqi and Man-Tak Shing

17
Fiber-Optic Interferometric Push-Pull Hydrophones
David A. Brown, David L. Gardner Steven L. Garrett

24
Determining Fatigue Crack Growth in Aircraft by Monitoring Acoustic Emission
Michael R. Gorman

28
Research In Ultra-Wideband Impulse Radar Target Identification
Michael A. Morgan

35
Liquid Immersion Cooling of Electronic Equipment
Yogendra K. Joshi
Matthew D. Kelleher

43
Research on Autonomous Underwater Vehicles at the Naval Postgraduate School
A. J. Healey, et al

Departments

23
Profiles in Science

51
Research Notes

CHIEF OF NAVAL RESEARCH
RADM William C. Miller, USN

DIRECTOR
Dr. Fred Saalfeld

CHIEF WRITER/EDITOR
William J. Lescure

SCIENTIFIC EDITORS
Dr. Robert J. Nowak
Dr. J. Dale Bultman

MANAGING EDITOR
Norma Gerbozy

ART DIRECTION
Typography and Design
Desktop Printer, Arnold, MD

About the Cover

Satellite image of the cloud destribution in Supertyphoon Flo on 0530 universal time (UTC) 16 Septemer 1990 during the Tropical Cyclone Motion (TCM-90) field experiment. The center of Flow is near 20.9°N, 134.4°E. (See article on page 5.

Naval Research Reviews publishes articles about research conducted by the laboratories and contractors of the Office of Naval Research and describes important naval experimental activities. Manuscripts submitted for publication, correspondence concerning prospective articles, and changes of address, should be directed to Code OPARI, Office of Naval Research, Arlington, VA 22217-5000. Requests for subscriptions should be directed to the Superintendent of Documents, U.S. Government Printing Office, Washington, DC 20403. *Naval Research Reviews* is published from appropriated funds by authority of the Office of Naval Research in accordance with Navy Publications and Printing Regulations. NAVSO P-35.

Note From the Superintendent

As the Navy is reduced in size it will rely more heavily upon technological prowess and sound management to accomplish its global peacekeeping mission. The 21st Century Navy must be able to provide stability and deter aggression in a new international security setting.

To meet these new challenges, the Navy must continue to ensure that it has educated and experienced leaders. The Naval Postgraduate School is playing a critical role in preparing officers to understand the subtleties of finance, geopolitics, science and technology.

The outstanding programs at the Naval Postgraduate School advance the talents, skills and insights of its officer students to prepare them for more complex and challenging assignments. With its unique series of academic programs, NPS studies have served to enhance officers' analytical skills and expand their intellectual horizons. The key to this success lies squarely on the shoulders of the NPS faculty. On a par with faculty at any university, they excel in the classroom and the laboratory. The research program at NPS is used to strengthen the educational experience of each student while simultaneously keeping our faculty current in their disciplines. The research program ensures the recruitment and retention of top quality faculty. Results of NPS research have provided answers to many difficult operational problems, from aircraft combat survivability to weapons systems engineering and military recruiting strategy. We are pleased to offer a perspective of recent research contributions from the Naval Postgraduate School in this issue of Naval Research Reviews.

Note From the Provost

In the post-World War II era, the Naval Postgraduate School has established a unique educational role with an impressive academic track record. It concentrates on keeping its curricula modern and tuned to the Navy's needs. It brings thousands of military officers out of their operational duties for brief periods – on the average, less than two years – and enables them to acquire those advanced skills needed by their service. All of these officers come here after a considerable absence from academics. On an unprecedented scale in a university setting, they pursue graduate studies in a discipline that is more technical than their undergraduate degree program. Nearly one half of them make the transition from a baccalaureate degree in the liberal arts and humanities to graduate study in a science or engineering field. Over 90% successfully complete a fully-accredited Master's degree. Through the academic programs at NPS, Naval officers prepare themselves for more demanding assignments and make themselves a more valuable asset to their service. This value-added educational process has become the hallmark of the Naval Postgraduate School.

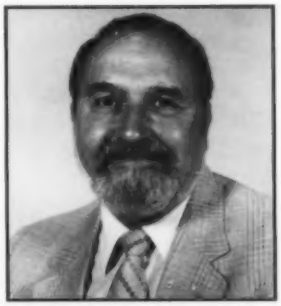

The individual thesis completed by each officer is especially important in the educational process, for the problem-solving skills developed during the thesis research remain embedded in a lifetime of service, never to be forgotten. The civilian faculty maintain a keen interest in cutting-edge research in their disciplines. The officer students bring the campus important insight from their operational environments. The faculty-student exchange that occurs while pursuing research reaps direct dividends for the Navy and other services, maintains a focus on relevant defense issues, and routinely leads to new and valuable results. In many cases, the research has helped to solve real-world problems on a real-time basis.

NPS education and research programs are relevant to tomorrow's Navy. With the troubling specter of future intellectual malaise on the horizon – visible in the inadequate science and math skills of American students – the value-added education programs at the Naval Postgraduate School will assume an increasing significance in the coming decades. Technological choices have strategic consequences, and the Navy and other military services must have leaders capable of understanding current and future technologies and making sound technological decisions. The links at the Naval Postgraduate School between education and research, scientific theory and naval operations, and civilian faculty and officer students serve the Navy and the Nation well, providing leaders who must be able to strike a bold and forward path into the early 21st Century, prepared to resolve unforeseen future national security challenges.

The Naval Postgraduate School Research Program

Jeffrey B. Knorr, Associate Dean of Reserach

Introduction

We at the Naval Postgraduate School are privileged to provide readers of Naval Research Reviews with an overview of the research being conducted at our unique institution. The broad responsibility of the School is reflected in its stated mission:

> To conduct and direct the advanced education of commissioned officers, and to provide such other technical and professional instruction as may be prescribed to meet the needs of the Naval Service, and in support of the foregoing, to foster and encourage a program of research in order to sustain academic excellence.

Thus, at the Naval Postgraduate School, the role of research is supportive of the educational mission of the School.

The Naval Postgraduate School research program is administered through the Research Office by the Dean of Research. The supportive role of research is reflected in the mission statement developed by the Research Office:

> To ensure that the Research Program provides a high quality, creative and relevant learning experience for NPS graduate students, and to encourage pursuit of new discoveries and applications which enhance the long term combat effectiveness of the Navy and other services.

The NPS Research Program

The research program at the Naval Postgraduate School consists of projects directed and executed by the School's 348 faculty with the participation of 1800 graduate students. The faculty, are associated with one of the 11 Academic Departments or 4 Academic Groups which serve the School's 39 curricula in science, engineering, information and policy sciences. The current annual level of the research effort is 122 faculty work years and $20M. Seventy percent of this research is conducted for the Navy and thirty percent is non-Navy. At present, sixty percent of the research is externally (i.e. reimbursably) funded and forty percent is internally (i.e. Navy O&MN) funded.

A. The Reimbursable Program

The Reimbursable Research Program consists of those projects which are externally funded on the basis of proposals submitted to potential sponsors by the School's faculty. Funding comes from a wide variety of sources including:

Office of Naval Research
Air Force Office of Scientific Research
Army Research Office
National Science Foundation
Defense Advanced Research Projects Agency

Navy Laboratories
Navy Systems Commands
Other DOD/Government Agencies and private sources

The Research Office reviews reimbursable proposals for appropriateness in the context of the School's mission and subsequently administers contracts awarded. The primary relationship, however, is between the principal investigator and the sponsor.

B. The Direct Funded Program

The Direct Funded Research Program is similar in nature to the IR/IED Programs at the Navy Laboratories. Proposals are prepared by the faculty and submitted to a Department Research Committee. Those proposals are evaluated by this Committee and by external referees throughout the Navy. Projects must be approved by the Research Committee, the Department Chair and the Dean of Research.

The Direct Funded Program has been carefully structured to complement the Reimbursable Program, thereby ensuring that the total program is flexible, responsive, balanced and supportive of the School's curricula. The Program supports a broad range of projects in accordance with an investment strategy which clearly delineates goals and priorities.

Overview of the Issue

This special issue of Naval Research Reviews contains articles by authors from various academic departments. The lead article by Elsberry reviews work on tropical cyclone motion. Prof. Elsberry was the Technical Director for the ONR Acclerated Research Initiative on this subject. The second article, by Luqi and Shing discusses a computer-aided prototyping system which provides an attractive alternative approach to more traditional software development methods. Following this is a paper by Brown, Gardner and Garrett which discusses some very innovative fiber optic hydrophone work. Devices such as these are required to achieve all fiber optic acoustic detection systems. The next article, by Gorman, discusses the use of acoustics to detect potentially damaging fatigue cracks in aircraft, a problem of great interest to the Navy. Work on identification of targets using impulsive radar is described in the paper by Morgan. This work has produced some basic results and the technique is attractive because it produces data which are aspect independent and depend only on target geometry. The article by Joshi and Kelleher discusses liquid cooling of electronic components. Interest in this approach has grown as circuit integration levels have increased; producing correspondingly higher heat fluxes. The final article by Healey et al. discusses a multidisciplinary project to develop an autonomous underwater vehicle. Such vehicles could be used in a host of Navy applications. The Research Notes which follow these articles provide an additional perspective on work being done at the School.

With this selection of articles and research notes, we have tried to convey some sense of the breadth and quality of the research work carried out at our institution in those areas of interest to ONR. It should be noted that several Departments are doing interesting research work in other areas which are not represented here. We sincerely hope that Research Reviews readers enjoy this selection of material. We invite your questions and comments which may be directed to either the authors or the Research Office.

Biography

Jeffrey B. Knorr is a Professor of Electrical and Computer Engineering and Associate Dean of Research at the Naval Postgraduate School. He received the BSEE Degree (1963) and MSEE Degree (1964) from the Pennsylvania State University and the Ph. D. degree (1970) from Cornell University. His research interests include microwave circuits and systems.

Tropical Cyclone Motion

Russell L. Elsberry
Department of Meteorology

The Threat

Although most people think of tropical ocean regions in terms of warm and pleasant weather, the tropical cyclone that forms over these oceans is one of the most destructive weather phenomena in the world. During May 1991, more than 135,000 people were killed when a tropical cyclone struck Bangladesh. Events such as this have led to the island native saying – "Typhoon come, all die." Typhoon is the local name in the western North Pacific for a similar tropical cyclone in the Atlantic that is known as the hurricane. In both cases, the maximum wind must exceed 64 knots (75 mph) and may be up to 150 knots (175 mph). Tropical cyclone is the general name for these storms and includes the weaker stages as well.

Disastrous encounters between typhoons and navy fleets have caused ship operations manuals to be rewritten. During World War II, U. S. Navy fleet units under Admiral Halsey sustained heavy losses and damage due to a typhoon. Survivors of a Japanese flotilla attempting to cross the path of a typhoon reported "huge and mountainous waves" across the bows of the ships. In many cases, ships can not make progress against the ocean currents and surface waves driven by the tropical cyclone winds. Once trapped, the normal option is to point into the waves and hopefully ride out the storm passage.

These naval encounters with tropical cyclones have led to the familiar "danger circle" of high winds and waves that all ships are to avoid. Gale force (35 knot or 41 mph) winds in large typhoons can extend 600 n mi (700 miles) from the center, but only extend 60 n mi (70 miles) from a midget typhoon. The typhoon forecaster uses surrounding ship reports and some satellite information to estimate the size of the danger circle. Drawing the danger circle around the predicted positions of the typhoon then defines the area that the ships must avoid. The problem is that the errors in the track forecasts have been so large that the danger areas have to be enlarged significantly to account for the uncertainty in the tropical cyclone motion.

Two important benefits can be achieved by an improvement in tropical cyclone track forecasts. Fleet units will be able to maintain readiness, accomplish training and achieve planned rendezvous points with other units in the battle group if accurate forecasts of the sizes and locations of the danger circle are available. Another situation in which accurate tropical cyclone track forecasts are required is when the ship is in a port, such as Norfolk in the Atlantic or Hong Kong in the Pacific. Just a few degrees change in track direction can mean the difference between riding out the storm in a safe harbor, and having to get underway quickly to cross out of the danger circle before the tropical cyclone traps the ship and drives it aground or into another vessel.

Recognition of the tropical cyclone threat to the Fleet, and that new scientific understandings were possible, led to a new research initiative in 1986. The role of the Naval Postgraduate School in that initiative will be described here.

ONR Initiative

The Office of Naval Research Marine Meteorology Program has just completed a five-year Accelerated Research Initiative to improve basic understanding of tropical cyclone motion. A key component of that program was a field experiment called Tropical Cyclone Motion (TCM-90) that acquired the best data set ever collected for typhoons. Operational fleet units participated in TCM-90, and the experiment operations center was at the Naval Oceanographic Command Center (NOCC)/Joint Typhoon Warning Center (JTWC) in Guam. This field experiment was also an excellent example of international cooperation. Four oceanographic research ships of the

USSR provided atmospheric and oceanographic observations along the path of the typhoons. Ten east Asian countries conducted a separate, but coordinated, field experiment to test improved techniques for track prediction. In addition, Taiwan made special observations to better predict the winds and heavy precipitation as typhoons pass over or around the mountainous terrain of that island.

The Naval Postgraduate School has had an integral role in the ONR research initiative. Department of Meteorology personnel participated in the research that led to the hypotheses for the field experiment, and contributed to the planning and execution of TCM-90. The discussion below will highlight some new understandings from the ONR initiative and preliminary results from TCM-90 that are expected to lead to better track predictions. Selections from a more comprehensive review[1] have been made to emphasize the NPS contributions because of the focus of this issue and of space limitations.

The Issues

Tropical cyclones usually form and move westward in the trade winds between the broad subtropical (around 30° lat.) high pressures and the lower pressure region near the equator (Figure 1). In the western North Pacific where three-eighths of all the world's named tropical cyclones form, this low pressure trough is deeper, so that the trade winds to the north are stronger. Furthermore, the deep trough pulls air from the Southern Hemisphere into a band of strong eastward winds on the equatorward side. It is within this favorable environment of westward winds on the poleward side and eastward winds on the equatorward side that contributes to the counterclockwise (in the Northern Hemisphere) rotation of tropical cyclones. The energy source for the development is provided by water vapor previously evaporated from the warm tropical ocean. This water vapor is then converted into heat energy in the eyewall clouds and the rainbands that spiral around the center. In the most intense stages, a clear region (called the eye) forms within this cloud mass, which then makes it relatively easy to locate the storm center from satellite images. In weaker stages in which this eye is not visible from satellites, the errors in locating the center are much larger. The challenge is to predict where this central region of high winds, waves and heavy precipitation (except in the eye) will move.

Storm Motion And Propagation

For a small tropical cyclone, the motion is similar to a cork in a stream. That is, the cyclone moves with the basic atmospheric current in which it is embedded. If this were the only effect, and the high and low pressure regions did not change, the tropical cyclone would simply move around the subtropical high into the cold midlatitude waters or hit land and die. For larger storms, deviations of 2-6 knots (2-7 mph) have been observed[2] between the typhoon motion and the

Figure 1.

Schematic of the environmental features during typhoon (symbol) formation over the western Pacific Ocean. Trade winds between the subtropical high and the low pressure trough near the equator form a basic current that moves most typhoons toward the west-northwest.

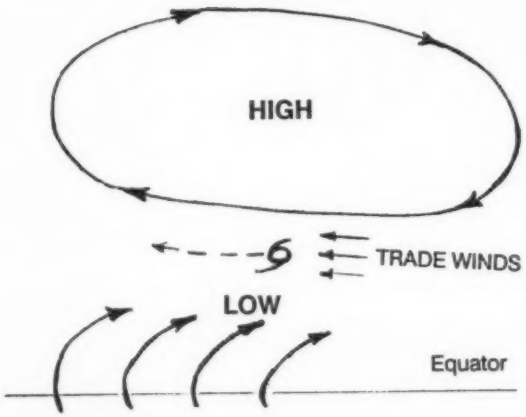

basic current. When the basic current is weaker than the normal 12 knots (14 mph), the addition of this deviation contributes a significant fraction of the total storm motion (Figure 2). This deviation will be referred to as a propagation vector because internal and external influences combine to deflect the storm relative to the basic current, and a combination of the basic current and propagation leads to the total storm motion.

A major effort in the ONR initiative has been devoted to understanding the physical causes of the propagation vector, and how the magnitude and direction of this vector depend on the storm structure and the environmental conditions. As suggested above, the magnitude of the propagation vector increases with size of the storm[3-5], which is defined here as the radial distance from the center to which 30 knot (35 mph) wind speeds extend. This effect has been demonstrated in numerical models in which no basic current is included. Nevertheless, the cyclone will propagate toward the west and toward the pole simply because the earth is curved and air parcels on the poleward side have more spin around a vertical axis than do air parcels on the equatorward side. Movement of these air parcels by the winds in the storm creates a counterclockwise rotating circulation to the west, and a clockwise circulation to the east (Figure 3). These counter-rotating gyres have a nearly uniform flow region between their centers, which typically are separated by 600-800 km (700-935 miles). It is this uniform flow region that propagates the tropical cyclone toward the west and the pole.[5]

Larger tropical cyclones produce stronger gyres that have stronger uniform flow between their centers, which results in larger propagation vectors. Very small tropical cyclones are not as effective in moving air parcels with different rotations about the vertical axis, thus the corresponding gyres are weaker and closer together. Only a weak uniform flow region is produced and the propagation vector is small.

It is the north-south difference in rotation about the vertical axis on a spherical earth that leads to the gyres in Figure 3. Such differences in rotation can also be created by the environmental flow. For example, clockwise rotation occurs in the subtropical high pressure cell in Figure 1 and counterclockwise rotation is found around the low pressure trough. This difference in rotation effect tends to offset the spherical earth effect. Farther to the north, the two effects act in the same sense. For the same size tropical cyclone, the westward and poleward propagation would be reduced south of the subtropical high and enhanced on the north side.[6]

Analytical models have been developed[7-10] that predict the amplitude of the counter-rotating gyres in Figure 3, and the magnitude and direction of the uniform flow between the gyre centers. It has been demonstrated[11] that a numerical track prediction model that does not include these counter-rotating gyres in the initial conditions will not have the proper propagation vector until the gyres are generated in 24-48 hours. Thus, the predicted storm motion initially is too slow. If the analytical model[7] is used to insert the counter-rotating gyres in the initial conditions, the propagation vector is present immediately and the correct storm motion results. This basic research result appears to be ready for transition to operational track prediction models[11], and should result in improved guidance to the tropical cyclone forecaster.

Time-Dependent Basic Currents

The tropical atmosphere is more complicated than the simple schematic in Figure 1. Presence of other weather disturbances that have similar horizontal scales as the tropical cyclone makes the determination of the basic current more complex. These disturbances may be confined to the lowest 5 km (18,000 feet) of the atmosphere, or only exist in a layer between 6-13 km (20,000 - 50,000 feet). As the tropical cyclone moves, these disturbances may become part of the environment, so that the basic current varies in time. The sparse meteorological observation network over the tropical oceans often prevents an accurate specification of the basic current. One goal of the TCM-90 field experiment was to collect a more complete data set to better define the basic current and its time variations.

Figure 2.

Storm motion is the vector sum of the basic current and a propagation vector that depends of the wind structure in the typhoon (symbol) and in the environment.

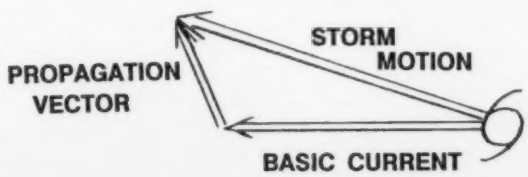

Figure 3.

Streamfunction of clockwise-rotating (solid) and counterclockwise-rotating (dashed) gyre circulations with a nearly uniform flow (equal spacing of the streamfunction) between the gyre centers. Dotted circles of 2°, 4°, 6°, 8° and 10° lat. are included to indicate horizontal scales of the gyres and the nearly circular flow around a large typhoon at the center of the grid.

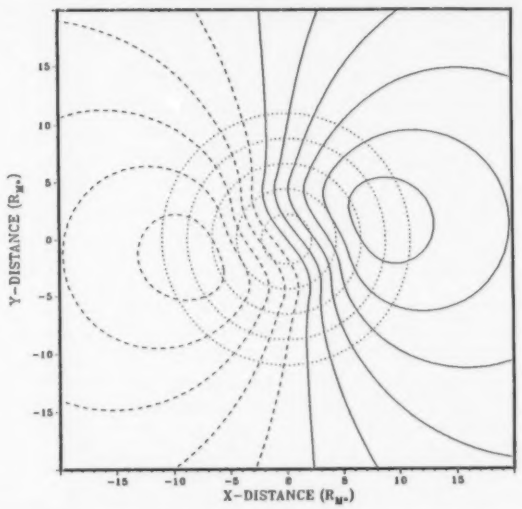

Each of these adjacent weather disturbances may interact with the tropical cyclone. In the western North Pacific, the adjacent disturbance may be another tropical cyclone because the region is so fertile for tropical cyclone formation that multiple cyclones frequently exist. When the separation between the two cyclones reaches some critical value around 600 n mi, they begin to rotate about a point between them in a counterclockwise orbit. This rotation is similar to a classical fluid mechanics experiment called the Fujiwhara effect. A re-examination[12] of many tropical cyclone interactions has shown that the two cyclones may rapidly begin to orbit, only later to escape. The classical merger of the two circulations does not occur very often. Rather the horizontal wind variations of the larger storm appear to destroy the smaller storm by tearing it apart. Some new theoretical treatments[13,14] of the

cyclone interaction problem have explored the capture, escape and merger phases. The rapid escape seems to occur when one of the orbiting cyclones comes under the influence of a neighboring circulation, and is captured by that circulation. The nonlinear interactions between more than two circulations can result in chaotic situations. Thus, chaos theory may provide guidance as to whether such cases are inherently not predictable. In such situations, the forecaster may be provided guidance that a critical interaction situation is approaching, and at best the outcome in terms of the possible tracks may be given only in a probabilistic sense.

Perhaps one of the most critical track forecast decisions is the time when the tropical cyclone moves northward around the subtropical high in Figure 1 and begins to move eastward rather than westward. The time when the cyclone begins to track eastward is called the recurvature time. The forecast is difficult because the cyclone may begin to move toward recurvature and then resume westward motion. Thus, the recurvature might be considered a time of low predictability, perhaps due to multiple interactions as described above.

At other times, large-scale circulations as in Figure 1 appear to determine whether the tropical cyclone will be a recurver or a straight-mover that will continue to move westward until it strikes land and dies. However, the large-scale circulation changes slowly in amplitude and relative location on time scales of more than 10 days.[15] While the circulation is locked in one mode, a sequence of tropical cyclones will all have the same track type. After the large-scale circulation changes into the other mode, the opposite track type will occur for some time. Thus, it is frequently possible to classify the track type by knowing the large-scale circulation at the time the tropical cyclone is first named (maximum winds exceed 34 knots or 40 mph). The NPS track-type forecast technique[15] is less reliable during transitions between modes of the large-

Figure 4.

Combined rawinsonde network for the four international tropical cyclone field experiments during 1990. The Asian nations regular rawinsonde networks with 12-hour soundings are indicated by small dots, and the special stations with 6-h soundings have large circles. The special 6-h soundings for TCM-90 are indicated by squares, and the Taiwan experiment 6-h soundings are indicated by triangles. Four USSR ships in stationary positions along 20°N are indicated by open ship symbols. Two Japan Weather ships are indicated with question marks because their schedule did not coincide with the TCM-90 operation periods. Two U.S. ships are indicated by solid ship symbols and other transmitting U.S. ships with rawinsonde launches over the Philippine Sea were withdrawn due to Desert Shield activities.

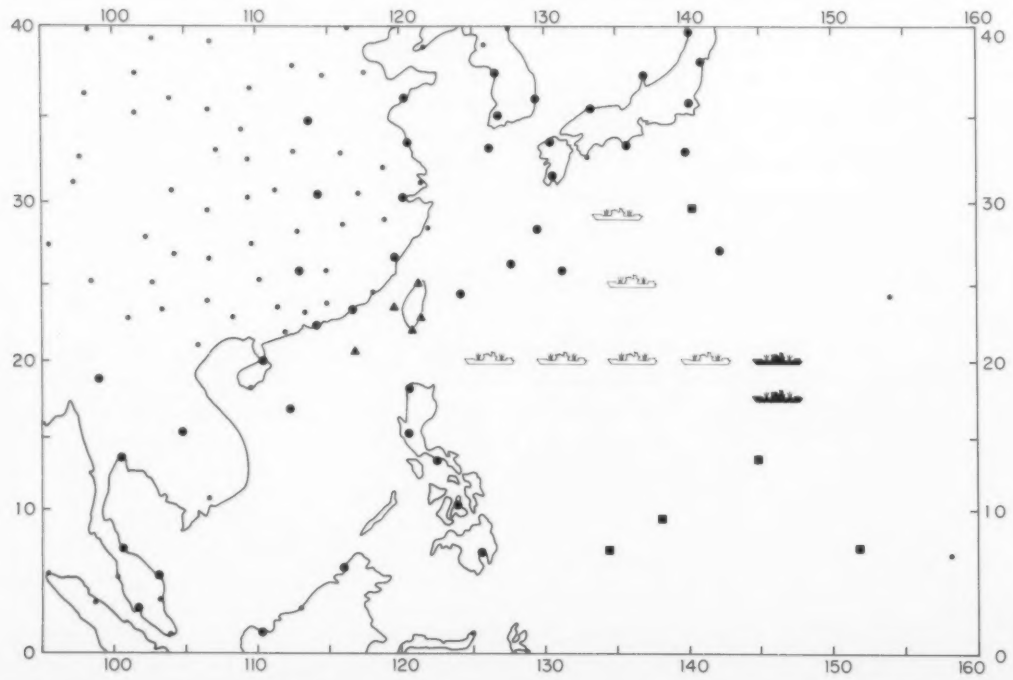

scale circulation, or when multiple cyclones exist. This technique is being prepared for operational testing at the JTWC.

TCM-90 Field Experiment

As indicated in the introduction, the Tropical Cyclone Motion (TCM-90) field experiment was carried out in conjunction with three other international experiments.[16] An overview of the combined network of upper air soundings is given in Figure 4. Instead of the normal two times per day, these stations provided four soundings per day during seven Intensive Observing Periods[17] lasting 36 to 48 hours. Furthermore, special sounding sites were added in the Philippines and on Saipan. The most important additions are the four USSR ships that maintained positions along 20°N, and a Japanese ship at 25°N. Navy Mobile Environmental Teams (MET) were onboard a stationary ship at 20°N and transiting ships, at least until the Desert Shield Operation took precedence. A MET group from Yokosuka also deployed to Iwo Jima on short notice to make soundings.

A new Doppler radar wind profiler at NPS was deployed to Kadena AFB, Okinawa during TCM-90. Three typhoons passed close enough to Okinawa to generate high winds that were measured each hour. For example, high vertical resolution winds (Figure 5) were measured each hour as Supertyphoon (winds exceeding 130 knots or 150 mph) Flo passed

Figure 5.

Wind speed (flag = 50 knots, long barb = 10 knots) and directions (wind from the north would be arrow pointing from top to bottom) measured by Naval Postgraduate School radar wind profiler at Kadena Air Base, Okinawa from 00 UTC 17 September (right side) to 23 UTC 17 September (left). The profiler provided observations each 360 meters (1180 feet) from 600 meters (1970 feet) above the ground to as high as 16,000 meters (52,000 feet) each hour as Supertyphoon Flo passed within 60 n mi to the east of Okinawa. The maximum wind speeds were greater than 85 knots (100 mph).

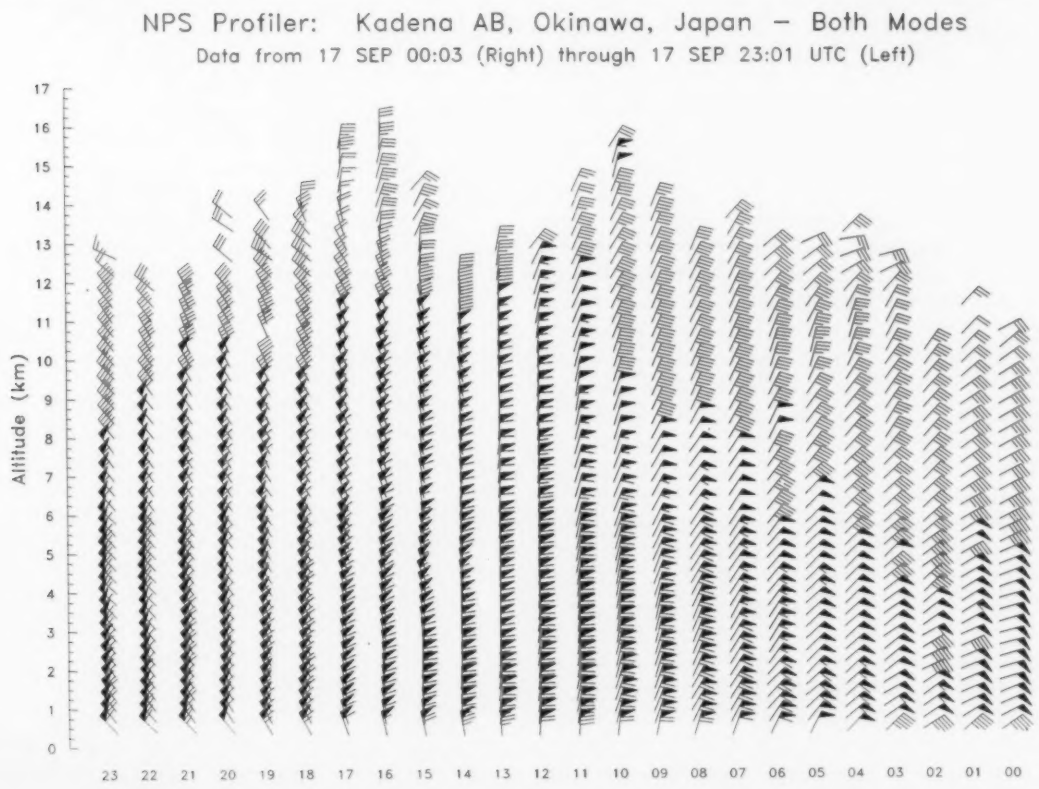

60 n mi (70 miles) to the east of Okinawa. During TCM-90, typhoons also passed by other radar wind profilers which provided unprecedented wind fields in typhoons. Correlations between the radar wind profiles at Okinawa and the hourly surface winds allow detailed comparisons over a larger range of speeds than achieved previously. New insights into how the surface wind gusts increase more rapidly than does the mean wind during the approach of the typhoon have also been gained from the NPS profiler observations.

The Naval Oceanography Command provided 12 prototype drifting buoys for TCM-90. These buoys were deployed via the launch tubes of P-3s from VQ-1. Eleven of 12 of the buoys were successfully deployed, and reported air and sea-surface temperatures plus the sea-level pressures each time a polar-orbiting satellite passed overhead. The buoys continued to report even in the high winds and waves as typhoons passed nearby. Decreases of the sea temperature by more than 1°C were measured in the wake of the typhoon. The surprising aspect was that the upper layers of the ocean continued to cool another 2°C even after the typhoon had passed. Although detailed confirmations have not been done, this decrease appears to be related to a surge of high winds, deep clouds and heavy precipitation that followed the typhoon. These changes could be expected to affect acoustical propagation along paths through the wake of the typhoon and surge.

LCDR George Dunnavan of NPS served as TCM-90 aircraft coordinator onboard the NASA DC-8 aircraft. TCM-90 funded the installation of a dropsonde launch tube on the DC-8 so that a new dropwindsonde developed by the National Center for Atmospheric Research could be deployed. Craig Motell of NPS and teams of Naval Reservists assisted in the dropwindsonde operations. In addition, the DC-8 carried the prototype satellite instrumentation for the Tropical Rainfall Measurement Mission (TRMM) that NASA will launch in the mid-1990's. Overflights of typhoons provided NASA scientists with the opportunity to test the TRMM instrument for high rainfall rates near the center and in the spiral rainbands. LCDR Dunnavan coordinated the flights so that the missions of TCM-90 and NASA were both accomplished.

An NPS team of Patrick Harr and Tamar Neta served as the Data Collection Center for TCM-90. As the result of full cooperation by the Fleet Numerical Oceanography Center (FNOC) in Monterey, about 90% of the observations were collected in real-time, and processed by the FNOC quality control procedures. Special experimental data and observations delayed in communication were collected after the experiment and merged with the real-time data. These observations[18] were distributed to participants of all four international experiments in July 1991.

The last data management goal for TCM-90 is to produce a set of final analyses on a 50 km grid at 18 levels in the vertical. This step is being accomplished at the National Meteorological Center using the newest version of an analysis system and the combined experiment data set. These analyses are expected to be used for many research studies to understand tropical cyclone motion using diagnostic techniques and advanced numerical models.

Summary

The goal of this Office of Naval Research Accelerated Research Initiative has been to improve understanding of tropical cyclone motion. The Naval Postgraduate School personnel are proud of their contribution to this ONR research initiative, which will contribute to improved tropical cyclone track predictions for the Fleet. One of those contributions has been in explaining the propagation of the cyclone relative to the basic current in which it is embedded. Differences in wind structure between large and small typhoons, and in the environment, have been demonstrated to affect the magnitude of the propagation. The control by the large-scale environmental flow on whether a tropical cyclone will be a recurver or a straight-mover has led to a prediction technique that appears to be operationally useful. However, more study is needed to understand special environmental flow conditions in which the future track is much less predictable. A major international field experiment during 1990 has resulted in the best data set ever collected for the study of typhoons. New technology in the form of radar wind profilers, drifting buoys and dropwindsondes from jet aircraft has been successfully applied. The raw observations have been distributed and final analyses with high horizontal and vertical resolution are being prepared with a state-of-the-art technique. These accomplishments offer hope for better track predictions for tropical cyclones in the future to the benefit of the Fleet and to civilian populations as well.

Acknowledgements

Dr. Robert F. Abbey, Jr., of the Marine Meteorology Program of ONR has directed the Accelerated Research Initiative. The Naval Postgraduate School Direct Funded Research Program also supported our participation in this research. Thanks are extended to our colleagues in the initiative who shared their inputs and results. Patrick Harr and John Sanders of the Naval Postgraduate School provided comments on the manuscript, which was carefully prepared by Mrs. Penny Jones.

Biography

Russell L. Elsberry is a Professor of Meteorology at the Naval Postgraduate School. He served as Technical Director of the ONR Accelerated Research Initiative on Tropical Cyclone Motion. He also was the Experiment Director for the

Tropical Cyclone Motion (TCM-90) field experiment during 1990. He is a Fellow of the American Meteorological Society and recently completed a three-year term as a Councillor for the Society.

References

1. Elsberry, R. L., and R. F. Abbey, Jr., 1991: Recent advances in understanding tropical cyclone motion. Technical Report NPS-MR-91-003, Naval Postgraduate School, Monterey, CA 93943, 92 pp.
2. Carr, L. E., III, and R. L. Elsberry, 1990: Observational evidence for predictions of tropical cyclone propagation relative to steering. J. Atmos. Sci., **47**, 542-546.
3. Chan, J. C.-L., and R. T. Williams, 1987: Analytical and numerical studies of the beta-effect in tropical cyclone motion. Part I. Zero mean flow. J. Atmos. Sci., **44**, 1257-1264.
4. DeMaria, M., 1985: Tropical cyclone motion in a nondivergent barotropic model. Mon. Wea. Rev., **113**, 1199-1210.
5. Fiorino, M., and R. L. Elsberry, 1989: Some aspects of vortex structure in tropical cyclone motion. J. Atmos. Sci., **46**, 979-990.
6. Evans, J. L., G. J. Holland, and R. L. Elsberry, 1991: Interactions between a barotropic vortex and an idealized subtropical ridge. I. Vortex motion. J. Atmos. Sci., **48**, 301-314.
7. Carr, L. E., III, 1989: Barotropic vortex adjustment to asymmetric forcing with application to tropical cyclones. Ph.D. dissertation, Naval Postgraduate School, Monterey, CA 93943, 143 pp.
8. Willoughby, H. E., 1988: Linear motion of a shallow-water barotropic vortex. J. Atmos.Sci., **45**, 1906-1928.
9. Peng, M. S., and R. T. Williams, 1990: Dynamics of vortex asymmetries and their influence on vortex motion on a beta-plane. J. Atmos. Sci., **47**, 1987-2003.
10. Smith, R. K., and W. Ulrich, 1990: An analytical theory of tropical cyclone motion using a barotropic model. J. Atmos. Sci., **47**, 1973-1986.
11. Carr, L. E., III, and R. L. Elsberry, 1992: Analytical tropical cyclone asymmetric circulation for barotropic model initial conditions. Mon. Wea. Rev., **120**, 644-652.
12. Lander, M., and G. J. Holland, 1991: On the interaction of tropical-cyclone scale vortices. Part I. Observations. Submitted to Quart. J. Roy. Meteor. Soc.
13. Holland, G. J., and M. Lander, 1991: On the meandering nature of tropical cyclones. Submitted to J. Atmos. Sci.
14. Ritchie, E. A., and G. J. Holland, 1991: On the interaction of tropical-cyclone scale vortices. II. Discrete vortex patches. Submitted to Quart. J. Roy. Meteor. Soc.
15. Harr, P. A., and R. L. Elsberry, 1991: Tropical cyclone track characteristics as a function of large-scale circulation anomalies. Mon. Wea. Rev., **119**, 1448-1468.
16. Elsberry, R. L., 1990: International experiments to study tropical cyclones in the western North Pacific. Bull. Amer. Meteor. Soc., **71**, 1305-1316.
17. Elsberry, R. L., B. C. Diehl, J. C.-L. Chan, P. A. Harr, G. J. Holland, M. Lander, T. Neta, and D. Thom, 1990: ONR Tropical Cyclone Motion Initiative: Field experiment summary. Technical Report NPS-MR-91-001, Naval Postgraduate School, Monterey, CA 93943, 106 pp.
18. Harr, P. A., T. Neta, and R. L. Elsberry, 1991: ONR Tropical Cyclone Motion Research Initiative: Data users guide to observations. Technical Report NPS-MR-91-002, Naval Postgraduate School, Monterey, CA 93943, 123 pp.

Notes on NPS participants cited in references: [2, 3 and 11] LCDR Lester Carr received his Ph.D. in September 1989. [3, 17] Dr. Johnny C.-L. Chan was an Adjunct Research Professor in 1986-87, and collaborated with Professor R. T. Williams. [5] Mike Fiorino completed his Ph.D. studies in December 1987. [6, 12, 13, 14, 17] Jenni Evans worked on her Ph.D. dissertation at the Naval Postgraduate School while her advisor Dr. Greg Holland was the G. J. Haltiner Research Chair occupant in 1988. [8] Dr. Hugh Willoughby was the Haltiner Research Chair occupant in 1991. [9] Dr. Melinda S. Peng is an Adjunct Research Professor. [15, 17, 18] Patrick Harr is an Adjunct Research Professor, and served with Tamar Neta as Data Managers for TCM-90.

CAPS – A Tool For Real-Time System Development and Acquisition

Luqi and Man-Tak Shing
Computer Science Department

Introduction

The Computer Aided Prototyping System (CAPS) is an integrated software development environment aimed at rapidly prototyping hard real-time embedded software systems, such as missile guidance systems, space shuttle avionics systems, and military Command, Control, Communication and Intelligence (C3I) systems. One of the major differences between a hard real-time system and a conventional system is that the application software must meet its deadlines even under worst case conditions[1]. The process of design and development of these systems is often plagued with uncertainty, ambiguity and inconsistency. The timing requirements are difficult for the user to provide and for the analysts to determine. It is also very difficult to determine whether a delivered system meets its requirements.

Traditional software development methods conduct extensive testing near the end of the project in an attempt to ensure proper functioning of the system. The major weakness of this approach is that there is no way to recover from major faults discovered at the end of the project, when available funds have been nearly exhausted. Furthermore, delivered systems that meet faulty requirements can satisfy a contract without being useful to the sponsor. The inadequacy of current software development methods is evident in high software costs and low programmer productivity. Recognizing the increased cost and importance of software development for Command and Control (C2) systems, the Secretary of Navy (SECNAV) promulgated an instruction addressing software development and acquisition[2]. This instruction documents SECNAV concern for defining a DoN acquisition policy for software-intensive systems and increasing user involvement during the design and development stages. The policy combining these two concerns states:

"To promote effective interaction between the user and the developer, software prototyping methods shall be used in the design and construction of C2 information systems. Early delivery of software systems is emphasized through the use of prototyping methods"[2].

The rapid prototyping approach to software development provided by CAPS[3] supports this policy. Rapid prototyping uses rapidly constructed prototypes to help both the developers and their customers visualize the proposed system and assess its properties in an iterative process. A prototype is an executable pilot version of the intended system that accurately reflects chosen aspects of the system. Rapid prototyping may be used in conjunction with or as an alternative to the traditional software development cycle.

The Computer Aided Prototyping System

The Computer Aided Prototyping System (CAPS) provides facilities for computer-aided design, software component reuse, and automated Ada code generation. These tools are developed to help software engineers rapidly construct and adapt software, validate and refine user requirements, and to

check consistency of proposed design[4]. The process supported by CAPS provides requirements and designs in a form that is useful in the construction of the operational system, as well as in the acquisition process to assess optimized implementations delivered by contractors, and to integrate independently developed subsystems. CAPS allows the user to specify the requirements of a proposed system informally in a structured top-down fashion using easy-to-understand graphics, assists the designer in augmenting the informal specifications with formal annotations, and automatically translates the result into executable Ada code.

The CAPS Method

There are four major stages in the CAPS rapid prototyping process: software system design, construction, execution, and debugging/modification.

The initial prototype design starts with an analysis of the problem and a decision about which parts of the proposed system are to be prototyped. Requirements for the prototype are then generated, either informally (e.g. English) or in some formal notation. These requirements may be refined by asking users to verify their completeness and correctness. After the requirements analysis is completed, the designer uses the CAPS graphic editor to draw dataflow diagrams with non-procedural control constraints as part of the specification of a hierarchically structured prototype, resulting in a preliminary, top-level design free from programming level details. The underlying computational model unifies dataflow and control flow, and provides a mechanism for developing top-down decompositions. The user may continue to decompose any software module until its components can be realized via reusable components drawn from the software base or new atomic components. The construction of the prototype is aided by the syntax-directed editor which helps the designer create syntactically correct timing and control constraints for the operators. This prototype is then translated into Ada for execution and evaluation. Debugging and modification utilize a design database that assists the designers in managing the design history and coordinating changes as well as the other tools described above.

Figure 1.

Iterative Prototyping Process in CAPS

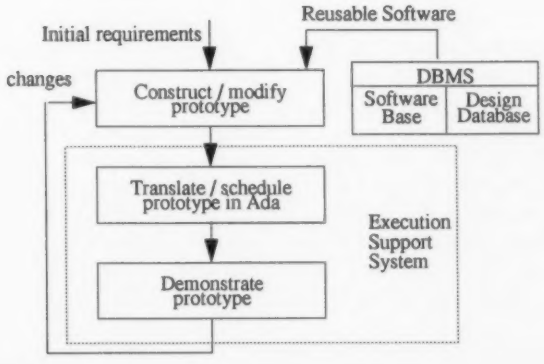

The Prototype System Description Language

The CAPS tools are based on the Prototype System Description Language (PSDL). PSDL is a high-level language designed specifically to support the specification of real-time software systems, as well as to organize and retrieve reusable components in the software base[5]. PSDL lets designers sketch a system using computation graphs, where the vertices are *operators* and the directed edges are *data streams*, and then refine the design by adding timing and control constraints in text form.

Operators are state machines whose internal states are modeled by state variables. Operators with an empty variable set behave like functions. PSDL operators can be triggered by data (*sporadic* operators) or by periodic timing constraints (*periodic* operators). When triggered, an operator will produce output based on input values and values of internal state variables. There are two kinds of operators: *atomic* operators and *composite* operators. An atomic operator is one that can be realized by an implementation stored in the software base or supplied by the software engineers, and a composite operator is one that can be decomposed into a network of more primitive operators represented as enhanced dataflow diagrams.

Operators communicate via two kinds of data streams: *dataflow* streams and *sampled* streams. A dataflow stream can be thought of as a FIFO buffer of capacity one that connects synchronized operators. Data in dataflow streams represents discrete transactions, and is removed from the stream when read. A sampled stream can be thought of as a single memory cell and connects operators with uncoordinated rates. This type of data usually comes from a continuous data source and can be used many times or written over before use, depending on the rate of its input and use.

Real-time applications motivate the timing and non-procedural control constraints of PSDL. Each time critical operator has a *maximum execution time* constraint, representing the maximum time the operator may need to complete execution after it is fired, given access to all required resources. In addition, each periodic operator has a *period* and a *deadline*. The period is the interval between triggering times for the operator and the deadline is the maximum duration from the triggering of the operator to the completion of its operation.

Each sporadic operator has a *maximum response time* and a *minimum calling period*. The minimum calling period is the smallest interval allowed between two successive triggerings of a sporadic operator. The maximum response time is the maximum duration allowed from the triggering of the sporadic operator to the completion of its operation. To model distributed systems, PSDL also provides the option of specifying the *maximum delay* associated with any data stream. Control constraints define data-triggered actions and provide conditional execution and output.

The CAPS Tools

The set of tools provided by CAPS includes the user interface, software database system, and execution support system.

The user interface in CAPS includes a graphic editor, a syntax-directed editor, and a browser. The graphic editor and the syntax-directed editor together provide a user-friendly environment for the user/software engineer to construct a prototype using graphical and textual objects. The browser allows software engineers to view reusable components in the software database system.

The software database system, which consists of a software base and a design database, provides facilities for software reusability, automated system management, and version control. The software base keeps track of the PSDL descriptions and Ada implementations for all reusable software components in CAPS. The design database coordinates the concurrent efforts of a team of software engineers and manages the different versions and alternatives of the design and documents they produce.

The execution support system consists of a translator, a static scheduler and a dynamic scheduler. The translator generates code that binds together the code supplied by the designer and the reusable components extracted from the software base. The static scheduler and the dynamic scheduler together create the real-time schedule and drivers needed for executing the prototype.

Application of CAPS in Real-time Software Development and Acquisition

Rapid prototyping under CAPS is a semi-formal approach to real-time software development. Like Structured Analysis[6], it uses a structured approach to enforce modular design. However, unlike Structured Analysis, CAPS provides tools which span the entire software development process, ranging from requirements analysis to system testing and integration.

CAPS as a Requirements Engineering Tool

The requirements for a software system are expressed at different levels of abstraction and with different degrees of formality. The highest level requirements are usually informal and imprecise, but they are understood best by the customers. The lower levels are more technical, precise, and better suited for the needs of the system analysts and designers, but they are further removed from the user's experiences and less well understood by the customers. Because of the differences in the kinds of descriptions needed by the customers and developers, it is not likely that any single representation for requirements can be the "best" one for supporting the entire software development process[4]. CAPS provides the necessary means to bridge the communication gap between the customers and developers. The Prototype System Description Language is designed specifically for specifying hard real-time systems. It has a rich set of timing specification features and offers a common baseline from which users and software engineers describe requirements. The PSDL descriptions of the prototype produced by the graphic and syntax-directed editors are very formal, precise and unambiguous, meeting the needs of the system analysts and designers. The demonstrated behavior of the executable prototype, on the other hand, provides concrete information for the customer to assess the validity of the high level requirements and to refine them if necessary. CAPS offers basic requirements traceability through the "by requirements" statement of PSDL, allowing software engineers to link actual requirements to the modules that realize the requirements. Requirement traceability is essential in the development of hard real-time systems, where user requirements change often over the course of the software development.

CAPS as a System Testing and Integration Tool

Unlike throw-away prototypes, the process supported by CAPS provides requirements and designs in a form that can be used in construction of the operational system. The prototype provides an executable representation of system requirements that can be used for comparison during system testing. The existence of a flexible prototype can significantly ease system testing and integration. When final implementations of subsystems are delivered, integration and testing can begin before the completion of all the subsystems by combining the final versions of the completed subsystems with prototype versions of the parts that are still being developed.

CAPS as an Acquisition Tool

Decisions about awarding contracts for building hard real-time systems are risky because there is little objective basis for determining whether a proposed contract will benefit

the sponsor at the time when those decisions must be made. It is also very difficult to determine whether a delivered system meets its requirements. CAPS, besides being a useful tool to the hard real-time system developers, is also very useful to the customers. Acquisition managers can use CAPS to ensure that acquisition efforts stay on track and that contractors deliver what they promise. CAPS enables validation of requirements via prototyping demonstration, greatly reduce the risk of contracting for construction of systems that do not meet the sponsors' needs. The validated high-level designs resulting from prototyping can be used to formulate subcontracts for subsystems that prevent many system integration problems. Other problems can be detected earlier by testing interactions between delivered subsystems and prototypes of subsystems not yet complete. Prototypes generated by CAPS include structures for experimentally measuring whether critical components meet their timing requirements. These structures can be used to evaluate real-time performance of systems delivered by contractors. Automated functional testing can compare results or delivered systems to results produced by the prototype.

Conclusions

The capabilities provided by CAPS are essential to rapid prototyping. In particular, automatic code generation and instrumentation let designers to try design variations quickly without cutting corners. The diagnostics provided by the automatic instrumentation helps to localize and fix bugs. Automated schedule construction and diagnostic information about timing constraints helps to navigate the maze of interacting resource constraints and evaluate the feasibility of the requirements.

We have recently completed an experiment to evaluate our rapid-prototyping methods and computer-aided design environment[7]. Our experiment was to prototype a generic command, control, communications and intelligence (C3I) station and generate the Ada code from the prototype's specifications automatically. The results of the experiment show that it is feasible to use computer-aided prototyping for practical, real-time Ada applications. Experience gained from the experiment also suggested many improvements to CAPS. Our long term plans include work on extending CAPS to a distributed computing environment, improved computer aid for managing and retrieving reusable software, and computer-aided generation and optimization of production-quality implementation code from specifications.

CAPS is unique in providing a computer-aided prototyping capability for hard real-time systems. Current CASE tools only support the static aspects of software development, while CAPS supports the dynamic aspects of the software life cycle. It will help the contracting and acquisition process for hard real-time systems in establishing that the initial requirements correctly capture the problem, checking that delivered systems meet their requirements, and ensuring that independently developed subsystems work properly when integrated together.

The substantial investment in real-time embedded systems in the Department of Defense (DoD) and the Department of Navy (DoN) points out the tremendous need for improved acquisition methods and supporting tools that can be used to test the design of a software system before coding. The Military Specification MIL-H-48655B calls for requirements analysis, functional specification and verification before the actual coding of the system[8]. The work described in this paper supports these objectives and enables DoN to make better decisions in acquiring systems useful to the Navy.

Biography

Luqi is an associate professor of computer science at the Naval Postgraduate School. She has also worked on software research and development in academia and industry. Her recent work includes rapid prototyping, real-time languages, design methodology, and software development tools. She has received an Engineering Initiation Award and a Presidential Young Investigator Award from NSF. Her research has been supported by ONR, AFSOR, CNO, NAVSEA, Navy Labs and computer industry. Luqi has a BS in computational mathematics from Jilin University, China, and an MS and a PhD in computer science from the University of Minnesota.

Man-Tak Shing is an associate professor of computer science at the Naval Postgraduate School. He has also been on the faculty of the University of California at Santa Barbara. His recent work includes path planning, genetic algorithms, and scheduling real-time systems. Shing received his BS degree from the Chinese University of Hong Kong in 1976, and MS and PhD degrees from the University of California at San Diego in 1978 and 1980.

Acknowledgment

The research reported in this paper was sponsored in part by the Computer System Division of the Office of Naval Research through the direct funding program.

References

1. J.A. Stankovic and K. Ramamritham, *Tutorial on Hard Real-Time Systems*, IEEE Computer Society Press, Washington, D.C., 1988.
2. Department of Navy, SECNAV INSTRUCTION 5200.37, "Acquisition of Software-Intensive C2 Information Systems," 5 January, 1988.
3. Luqi, "Software Evolution via Rapid Prototyping," *Computer*, vol. 22, pp. 13-25, 1989.

4. Luqi, R. Steigerwald, G. Hughes, F. Naveda, and V. Berzins, "CAPS as Requirements Engineering Tool," *Proc. Requirements Engineering and Analysis Workshop*, Software Engineering Institute, Carnegie Mellon University, Pittsburgh, Pennsylvania, 1991.

5. Luqi, V. Berzins, and R.T. Yeh, "Prototyping Language for Real-Time Software," *IEEE Transactions on Software Engineering*, vol. 14, pp. 1409-1423, 1988.

6. D. Hatley and I. Pirbhai, *Strategies for Real-Time Systems*, Dorset House Publishing Co., New York, NY, 1988.

7. Luqi, "Computer-Aided Prototyping for Command-And-Control Systems using CAPS," *IEEE Software*, pp. 56-67, Jan 1992.

8. Department of Defense, Military Specification MIL-H-48655B, "Human Engineering Requirements for Military Systems, Equipment and Facilities," 31 January 1979.

Fiber-Optic Interferometric Push-Pull Hydrophones

David A. Brown, David L. Gardner, and Steven L. Garrett
Physics Department

Introduction

Transmitting information with optical fibers has many advantages over using metal wires including: immunity to electromagnetic interference, increased bandwidth, lighter weight, lower cost, reduced risk of spark hazards, and low transmission loss. These advantages summarized in Table 1, make fiber-based systems attractive for both commercial and military applications. One important difference is that commercial systems are operated with cooperative users (allowing two way communication and synchronous timing), while military systems must operate with both cooperative and uncooperative users. The Navy has recognized benefits of fiber optic technology and has been exploiting its potential in underwater acoustic detection systems such as towed arrays, sonobuoys, bottom mounted systems, tracking ranges, and hull mounted arrays. This paper summarizes a few of the recent developments at the Naval Postgraduate School in all optical fiber acoustic detection systems.

In order to exploit the full benefits of using optical fibers in acoustic detection systems, the sensors must be optically interrogated. Therefore, conventional sensing technologies, such as piezoelectrics, will be replaced with optical-based sensing technologies compatible with optical fiber transmission lines. Using electrical-based sensors in combination with fiber transmission lines mandates either battery power at the sensor location or parallel electrical lines to power the wet-end electronics (amplifiers/multiplexers), thus, negating many of the advantages achieved by using optical fiber.

The cost of this technology is an important issue. Historically, the military has been forced to carry the burden of expense in developing new technologies to support its mission. In contrast, the military research and development in fiber optic sensing and communications is heavily leveraged by industry. The market developed by long haul communications and Local Area Networks (LANs) has driven the price of optical fiber from 4 dollars a meter to 4 cents a meter in just the last ten years. Likewise, we have seen a two order of magnitude decrease in the price of quality laser diodes due to the tremendous use of lasers in bar code readers and compact disk (CD) players. Fiber optic couplers/splitters, a common component in interferometric sensors, have seen an order of magnitude drop in price over the same time period.

Table 1.

Advantages of fiber optics over conventional technologies.

Data Transmission Advantages	Sensing Advantages
Increased bandwidth	Compatibility with fiber transmission
Higher data rates	Large Dynamic Range (Phase sensors)
Lower cost	Long continuous sensing medium
Low attenuation	New multiplexing capabilities
Lighter weight	Lighter weight
EMI immunity	EMI immunity
Reduced risk of spark hazards	Reduced risk of spark hazards
Low crosstalk	Covert Deployment
Small size, easily packaged	No EM radiation

Fiber Optic Sensors

All fiber optic sensors have similar characteristics. They share common components including: a light source, an optical fiber transmission line, a transducer, a photodetector, and supporting electronic instrumentation. Depending on the requirements of the system, the light source may be a light emitting diode or a laser, the fiber may allow multimode or single mode propagation, and the demodulation electronics can range from simple linear scaling and ratio circuits to more complicated phase modulation recovery algorithms.

The most general way to classify fiber sensors is by the parameter of the light that is varied e.g. intensity, polarization, or phase. In general, phase based sensors using interferometry offer the best sensitivity and dynamic range and have consequently received the most attention for Navy acoustic detection systems. These systems can require below sea state zero (SSO) detection, dynamic range in excess of 100 dB, large bandwidth, multiplexing capabilities, low power loss, and/or long distance repeaterless transmission.

Phase Modulated Sensors (Interferometers)

Photodetectors are not capable of directly detecting the phase changes of light, since the frequency of light is on the order of 3×10^{14} Hz. In order to detect phase changes, two light waves of exactly the same frequency are combined interferometrically to produce an intensity pattern that can be converted to a voltage with a photodetector cell and a transimpedance amplifier. The phase differences between the two light waves can then be determined by examining the resulting intensity pattern.

When the two waves of the same intensity and polarization are in phase and at the same spatial location, they add constructively to produce a waveform of the same frequency with twice the amplitude. If the phase relationship is such that the waves are 180 degrees (π radians) out-of-phase, the waves add destructively and are extinguished. Interferometry has been used for many years to make measurements of small path length changes. Fiber interferometry differs from interferometers using bulk optics in that the waves are totally contained in a flexible inexpensive optical fiber waveguide.

A Mach-Zehnder fiber optic interferometer which is commonly used for acoustic sensing is illustrated in Figure 1. It consists of a coherent single frequency light source, a splitter/coupler, which divides the light in order to produce two waves of the same frequency, a second coupler, which allows the two lightwaves to combine interferometrically, a photodetector, which can be kilometers away from the actual sensor, and a demodulator which converts the phase/interferometric encoded information into a voltage that is proportional to the stimulus inducing the phase modulation.

Figure 1.

Mach-Zehnder Interferometer.

The output intensity of the interferometer varies from bright to dark having a periodicity that is proportional to the amplitude of the phase variation between two interfering waves. The intensity observed is proportional to sum of the squares of the electric field vectors, E_1^2, and E_2^2, and the cosine of the phase angle, Φ, between the two light waves:

$$E_3^2 = E_1^2 + E_2^2 + 2E_1 E_2 \cos \Phi \qquad (1)$$

Acoustically induced phase changes in fiber optic interferometers

An interferometer leg of length L has a corresponding radian length given by

$$\Phi = \frac{2\pi}{\lambda} n L \qquad (2)$$

where λ is the vacuum wavelength of the laser light and n is the index of refraction. When the fiber is subjected to an external positive pressure the fiber gets smaller and the speed at which the light propagates increases slightly. The pressure induced phase change is therefore

$$\frac{\Delta\phi}{\Delta P} = \frac{2\pi}{\lambda} n \frac{\Delta L}{\Delta P} + \frac{2\pi}{\lambda} L \frac{\Delta n}{\Delta P} \qquad (3)$$

As an example, suppose a leg of an interferometer is subjected to a monofrequency acoustic pressure and a slowly drifting temperature such that the resulting phase difference between the two legs can be expressed as, $\Phi = C \cos(\omega t + \phi_d)$. The output of the interferometer is clearly not linear with the acoustic pressure. Noting equation 1 above, the resulting intensity pattern is given by the expression

$$i(t) = A + B \cos(C \cos \omega t + \phi_d) \qquad (4)$$

Demodulation of phase encoded signals in fiber optic sensors

There are only a few practical techniques that can be used to unambiguously recover (demodulate) the induced phase modulation. In one form or another, a sine-cosine demodulator is typically used such as that illustrated in the block diagram

Figure 2.

Block diagram of a sine-cosine demodulator.

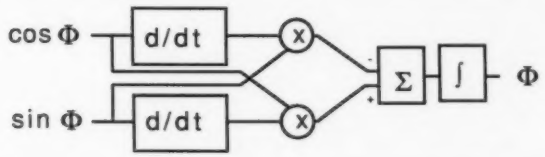

in Figure 2. In order for this style demodulator to be effective, the inputs must be orthogonal. Thus, obtaining the sine and cosine of the relative phase difference is usually the first step in demodulating an interferometric waveform.

The most common method of obtaining the two orthogonal inputs is to create a known carrier phase modulation by externally modulating the wavelength of the laser. A signal proportional to the sine and cosine can then be extracted from the carrier waveform using heterodyne techniques. This phase generated carrier (PGC) technique is capable of detecting phase modulations of 2μrad/√Hz.[1].

A second approach to demodulate the phase encoded information is to terminate the interferometer with a 3x3 coupler instead of the more conventional 2x2 coupler. Ideally a 3x3 coupler produces outputs that intrinsically contain orthogonal information since they are 120 degrees out-of-phase. In a 2x2 coupler the outputs differ by 180 degrees. The three signals can then be processed to obtain sinΦ and cosΦ.[2] A third approach that we have recently developed at NPS is to process the three outputs of a 3x3 coupler directly in a symmetric manner.[3,4]

Transducers and design philosophies

In order to exploit the advantages of interferometric detection adequate phase shifts must be induced in the arms of the interferometer. Most of the early work in fiber optic sensing was based on coating one fiber with a thin layer of plastic to enhance the compressibility of the glass fiber waveguide and using the second leg of the interferometer as a reference by attempting to decouple the outer plastic jacket from the fiber and/or by wrapping the leg under tension on an incompressible mandril.

There are a number of problems with this approach. Silica glass optical fiber alone or with a plastic coating is neither very compliant nor selective. Subjecting the optical fiber to a pressure resulted in only a very small deformation and corresponding small phase change in the interferometer. In addition, using a reference leg severely compromises not only the sensitivity but also the selectivity of the interferometer.

The approach we have taken is to use air backed transducers and to remove the reference leg, replacing it with a second sensing leg. It is important to recognize that an interferometer is intrinsically a differential device, responding to the relative phase changes in the two legs of the interferometer. Exploiting this, we have developed and patented air backed flexural disks and ellipsoidal shell transducers that produce acoustically induced phase modulations that are 180 degrees out-of-phase, but generate phase changes in each leg that responded in phase to temperature fluctuations and accelerations. Using this philosophy, the Naval Postgraduate School has developed push-pull accelerometers, geophones, seismometers, pressure gradient, directional hydrophones, and omnidirectional hydrophones.

Omnidirectional push-pull hydrophones

Designing a push-pull transducer for directional stimuli such as acceleration or pressure gradients is fairly straightforward. Producing differential strains when the field of interest is uniform is less obvious. The first push-pull omnidirectional sensors were built at the Naval Postgraduate School using flexural disk transducers.[5] These flexural disk sensors produced the highest sensitivity for a given depth tolerance of any previous fiber optic interferometric sensor reported.[6] In addition to improved sensitivity, the selectivity was also enhanced due to its temperature and acceleration canceling design. The second omnidirectional push-pull sensor that we have developed and patented relies on the differential strains that are

Figure 3.

Schematic diagram of the dual-plate, four-coil acceleration cancelling hydrophone. The gap between the two plates is chosen based on the strength of the plastic and the required maximum operating depth.

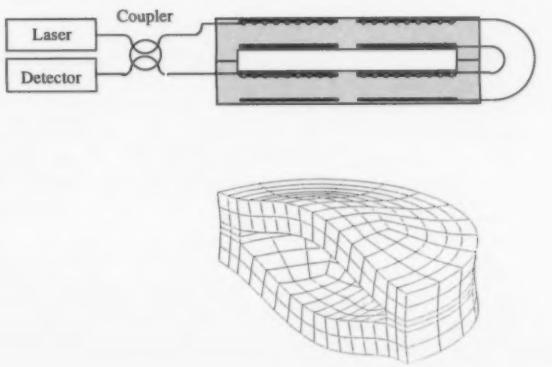

Figure 4.

Photograph of a flexural disk hydrophone capsule that is cast and cured as a single unit.

produced on the surface of an oblate ellipsoidal shell.[7] Uniform pressure induced push-pull strains can also be produced when using two concentric cylinders.[8]

Flexural disk hydrophones

When an air backed thin circular plate is subjected to a uniform pressure on one side, strains are produced that are compressive on one side and tensile on the other. By bonding flat spiral coils of optical fiber to both surfaces of the plate, the strain can be detected interferometrically in a push-pull fashion. If the flat fiber coils make up the two legs of an interferometer, the phase modulations that are produced are 180 degrees out-of-phase. Temperature induced signals are canceled since each leg will strain in-phase. Acceleration induced signals can also be canceled by using a second plate mounted on the opposite end of a cylinder and winding the optical fiber as illustrated in Figure 3. We have built and tested prototype flex disk sensors using aluminum, castable epoxies, castable elastomers, and composite materials.

An acceleration canceling hydrophone made entirely from a high tensile strength material is shown in Figure 4. In this particular design the four coils and coupler are cast into a single unit and the gap between the plates is chosen so that the plates touch at the designed maximum operating depth. This permits the plate strength to correspond with the breaking strain of the optical fibers. This design is also particularly well suited for bottom mounted high pressure application. By introducing a small orifice in the wall of the housing, the pressure within the sensor can reach equilibrium with the ambient pressure while frequencies higher than the associated cutoff frequency are detected. The frequency response of one of the castable epoxy flex disk sensors is shown in Figure 5. This particular calibration curve was obtained at Underwater Sound Reference Detachment of the Naval Research Laboratory. Having constructed and tested several of these flexural plate hydrophones, we have found that their measured sensitivity and their theoretical sensitivity, based on the elastic properties of the plate material and the boundary conditions, are in excellent agreement for both hydrostatic and acoustic pressure fields. The temperature and depth dependance of the sensitivity is also in good agreement with that predicted by the theory. Because of their geometry, high acoustic sensitivity, and cancellation of accelerations, flexural disk sensors are particularly suited for hull mounted arrays, bottom mounted arrays and in sonobuoy applications.

Ellipsoidal Flextensional Hydrophone

While developing the flex disk sensors, the Postgraduate School has also been designing and fabricating a second class of omnidirectional push-pull hydrophones by taking advantage of the differential strains generated on the surface of an (oblate) ellipsoidal shell. When an oblate spheroidal shell having an aspect ratio, $a/b > (2-\nu)^{1/2}$, where ν is Poisson's ratio, is subject to hydrostatic or low frequency compression, the semi-major axis (a) and semi-minor axis (b) experience strains

Figure 5.

Frequency response of a dual-plate, four-coil acceleration cancelling hydrophone capsule that is cast and cured as a single unit. Data obtained at the Underwater Sound Reference Detachment of the Naval Research Laboratory.

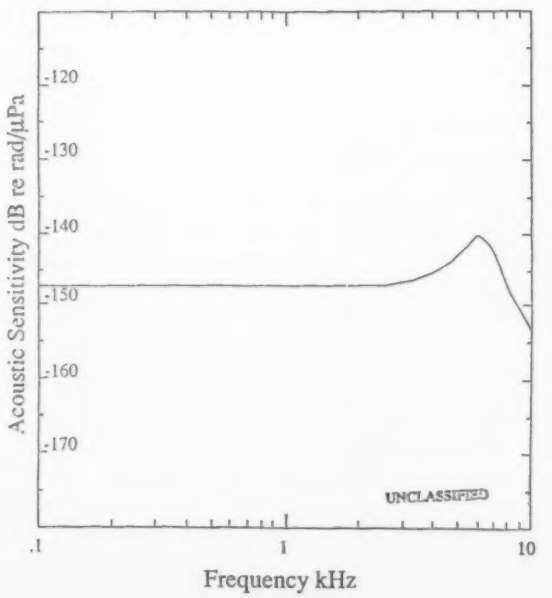

Figure 6.

a)Cross-sectional view of cross wrapped fiber-optic interferometric oblate spheroidal flextensional hydrophones showing the equatorial and meridional coil pairs.
b)Cross-sectional view of parallel wrapped oblate spheroidal hydrophones showing the equatorial and polar coils.

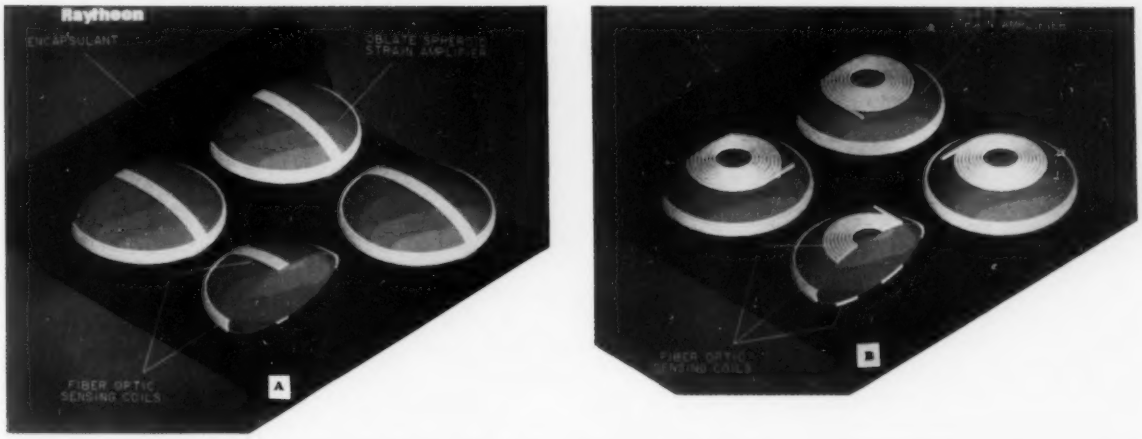

of opposite sign.[9] There are a number of ways one can transduce these strains. When the arms of an interferometer are wound separately around the equatorial and meridional circumferences of the oblate spheroid, strains produced in the optical fibers will be of opposite sign. The second implementation replaces the meridional interferometer leg with a circular or parallel winding of optical fiber nears the pole(s). Illustrations of the cross wrapped and parallel wrapped oblate spheroidal hydrophone are shown in Figure 6.

As in the case of the flexural plate design, we have developed closed form analytical equations describing the sensitivity, resonance frequency, and depth tolerance of this hydrophone. The oblate spheroid designs have the advantage of requiring no internal access so that the shells can be fabricated by inexpensive methods (e.g., injection molding) and the optical fibers can then be placed entirely on the exterior.

This geometry also provides the flexibility of allowing the hydrophone element or an array of elements to be "shaded" by varying the number of turns taken around each shell. Hydrophone element shading can suppress side lobes when beamforming.

Conclusions

This paper has summarized the research on fiber-optic push-pull interferometric hydrophone systems which have been developed and tested at the Naval Postgraduate School from 1983 through 1992. In general, the fiber optic hydrophones are designed to be air backed and push-pull in order to produce high sensitivity. Since no reference fiber leg is used the sensors are capable of common mode cancellation of unwanted environmental noise such as accelerations and temperature fluctuations. In most cases, these sensor designs and interferometric demodulators schemes have been patented by the U.S. Navy.

While this relatively new technology has been proven at sea in Advanced Technology Demonstrations under numerous sea trials, for different programs, and in large arrays with multiplexing, many challenges still remain in reducing cost, further improving performance, reaching production, and in educating the potential users.

Acknowledgements

Over the past seven years this work has been supported by the Office of Naval Research – Physics Division, the Office of Naval Technology, Space and Naval Warfare Systems Command, Naval Sea Systems Command, and the Naval Postgraduate School Direct Funded Research Program. Most of the actual fabrication and testing was accomplished by students at the Naval Postgraduate School in partial fulfillment of their Master's degrees LCDR G.B. Mills, LCDR G.E. MacDonald, LT P.A. Feldmann, LT C.M. Crooker, LT J.A. Flayharty, LT B.M. Fitzgerald, LCDR J. Olcott, LT B.L. Beaton, LT J. Serocki, LT K. Wetterskog, LT J. Kreijger, LT B. Flaskerude, Mr. Beng Hock Tan, Mr. D. Bartlett, LT M. Chipkovich, and LT D. Kapolka. Two of the authors, D. Gardner (1987) and CDR D. Brown (1991), and a third LCDR C. Cameron (1991), wrote their Doctoral Dissertations on fiber optic sensing related research.

Biographies

David A. Brown received his B.S.E.E. from the University of Rhode Island and his M.S. and Ph.D. degrees in Engineering Acoustics from the Naval Postgraduate School. His research areas have included fiber-optic interferometry, transducer design, and viscoelasticity. After receiving his Doctorate, Dr. Brown stayed on board to do his postdoctoral research at NPS as the principal investigator for fiber optic sensor research. He has also worked at McDonnell Douglas Astronautics Co. and at the Naval Underwater Systems Center, in Newport, RI.

David L. Gardner is a Commander in the National Oceanic and Atmospheric Administration (NOAA). CDR Gardner holds B.S. and M.S. degrees in Ocean Engineering from Florida Atlantic University, and a PhD. degree in Engineering Acoustics from the Naval Postgraduate School; he is currently assigned to the Naval Postgraduate School as an Adjunct Professor. CDR Gardner is active in fiber-optic acoustic sensor and thermoacoustic engine research.

Steven L. Garrett received his B.S., M.S., and PhD. degrees in physics from the University of California at Los Angeles with specializations in quantum fluids, condensed matter physics, and acoustics. After completing his degrees he did postdoctoral research in ultra-low temperature physics at the University of Sussex in England and the University of California, Berkeley. Since 1982 he has been at the Naval Postgraduate School where he is a Professor of Physics. His current research interests include fiber optic sensors and thermoacoustic refrigerators. He is a fellow of the Acoustical Society of America.

References

1. A. Dandridge, A.B. Tveten, and T.G. Giallorenzi, "Homodyne demodulation scheme for fiber optic sensors using phase generated carrier", IEEE J. Quantum Electron. **QE-18**, 1647 (1982).
2. K.P. Koo, A.B. Tveten, and A. Dandridge, "Passive Stabilization Scheme for Fiber Interferometry Using (3x3)Fiber Directional Couplers, Appl. Phys. Lett. **41**, 616 (1982).
3. C.B. Cameron, R.M. Keolian, and S.L. Garrett, "A Symmetric Analogue Demodulator for Optical Fiber Interferometric Sensors", *Proc.34th Midwest Symposium on Circuits and Systems* (IEEE), Monterey, CA, May 14-17, 1991.
4. C.B. Cameron, "Recovering Signals from Optical Fiber Interferometric Sensors", PhD. Dissertation, Electrical Engineering, Naval Postgraduate School, Monterey, CA, June, 1991. DTIC Report No. ADA 240-062.
5. D.A. Brown, T. Hofler, and S.L. Garrett, "High sensitivity, fiber-optic, flexural disk hydrophone with reduced acceleration response", Fiber and Integrated Optics **8**(3), 169-191 (1989); and "A fiber-optic flexural disk microphone" in *Fiber Optic and Laser Sensors IV*, Proc. Soc. Photo-Optical Instrumentation Eng. (SPIE) **985**, 172-182 (1988) and U.S. Pat. No. 4,959,539 (Sept. 25, 1990).
6. Previous claims to the highest sensitivity were made in this journal without knowledge of our work. P.C. Shang, P.J. Zoccola, S.A. Fisher, Y.F. Hwang, "Development of a Planar Fiber Optic Hydrophone for Measuring the Low Wavenumber Pressure Components of Turbulent Boundary Layers", *Naval Research Reviews*, Office of Naval Research, **1**, **XLIII**, 30-39 (1991).
7. D.A. Brown, S.L. Garrett and D.A. Danielson, "Fiber-optic ellipsoidal flextensional hydrophones", in Fiber Optic and Laser Sensors VII, Proc. Soc. Photo-optical Inst. Eng. (SPIE), **1169**, pp. 240-248, (1989) and S.L. Garrett, and D.A. Danielson, U.S. Pat. No. 4,951,271 (Aug. 21, 1990).
8. G.F. McDearmon, "Analysis of a push pull fiber optic hydrophone", J. Lightwave Tech., **5(5)**, 647-652, (1987).
9. D.A. Danielson, and S.L. Garrett, "Fiber-optic ellipsoidal flextensional hydrophones", J. Lightwave Tech. **7**(12), 1995-2002 (1989).
10. D.A. Brown, "Optical fiber interferometric acoustic sensors using ellipsoidal sell transducers", Ph.D. Dissertation, Engineering Acoustics, Naval Postgraduate School, Monterey, CA, June, 1991; and D.A. Brown, "Parallel-Wrapped Optical Fiber Interferometric Ellipsoidal Shell Acoustic Sensors", paper F1.2, *Proc. Optical Fiber Communications Conference*, Monterey, CA, Jan. 29-31, 1992.

Profiles in Science

Turgut Sarpkaya

Dr. Turgut (Sarp) Sarpkaya, a Distinguished Professor of Mechanical Engineering, joined the Naval Postgraduate School in 1967, after twelve years of teaching and research at various institutions, including MIT and the University of Manchester (England). During the past thirty-seven years, with the support of the Office of Naval Research and the National Science Foundation, he has made seminal contributions to the understanding of vortex-shedding in time-dependent flows, vortex breakdown, wave forces on offshore structures, computational methods with vortices, vortex-induced oscillations and cable strumming, and, more recently, to his pioneering work on vortex/free-surface interactions (scars and striations). His contributions to marine hydrodynamics became part of the international design codes for offshore structures. He also made major contributions to the stability of oscillating flows, dynamics of submarines, trailing vortices of submerged bodies in density-stratified medium, hydroelastic response of flexible structures, and collapse of large parachutes. His oscillating flow tunnel and the vortex-breakdown apparatus are two truly unique research facilities in the world.

A Fellow of the American Society of Mechanical Engineers (ASME) and the Royal Society of Naval Architects (RINA), author of a book, more than 150 journal articles, and editor of several books, Sarpkaya continues, with ONR, NSF and DARPA support, active research on the stability of time-dependent flows and on free-surface signatures of submerged bodies and vortices.

Sarpkaya's contributions have been recognized numerous times over the years: Collingwood Prize in 1957, Lewis F. Moody Award in 1967, Sigma Xi Research Award in 1971, Freeman Scholar Award in 1988, and the Fluids Engineering Award of ASME in 1990 "for his pacesetting leadership in research, for his tireless work in professional societies and journal reviewing and for his superb teaching."

Determining Fatigue Crack Growth In Aircraft By Monitoring Acoustic Emission

Michael R. Gorman
Department of Aeronautics and Astronautics

Introduction

A description of acoustic emission (AE) based on plate wave theory has been proposed which has the potential to affect AE practice in the near term[1,2]. While being more limited theoretically it has certain practical advantages. It is computationally simpler, can predict waveforms in finite media, and readily meshes with lamination theory for composite materials. Some of the results of this approach are described below. It will be seen that there is good potential for new practices to be based on the insights from plate wave theory. If this potential is realized, the result will be a large enhancement of the technology because of the quantitative nature of the information it provides.

A lead break (fracture of pencil lead is a commonly used source of simulated acoustic emission) on the surface of a laminated composite plate excites a relatively large flexural mode. The larger waveform seen in Figure 1 is the flexural mode and the smaller waveform at the left hand edge of the figure is the extensional mode. A lead break on the edge produces a larger extensional mode which is exhibited in Figure 2. A broadband transducer was used in the measurements above and the narrow width of the pulse should be noted. Under the same test conditions a resonant AE transducer produces the type of signal seen in Figure 3. To digitize this kind of signal not only consumes more memory but more processing time. Thus, in addition to providing more information, the broadband sensor has a practical advantage.

Theory

For in-plane disturbances in a plate, the governing equations of motion are

$$\frac{\partial^2 u}{\partial x^2} + \frac{1-\nu}{2}\frac{\partial^2 u}{\partial y^2} + \frac{1+\nu}{2}\frac{\partial^2 v}{\partial x \partial y} = \frac{(1-\nu^2)\rho}{E}\frac{\partial^2 u}{\partial t^2}$$

$$\frac{\partial^2 v}{\partial y^2} + \frac{1-\nu}{2}\frac{\partial^2 v}{\partial x^2} + \frac{1+\nu}{2}\frac{\partial^2 u}{\partial x \partial y} = \frac{(1-\nu^2)\rho}{E}\frac{\partial^2 v}{\partial t^2}$$

where u and v are the displacements in the in-plane x and y directions. E is Young's modulus, ρ is the density and υ is Poisson's ratio. If the above equations are solved for an in-

Figure 1.

Waveforms produced by a lead break on the surface of a plate. Broadband measurement.

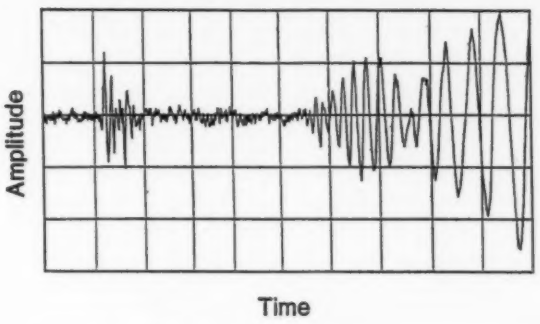

plane harmonic wave of the form $u = Ae^{i}(kx\text{-}t)$, $v = 0$, it can be shown that the velocity for this disturbance is

$$c_e = \sqrt{\frac{E}{\rho(1-\nu^2)}}$$

This is analogous to the bar velocity in a rod, and is known as the extensional plate wave velocity. The largest displacement of this mode is in-plane. Due to the Poisson effect there is an out-of-plane motion propagating at this velocity as well. In the typical AE test where the sensor is sensitive to motion perpendicular to its face, it is this motion which is measured. From the above equation it is seen that the mode propagates nondispersively.

Figure 2.

Waveform produced by a lead break on the edge of a plate. Broadband measurement.

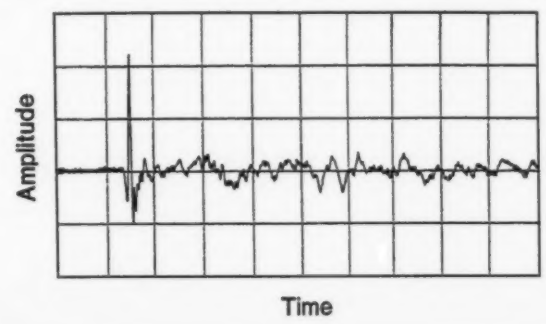

For out-of-plane disturbances the governing equation is

$$D\left(\frac{\partial^4 w}{\partial x^4} + 2\frac{\partial w^4}{\partial x^2 \partial y^2} + \frac{\partial w^4}{\partial y^4}\right) = -\rho h \frac{\partial^2 w}{\partial t^2}$$

where w is the out-of-plane displacement, h is the plate thickness and $D = Eh^3/12(1\text{-}\nu^2)$. Solving this equation for a harmonic wave disturbance, $w = Ae^{i(kx\text{-}t)}$, results in the flexural plate wave velocity

$$c_f = \left[\frac{D}{\rho h}\right]^{1/4} \omega^{1/2}$$

As can be seen, the velocity for this propagation mode is a function of frequency and therefore dispersive. Thus, the shape of the pulse changes as it propagates. As can be imagined, this can lead to problems in location analysis and waveform identification if not taken into account properly.

Figure 3.

Output of conventional resonant AE sensor for lead break on edge of plate. Pulse measured at same position as broadband transducer used for Figure 2.

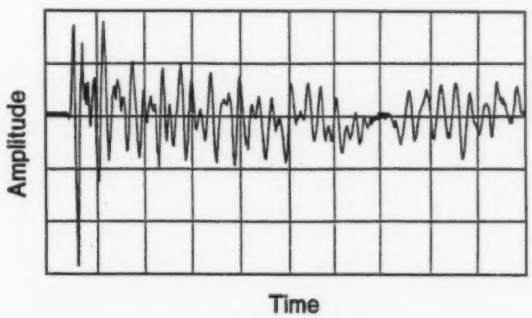

Monitoring Fatigue In Aircraft

One of the main problems in monitoring acoustic emission in aircraft has been the problem of separating crack events from noise events. A study of crack growth in 7075 aluminum was carried out in order to investigate whether the extensional mode plate wave would be the type of wave produced by fatigue crack growth. A coupon specimen was used to study a particular problem involving fatigue cracking in an E2-C[3]. The E2-C is a carrier based airplane that is used for guidance and control. It carries a large radar dome, shown schematically in Figure 4, as part of an advanced warning system (AWACS) with concomitant support electronic gear. The aircraft was found to have a crack growing in the web section of its main wing beam which is made of 7075 aluminum. The crack

Figure 4.

Schematic of E2-C Hawkeye wing center section.

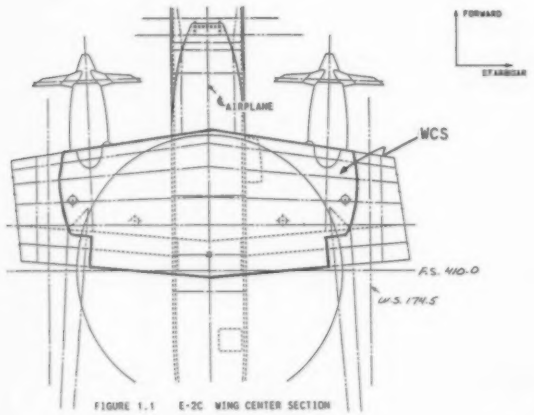

propagates between a fastener hole at wing station 49 (49 inches out from the centerline of the fuselage) and a cutout in the beam's web at that point. This section was modelled using finite elements to design a specimen which could be fatigued in a laboratory setting yet yield representative fatigue data. Grumman Aircraft Corporation kindly supplied drawings and stress data against which to check the model, and also provided the flight loading spectrum for this point in the aircraft. A schematic of the specimen is shown in Figure 5.

The specimen was inserted directly into the jaws of the grips which were attached to a mechanical test machine. The test machine (MTS) was a servohydraulic type with closed-loop feedback control. The flight loading spectrum was loaded into a personal computer which was used to program the controller. Thus the specimen underwent realistic loading and was "flown" a nominal 20,000 experimental flight hours or until cracked.

The transducers were attached with vacuum grease and tape. Due to the Mode I type crack growth between fastener hole and cutout the extensional mode was expected to be larger than the flexural mode. In order to separate the extensional and flexural modes broadband transducers were used (Harisonic, G0504) and the signals observed with a digital oscilloscope (DSO)(LeCroy, 9400A). Lead breaks were performed both inside the hole to create primarily an extensional mode pulse and on the surface right next to the hole to observe a larger flexural mode pulse. 125 Khz to 1 Mhz bandpass filters were then inserted into the preamplifiers which eliminated most of the flexural mode. This was done as suggested in[2] so that the signal going into the conventional AE analyzer(HSBIT, AET 5500B) would be dominated by a single mode. That is because this type of analyzer uses threshold triggering to start and stop the internal clocks which are used to determine the sequence in which the transducers are struck by a pulse and thus, triangulate the source. This information was useful initially in identifying the pulses emanating from the crack as opposed to grip and other noise.

A noise event, a crack event near initiation and a crack event after the crack had been growing for some time are shown in Figure 6. Their corresponding frequency spectra (uncorrected for transducer response but the transducer is almost flat in this frequency range, 100 Khz-1 Mhz) show that although the pulses look somewhat similar the noise contains lower frequencies mostly below 300 Khz while the spectra of the crack events contain frequencies above 700 Khz. By shifting the spectra of the two crack events on top of one another it will be seen that they are nearly identical except in amplitude. The velocities of these and all of the crack event waves coincided perfectly with the velocity of the extensional mode as predicted by plate wave theory. A crack easily was detectable before it reached the 0.005 inch length. Many others have studied this material and have tried monitoring aircraft (see[4] for some references). Various schemes for detecting crack growth emission were employed. Space does not permit an in-depth discussion, however the results of this work do confirm or reject and explain many previous ones. Suffice it to say that it does seem possible to separate crack events from noise based on this new understanding of the wave mechanics.

Figure 5.

7075 aluminum coupon specimen used for spectrum fatigue test showing cutout in center. Crack started at fastener hole after 20,000 experimental flight hours.

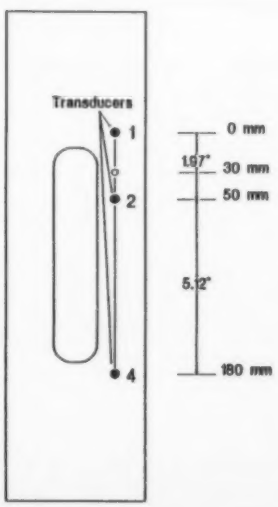

Figure 6.

Waveforms and frequency spectra for cracks and noise. Small 0 on next to top division is zero Db for the spectra.

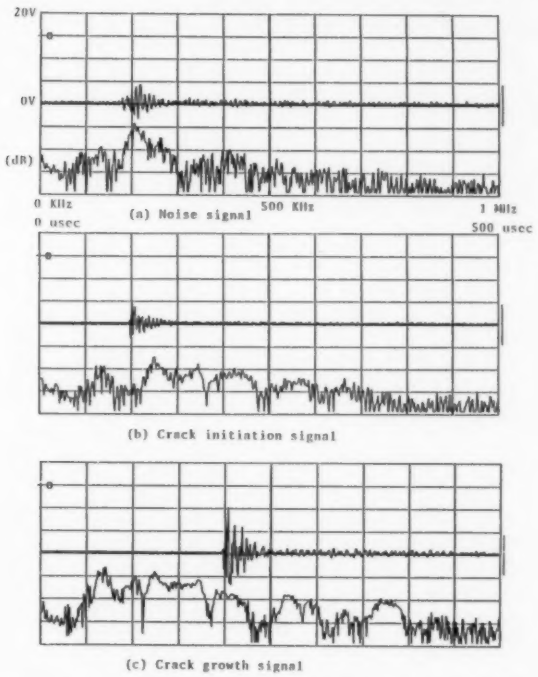

Figure V.5: DSO plots of Noise, Crack Initiation and Crack Growth

Conclusions

Plate wave theory is useful for describing acoustic emission pulse propagation when the thickness of the part under test is much less than the wavelengths contained in the pulse being measured. This condition obtains in many real structures such as aircraft components. In the E2-C Hawkeye aircraft, the main wing beam web is made of 7075 aluminum plate and crack growths smaller than 0.005" could be identified by the extensional mode detected during spectrum fatigue loading by monitoring acoustic emission. Detecting the extensional mode waveform in aircraft subassemblies should be studied next folowed by monitoring components in aircraft in flight.

Biography

Michael R. Gorman received his Ph.D. in Physics from the University of Pittsburgh, in 1981. He was a Staff Engineer at Hercules Aerospace, Magna, Utah from 1981 to 1984. While at Hercules he was the Principal Investigator of acoustic emission for the NASA Filament Wound Case Program and the Navy Trident II Rocket Motor Program. He developed the techniques still used today for monitoring these large structures including the design of a new instrument for handling high data rates. He moved to the University of Nebraska in Lincoln as an Assistant Professor of Engineering Mechanics where he worked on understanding acoustic emission and damage in composite materials under all types of loadings. He is now an Associate Professor of Aeronautical Egineering at the Naval Postgraduate School, Monterey, California. He has been working in the field of acoustic emission for ten years and has published many papers and given numerous invited talks on the subject.

References

1. M. R. Gorman, *J. Acoust. Soc. Am.* **90** (1), 358-364 (1991).
2. M. R. Gorman and S. M. Ziola, *Ultrasonics* **29**, 245-251 (1991).
3. Smith, W. D., M.S. Thesis, Naval Postgraduate School (1990).
4. S. L. McBride, W. Boyce, Perschbacher and W. Pless, *Nondestructive Testing Handbook*, R. K. Miller and P. McIntire, editors, Vol. 5, Sect. 12 (1987) ASNT, Columbus, Ohio.

Research In Ultra-Wideband Impulse Radar Target Identification

Michael A. Morgan
Department of Electrical and Computer Engineering

Abstract

A research program in impulse radar non-cooperative target recognition (NCTR) using natural resonances is reviewed. Program facets include fundamental discoveries in electromagnetics, leading-edge experimentation in impulse scattering, and advances in signal processing for recognition of the natural resonance "fingerprint" of a radar target. We first review essential physical concepts of impulse scattering which lead to the properties of natural resonances and their utility in NCTR. The unique NPS ultra-wideband impulse scattering range is then considered. Measured signatures from scale-model tactical aircraft are used for natural resonance estimation. Full-scale impulse radar implementation is discussed.

Introduction

The need for long-range identification of friend or foe in confrontational or wartime situations certainly predates written history. In modern times, with rapidly moving and highly lethal weapons this need has grown in importance to the Navy and to DoD. Current NCTR technology within the Navy spans the gamut of information acquisition and processing, from simple line-of-sight visual observations to elaborate strategic systems which couple satellite based intelligence data and over-the-horizon radar. The mandate for development of future radar capabilities in NCTR is clearly stated as two areas within the DoD Critical Technologies Plan of 1990: "sensitive radars" and "automatic target recognition."

Two main categories of radar NCTR techniques are imaging and parameter identification. Imaging radars provide a visual representation of the target geometry in either two or three dimensions using such techniques as focused spot scanning and inverse synthetic aperture. Parameter identification radars sense unique, often non-visual aspects of the target. These radars typically utilize Doppler information in the received signal to detect differential motion of portions of the target structure, including rotating blades and hull vibration. Recognition of aircraft and helicopters, as well as ground vehicles, is possible using this approach if aspect dependence of observations is considered.

Use of electromagnetic (EM) natural resonances as NCTR parameters is quite different from the conventional Doppler-based radar approach. EM natural resonances are innate properties of the target structure in a manner analogous to that of acoustical natural resonances. Natural resonances are independent in form to the excitation which causes them. Consider, for example, the plucking of a guitar string. The resultant vibration which produces the sound will be a mixture of harmonically related natural resonance vibration modes. Although the amounts of each mode in the mixture will depend upon how and where the string was excited, the individual modes, including frequency and spatial form, will be independent of this excitation. If one were to digitize and process the acoustic signal provided by the string to deduce the harmonics present, it would be easy to identify which string on the guitar had been excited, independent of where or how it had been plucked. In a like manner, EM natural resonances do not

depend upon the directions of arrival or reflection of the incident radar signal, nor upon the orientation of the target. NCTR using a very small database is possible.

The idea of EM natural resonances was formalized in 1971 by Baum's singularity expansion method,[1], and was applied to describing nuclear electromagnetic pulse effects on aircraft. In 1975, Moffatt and Mains proposed that natural resonances could serve as an aspect-independent basis for radar NCTR,[2]. Van Blaricum and Mittra,[3], as well as others, set out to estimate natural resonant modes in transient scattered fields by modeling the signature as a simple sum of exponentials, as was done in (circa 1795) Prony's method. Early attempts in this program to estimate resonances from experimental scattering data indicated that the simple signal model was in error. In 1984, Morgan derived new signal models based upon a rigorous analysis of transient EM scattering,[4].

The NPS research program in natural resonance NCTR has focused on three issues: (1) better understanding of the phenomenology; (2) enhanced experimental capabilities, and; (3) development and evaluation of signal processing strategies for reliable NCTR. These areas of the program are covered in the three sections that follow.

Physics of Impulse Radar Scattering

We will now consider the basic physics of electromagnetic scattering and introduce the concept of natural resonances using minimal mathematical development. Important ideas will be explained using physical insight, with minimal mathematics.

Consider a conducting radar target, such as an aircraft, being illuminated by an impulsive plane wave field having finite time duration, as depicted in Figure 1. The incident pulse induces currents as it travels at light velocity over the target's metal surface. These currents are influenced at each point by two factors: (1) behavior of the illuminating pulse at that spatial point, and; (2) behavior of the current at all other points on the surface at earlier times, expressed as a weighted integral. This relationship is expressed by the time-domain magnetic field integral equation,[5]. A discretized version of this equation is given by

$$\mathcal{J}(p,t) = \overline{F}(p,t) + \sum_{p'} \overline{\overline{K}}(p',p) \cdot \mathcal{J}[p', t - T(p',p)] \qquad (1)$$

where the continuous current is interpolated using values at selected spatial nodes, which we index as p. The *p-th* node surface current at time t is denoted by $\mathcal{J}(p,t)$, while $\overline{F}(p,t)$ is proportional to the incident field. The time delay, $T(p', p)$, is for straight-line travel at light velocity between nodes p' and p, and the weighting kernel,

$$\overline{\overline{K}}(p', p),$$

also depends upon this path length.

The "physical optics" portion of the induced current is formed from $\overline{F}(p,t)$ while the summation provides the "feedback" current to each node from the induced current at all other nodes. At sufficiently high frequencies, the feedback current becomes small on the illuminated side of the target, while it tends to cancel the physical optics current on the shadow side. This behavior is the basis for the high-frequency "physical optics" approximation for radar cross section where the induced current is assumed to be equal to that due to $\overline{F}(p, t)$ on the lit side and equal to zero on the shadow side.

Figure 1.

Impulse Radar Scattering

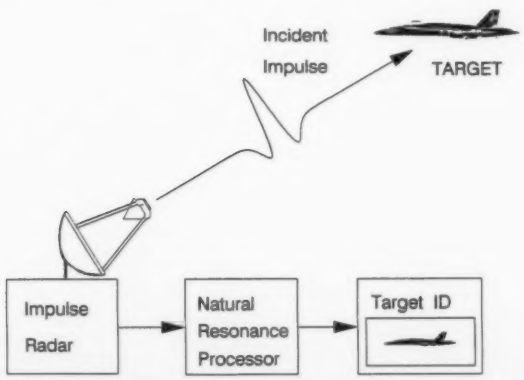

Figure 2.

Transient Electromagnetic Scattering Laboratory

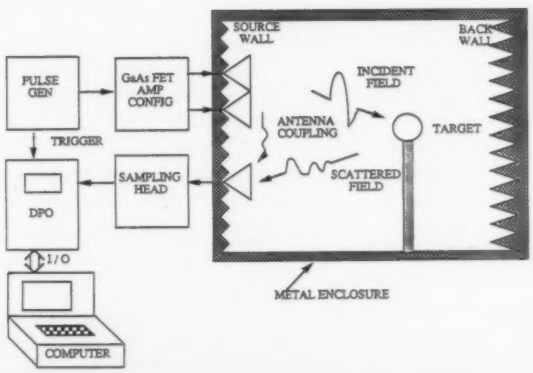

Figure 3.

Measured and Computed Scattering for Thin-Wire

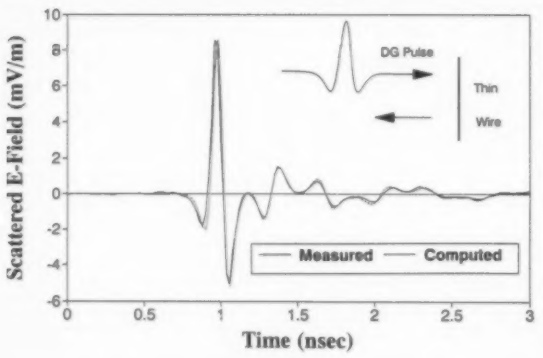

At somewhat lower frequencies, termed the resonance region, where major structural dimensions of the target are from a fraction to several wavelengths, the feedback current and the resultant natural resonance modes become quite significant. Once the incident pulse has completed its illumination, so $F = 0$ in (1), the induced current will continue to circulate back upon itself (via the summation) in the form of natural modes as it radiates its energy outward into the scattered field. The scattered field is produced as a weighted integral of this induced current, taking on the following form at the location of the radar receiver, as well as at other points in space,[4]:

$$\overline{E}^s(R,t) = E_{po}{}^s(R,t) = \sum_{n=0}^{\infty} \overline{E}_n^s(R,t)\, e^{\sigma_n t} \cos(\omega_n t + \theta_n) \qquad (2)$$

The physical optics induced current generates $\overline{E}_{po}^s$ while the natural resonance summation in (2) is due to the feedback process in the summation of (1). Complex resonant frequencies, $s_n = \sigma_n + j\,\omega_n$ formed from the damping factor and oscillating frequency of each mode in (2), are the parameters of interest in this form of NCTR. These resonances depend only upon physical structure (geometry and composition) of the radar target and are independent of the illuminating field.

Time-variation in each $\overline{E}_n^s(R,t)$ is due to the startup of the corresponding induced current mode as it reacts to the incident pulse moving across the radar target. Once the pulse completes its illumination of the target the induced current modes will have established their full spatial distribution. Resultant modal amplitudes, $\overline{E}_n^s(R)$, then become time-independent and the physical optics field vanishes. This transition time separates the "early-time" and "late-time" intervals; it depends upon the object geometry, the incident field behavior (e.g. pulse width), and the observation point,[4].

Natural resonance NCTR is most effective using frequencies within the resonant region of the target. A somewhat arbitrary criterion is that major target dimensions are in the range of, say, 0.4 to 4 wavelengths. For the case of a tactical fighter aircraft, with typical length or wingspan of 25*m*, this criterion gives a resonance region of 4.8 to 48 MHz. Such a 10:1 bandwidth is only hypothetical and may be much less in practical NCTR. Natural resonance NCTR will, in any case, require an ultra-wideband radar system which excites full structure resonances on the target, typically operating in the HF to VHF frequency bands for air targets. A discussion of real world implementation appears in the conclusions.

Impulse Radar Scattering Measurements

EM scattering measurements are usually performed using a stepped frequency coherent system. This approach can be used to estimate the impulsive response of a target using inverse Fourier transformation, with caveats that the scattering process is linear and time-invariant. However, time-domain measurements using impulsive sources can offer a faster and less expensive alternative to the stepped-frequency method. Such an approach is also essential for non-linear or non-stationary scattering cases. Impulse scattering was made possible

Figure 4.

Estimated Z-Plane Poles for a Thin-Wire at Four Aspects

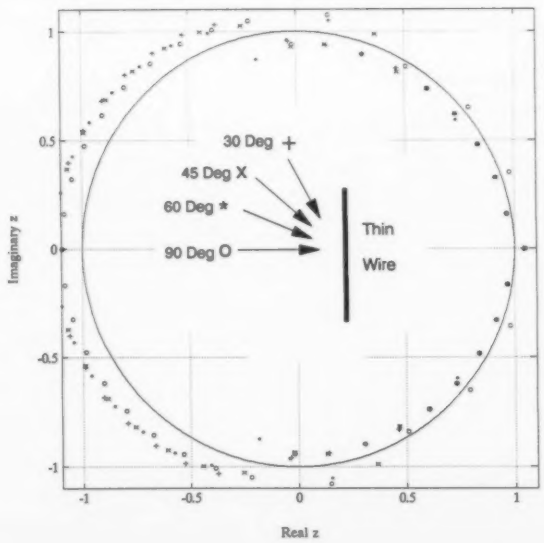

by the advent of fast pulser generators and sampling oscilloscopes in the 1960's.

The Transient Electromagnetic Scattering Laboratory (TESL) has evolved in form and function since 1980, when it employed an outside ground-plane range, measuring $12m$ square. In 1983 the TESL was rebuilt using a shielded anechoic chamber with scattering targets suspended on a virtually transparent support. This eliminated severe restrictions of the ground-plane range to mirror-symmetric targets and fixed polarization, in addition to reducing noise and interference with shielding.

Further upgrades of the TESL came in 1985, 1988 and 1990 with development of a novel form of highly stable impulse generator and addition of a new low-noise digital processing oscilloscope (DPO),[6]. The TESL currently employs ultra-wideband (exceeding 1-12 GHz) impulsive target illumination. Further enhancement of bandwidth to 50 GHz is planned for 1993.

The TESL incorporates a shielded anechoic enclosure having dimensions of $3m$ square by $6m$ long, as depicted in Figure 2. Pyramidal absorber covers the front and back walls while longitudinal wedged absorber covers other surfaces and acts to channel energy towards the back-wall, with minimal reflections. A low density styrofoam column supports targets.

The unique impulse-generator, developed at NPS, uses a fast step-generator to drive two solid-state bandpass 1 watt power amplifiers which have overlapping passbands of 1 to 6.5 GHz and 5.5 to 12 GHz. These amplifiers each feed a broadband horn antenna. Incident fields from both horns illuminate the target to provide a combined pulse with 1-12 GHz bandwidth.

Special software was developed to synthesize the target scattering for any specified incident waveform whose spectrum fits within the measurement bandwidth. This process eliminates the effects of the other frequency-dependent elements of the system (e.g. amplifiers, antennas, chamber reflection, etc.) which are embedded in the measurements. Three waveforms are measured: (1) an empty chamber; (2) the desired target, and; (3) a metal calibration sphere. These signals are digitized to 12 bit accuracy, usually with 1024 time-samples in a 20 nsec time-window. Averaging of as many as 2048 measured waveforms greatly improves the ratio of signal strength to noise. To eliminate echoes from the chamber (termed clutter) and antenna coupling signals, which appear identically in all three measurements, the empty chamber (background) measurement is subtracted from the target and calibration measurements.

Deconvolution is next, whereby transmitted signal and antenna effects are eliminated and the target response is estimated for a specified incident field waveform. This process uses the computed field scattered by the metal calibration sphere when illuminated by the desired incident waveform. A double-Gaussian has been the incident waveform of choice in this program. It is composed of two overlaid Gaussian functions of opposite polarity, with different amplitudes and effective widths, as shown in Figure 3. The widths are adjusted to control the upper and lower frequency rolloff of the spectrum. Estimation for the desired scattered waveform is made using a method developed by Riad,[7]. Results of this process for measured scattering from a $10cm$ long thin-wire are compared in Figure 3 to that computed using an accurate integral equation,[6].

Figure 5.

Estimated Z-Plane Poles for a Model Aircraft at Three Aspects

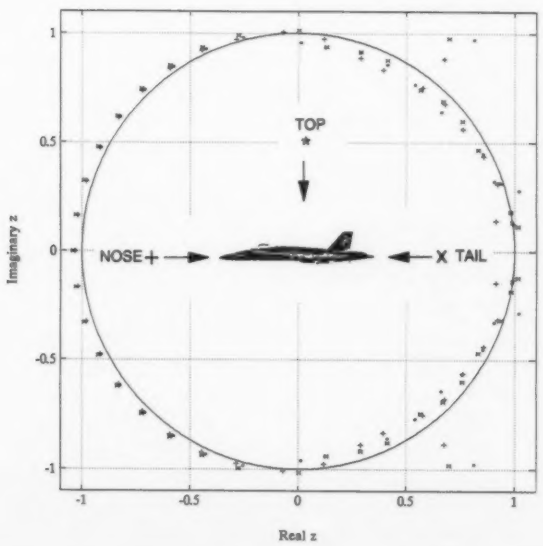

Natural Resonance Estimation

Natural resonance NCTR approaches require identification of the target's complex resonances using the measured radar signature. This can occur either through comparison with a pre-established resonance data base or through processing of the measured signature using target-specific resonance filters. A library of complex resonances is needed in both cases, to either compare signature resonances or as the basis for filter design.

The resonance filter concept includes the K-pulse method of Kennaugh[8], the E-pulse approach of Chen, et al,[9], and the resonance annihilation filter concept of Morgan[10]. Further efforts in NCTR filtering are discussed in the conclusions. Due to the brevity required in this review, we will only discuss estimation of complex natural resonances from impulse radar scattering data.

Consider sampling the transient scattered field in (2) at the location of the radar receiver at $t = m\,\Delta\,t$. The sampled signal can be written in the exponential form:

$$E^s[m] = \begin{cases} E_e^s[m] & \text{for } 0 \le m \le M \\ \sum_{N=-\infty}^{\infty} A_n (Z_n)^m & \text{for } m > M \end{cases} \quad (3)$$

where $E_e^s[m]$ is the early-time scattered field which ceases for $m > M$. This term includes both physical optics and initializing resonance series contributions. The late-time summation of resonances is turned on at $m > M$. The z-plane poles in (3) contain the s-plane natural resonances of the radar target $Z_n = e^{s_n \Delta t}$. These complex poles are to be estimated.

The sampled signal solves an auto-regressive moving-average (ARMA) difference equation,

$$E^s[m] = \sum_{k=1}^{N} b_k E^s[m-k] + \sum_{i=0}^{L} a_i E^i[m-i] \text{ for } m \ge 0 \quad (4)$$

where $E^i[m]$ is the time-sampled incident field. The second sum represents the sampled physical optics scattered field in (2) while the recursive sum corresponds to the resonance series.

Figure 6.

Estimated Z-Plane Poles for Four Model Aircraft at Nose-On Aspect

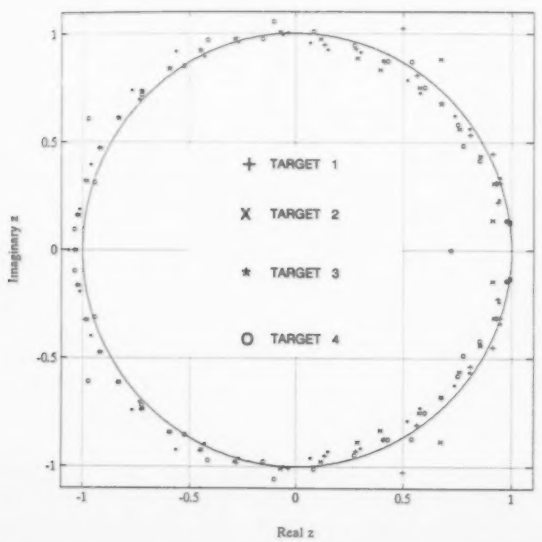

Once the incident pulse has completed its illumination of the target the radiated field will solve an auto-regressive (AR), form of (4), without the sum on $E^i[m-i]$. This late-time AR signal model is the basis for Prony's two-step method. First, the $E^s[m]$ values are used to estimate the b_k coefficients. The poles are then found as the complex roots of an ***N-th*** order polynomial in z, having the b_k as coefficients. This procedure is simple but is highly sensitive to noise or errors in the measured signal. This sensitivity results in part because the noise does not satisfy the system model in (4). Secondly, the system order, N, is generally not known. When the estimated order is greater than the actual order, poles due to noise are generated. Prony's method offers no technique for distinguishing signal poles from the extra poles caused by overestimation of the system's order. If the estimated system order is less than the actual order, actual poles are lost and the remaining poles are perturbed from their true positions.

Various new approaches to this difficult estimation problem have been developed in the last decade. That due to Kumaresan and Tufts,[11], uses a late-time AR signal model which is rearranged into a reversed-time recursive equation. The system order is overestimated to allow data fitting to the noise and an overdetermined system is formed. A pseudoinverse is found using the singular value decomposition (SVD) algorithm,[12]. The SVD algorithm allows discrimination of target and noise poles by forcing them into distinct regions of the z-plane. This approach was found to work well with moderate amounts of noise, but is inefficient because the early-time signal, where much of the energy is concentrated, is not processed.

Improvement came with the ARMA based algorithm by Cadzow and Solomon,[13], which models the input and output of the system to yield both the poles and zeros of the transfer function. Performance of the Cadzow-Solomon algorithm is generally better for the class of impulse radar scattering signatures than any other method thus far used in this research,[14]. Examples of estimated z-plane poles are shown in Figure 4 for scattering at four different incident angles on the thin-wire previously considered. Estimated target poles are inside of the unit circle, while numerous extra poles required to model the noise are also shown, but outside of the unit circle. Clustering of the target poles is due to their theoretical aspect independence. Tightness of these clusters is an indication of how well the algorithm is estimating the actual pole locations. It should be noted that only half of the target poles are found for broadside (90°) illumination because resonances having odd symmetry are not excited in this special case where there is even symmetry in both the incident field and the structure.

TESL measured scattering from four silver coated scale model aircraft is considered next. These are tactical fighters of similar size and shape. Results of pole estimation for one such target is shown for three radically different aspects in Figure 5, with clearly defined clusters being apparent. Poles esti-

mated for nose-on measurements of all four scale model targets are compared in Figure 6. The poles for each target are sufficiently different in this single measurement to identify each aircraft individually.

Conclusions

A research program in ultra-wideband impulse radar and natural resonance target identification has been reviewed. This research provides the promise for a new generation of tactical and strategic radars which support the needs of the Navy and DoD in non-cooperative target recognition. An additional realm of significant military interest is in counter-stealth, which was not addressed in this review.

Fundamental concepts were first used to explain the form of the impulse radar signature and the reason for aspect-invariance in natural resonance NCTR. A unique impulse radar facility (TESL) was then described and example measurements were shown to illustrate the outstanding measurement accuracy available. Finally, a brief overview of signal processing for natural resonance estimation was given. Estimated resonances from measured radar target signatures were shown to be relatively independent of object orientation.

Efforts are underway to extend this work. In the experimental realm, both increased bandwidth and higher impulse power are planned. The present system will be replaced in 1993 with a new digital processing oscilloscope and dual impulse sources, providing an effective pulse bandwidth of 1 to 50 GHz. This may well have the widest relative bandwidth of any real-time impulse radar in the world, and will support research in high resolution imaging, counter stealth, and enhanced natural resonance discrimination.

Advanced estimation processes for natural resonance based NCTR are being investigated. A new resonance estimation technique is being investigated which combines a modified Yule-Walker approach with iterative pre-filtering. Aspect-averaged poles are also being used to construct resonance annihilation filters, one for each target. Relative probability of correct identification is being assessed under varying noise and bandwidth conditions to predict needed system performance for reliable full-scale NCTR.

Although an impulse radar is used in the shielded NPS TESL, such an approach on a full-scale basis is wrought with the side effects of indiscriminant electromagnetic interference to communications, telemetry, signal intercept, and radars. Proponents of impulse radars argue that energy transmitted to any narrow bandwidth system will be small and cyclic, at the impulse rate used. This periodic interference may have very serious effects in some systems, particularly digital, with increases in the bit-error rate. An adaptive stepped-frequency system is the viable alternative to impulse radar in real-world applications requiring ultra-wide bandwidth. Spectrum control would allow the radar to step over any designated frequency ranges, thus avoiding interference. An ultra-wideband impulse response could be obtained, if desired, using high-speed signal processing and inverse transforms.

In conclusion, it should be noted that natural resonance based NCTR, if implemented, will most likely be to augment more conventional long-range search and tracking radars. The resonance information provided can be combined with other deduced features, such as high-resolution imaging and trajectory dynamics, to provide the final NCTR assessment.

Biography

Upon receiving the Ph.D. from U.C. Berkeley in 1976, Dr. Morgan worked as a research engineer at SRI International. He then accepted the position of Assistant Professor at the University of Mississippi in 1977. Professor Morgan has been a faculty member at the Naval Postgraduate School since 1979, with a leave of absence taken during 1985-86 to manage the basic research program in electromagnetics at the Office of Naval Research. He has been the Chairman of the Electrical and Computer Engineering Department at NPS since 1990. His research interests include computational electromagnetics, impulse radar scattering measurements and target classification, as well as the control of scattering mechanisms.

Acknowledgements

This research program in impulse radar and target identification was initiated in 1979 with support by the ONR/ONT funded NPS Research Foundation Program. In 1981, the program began five years of sponsorship from the Electronics Division of ONR. Follow-on funding during 1986-90 came from the Tactical Technology Office of DARPA. Current support comes from the U.S. Army Redstone Arsenal.

References

1. C.E. Baum, "On the singularity expansion method for the solution of electromagnetic interaction problems," Air Force Weapons Laboratory, Interaction Note 88, December 1971.
2. D.L. Moffatt and R.K. Mains, "Detection and discrimination of radar targets," *IEEE Trans. on Antennas Propagat.*, vol. AP-23, pp. 358-367, May 1975.
3. M.L. Van Blaricum and R. Mittra, "A technique for extracting the poles and residues of a system directly from its transient response," *IEEE Trans. Antennas Propagat.*, vol. AP-23, pp. 777-781, Nov. 1975.
4. M.A. Morgan, "Singularity expansion representations of fields and currents in transient scattering," *IEEE Trans. Antennas Propagat.*, vol. AP-32, pp. 466-473, May 1984.

5. R. Mittra, "Integral equations in transient scattering," in *Transient Electromagnetic Fields*, L. Felsen, Ed., New York: Springer-Verlag, 1976, pp 75-127.

6. M.A. Morgan and N.J. Walsh, "Ultra-wide-band transient electromagnetic scattering laboratory," *IEEE Trans. on Antennas Propagat.*, vol. AP-39, pp. 1230-1234, August 1991.

7. S.M. Riad, "Impulse response evaluation using frequency-domain optimal compensation deconvolution," 23rd Midwest Symposium on Circuits and Systems, August 1981, University of Toledo.

8. E.M. Kennaugh, "The K-pulse concept," *IEEE Trans. Antennas Propagat.*, vol. AP-29, pp. 327-331, Mar. 1981.

9. K.M. Chen, D.P. Nyquist, E.J. Rothwell, L.L. Webb, and B. Drachman, "Radar target discrimination by convolution of radar returns with extinction-pulses and single-mode extraction signals," *IEEE Trans. Antennas Propagat.*, vol. AP-34, pp. 896-904, July 1986.

10. M.A. Morgan, "Scatterer discrimination based upon natural resonance annihilation," *J. Electromag. Waves Appl.*, vol. 2, no. 5/6, pp. 481-502, 1988.

11 R. Kumaresan and D.W. Tufts, "Estimating the parameters of exponentially damped sinusoids, and pole-zero modeling in noise," *IEEE Trans. Acoustics, Speech, and Sig. Proc.*, vol. ASSP-30, pp. 833-840, Dec. 1982.

12. G.H. Golub and C. Reinsch, "Singular value decomposition and least squares solutions," *Numer. Math.*, 14, pp. 403-420, 1970.

13. J.A. Cadzow and O.M. Solomon, Jr., "Algebraic approach to system identification," *IEEE Trans. Acoustics, Speech and Sig.* Proc., vol. ASSP-34, pp. 462-469, June 1986.

14. M.A. Morgan and P.D. Larison, "Natural resonance extraction from ultra-wideband scattering signatures," in *Ultra-Wideband Radar: Proceedings of the First Los Alamos Symposium*, B.W. Noel, Ed., Boca Raton: CRC Press, 1992.

Liquid Immersion Cooling of Electronic Equipment

Yogendra K. Joshi
Matthew D. Kelleher
Department of Mechanical Engineering

Introduction

Starting from the 1920's when temperature distributions within laminated transformer cores were first studied[1], the thermal management of electronic equipment has assumed an ever important role. During the next twenty years, specially following World War II, significant advances in cooling technology were made for vacuum tubes used in military as well as commercial applications. The invention of the transistor resulted in a dramatic reduction in the size and power dissipation per device. However, the need for precise control of junction temperatures for reliable device operation remained a critical issue. The power dissipation per unit volume started to increase dramatically following the introduction of the integrated circuit. This trend has continued with the evolution of the LSI (Large Scale Integration), VLSI (Very Large Scale Integration) and ULSI (Ultra Large Scale Integration) technologies.

It is not uncommon today for a mainframe computer chip with a base area of 5 mm by 5 mm to dissipate 10 W of power[2]. The resulting average heat flux of 4×10^5 W/m^2 is only two orders of magnitude less than that on the surface of the sun and only an order of magnitude below that resulting from a nuclear blast 1.5 km away. While the solar surface temperature is about 6300°C and that associated with a nuclear blast well above 1000°C, modern semiconductor device junctions must be maintained typically below 85°C in order to meet acceptable reliability standards. For every 10°C rise in junction temperature there is a reduction in the mean time between failures by almost a factor of two.

The Navy Standard Hardware Acquisition and Reliability Program (SHARP) has projected future power dissipation levels of at least 200 Watts in the commonly used Standard Electronic Modules (SEMs). Currently, the SEMs are typically cooled by conducting heat to a card cage or by forced convection using air and are limited to dissipation levels of approximately 35 Watts. The large increases in power dissipation will result due to the high density packaging schemes required to meet the increased speed and performance requirements of future systems. These schemes are likely to include the use of multi chip module (MCM) and chip-on-board packaging technologies. One promising approach to meeting future power dissipation requirements is the use of single phase or phase change liquid immersion cooling, due to the inherently better heat transfer capability of such schemes over air cooling. Dielectric liquids such as the Fluorinert family[3] have been developed during recent years as chemically inert, non-toxic and environmentally safe alternatives to conventional refrigerants for electronics cooling applications.

At the Naval Postgraduate School (NPS), a number of recent studies have investigated the liquid cooling of electronic components under natural convection, i.e. in the absence of external forced circulation of the coolant. This cooling option offers increased heat transfer capability compared to air cooling (see Figure 1) and at the same time results in considerable design simplicity and high reliability. Figure 1 shows the relative cooling capabilities of three fluids during laminar natural convection along a vertical flat plate of height L dissipating a uniform surface heat flux q" in terrestrial

gravity field of intensity g. The temperature rise of the surface at its trailing edge above the ambient, $[T_S(L) - T_\infty]$, depends only on the thermophysical properties of the fluid. This dependence, displayed on the right side of the equation in Figure 1 involves the volumetric expansion coefficient, β, the thermal conductivity, k, the kinematic viscosity, ν, and the Prandtl number (ratio of kinematic viscosity to thermal diffusivity), Pr. Both Fluorinert FC-75 and water are seen to result in a much smaller temperature rise compared to air at the three reference temperatures examined.

Figure 1.

Cooling capability of three fluids during laminar natural convection along a vertical flat plate.

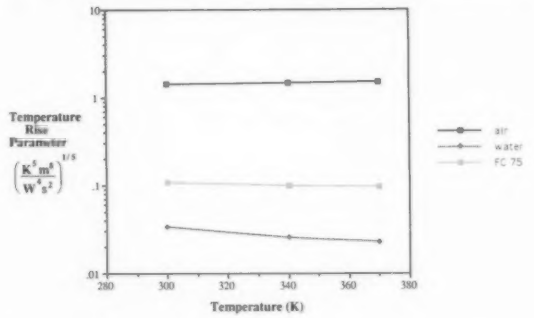

$$\text{Temperature Rise Parameter} = \left(\frac{g}{q''^4 L}\right)^{1/5} [T_s(L) - T_\infty] = \frac{1}{F(Pr)}\left[\frac{\nu^2}{\beta k^4 Pr}\right]^{1/5}$$

$$\text{where } F(Pr) = \left[\frac{Pr}{4 + 9\sqrt{Pr} + 10Pr}\right]^{1/5}$$

Studies of Natural Convection From Simulated Electronic Components

Analysis of heat transfer from miniature heat sources involves a number of fundamental issues never before addressed. The geometrical complexity associated with the heating and flow passages, possible onset of flow turbulence, participation of the substrate in the heat transfer process, all pose considerable challenges to the thermal designer. In order to understand the heat transfer and fluid flow characteristics in such systems in a systematic manner, idealized model packaging configurations that are representative of applications must be identified.

At NPS three such arrangements have been examined, as illustrated in Figure 2. Both experiments and computations have been carried out. These geometrics model the structural layouts of devices and coolant passages for many common types of electronic equipment. The device temperatures are to a large extent determined by the thermal environment in their immediate vicinity. As a result, while the geometries in Figure

Figure 2.

Geometrical configurations simulating electronic cooling applications.

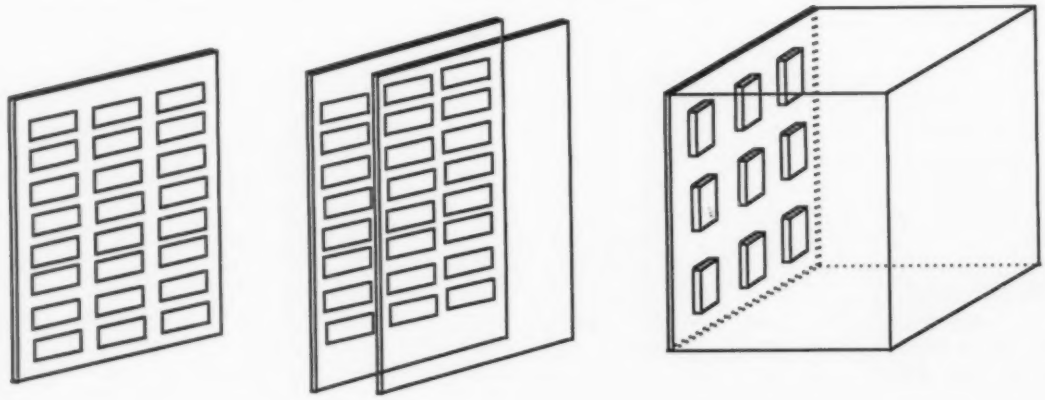

(a) ISOLATED SURFACE (b) CHANNEL (c) ENCLOSURE

2 do not model entire electronic systems in many cases, they provide valuable insight into the fundamental thermal processes at work. Some of these studies are described next.

Simulated Components on an Isolated Surface

When the substrate boards or cards on which electronic components are mounted are placed sufficiently far apart, the model geometry for heat transfer studies can be approximated as a flat plate with an array of protruding or flush heat sources, as in Figure 2(a). The liquid cooling behavior of protruding heat sources placed on a substrate has been extensively investigated in a natural convection test facility[4-6]. The test surfaces containing the heat sources are placed in a cubic tank of side 1 m made of plate glass, filled with deionized water. Water is used as the liquid cooling medium for these experiments due to the much higher cost of such a large volume of the dielectric liquids such as the Fluorinerts. The heat transfer and fluid flow information obtained from water experiments can be used for predicting the transport in fluorinerts through the use of non-dimensional parameters.

The power dissipated by each component and its resulting temperatures at selected locations provide the means for determining the non-dimensional heat transfer correlations for the configuration. Flow visualizations using a Helium Neon laser sheet facilitate the physical interpretation of this heat transfer data. Figure 3 shows the flow pattern in the vertical, spanwise centered plane resulting from an in-line column of eight stainless steel protruding heat sources placed on a vertical plexiglass substrate. The geometric dimensions of the protrusions (23.9 mm by 6.1 mm and 7.8 mm high) closely match those of 20 pin DIPS (Dual in line Packages). The protrusions are heated at their bases by 0.2 mm thick thermofoil heaters.

The flow pattern away from the protrusions in Figure 3 clearly shows the formation of a downstream growing boundary layer. However, near the test surface this flow is considerably altered as it tends to follow the protrusion contours. The boundary layer pattern suggests generally increasing average protrusion temperatures in the downstream direction due to the growing net energy convected by the flow. Also, on each protrusion the average surface temperature of the top face is expected to be the highest due to the almost stagnant region immediately above it. Only a weak influence of the downstream components on the upstream temperatures is expected. These trends are confirmed by detailed surface temperature measurements[4-6] which also allow the determination of a correlating equation for the average protrusion temperatures over a range of power levels.

A column of flush heat sources of the same size and spacing as in Figure 3 has also been examined [7]. Again a boundary layer type flow is observed, resulting in generally increasing heat source temperatures downstream. By powering only some of the heat sources in the column, the spacing between the active components was increased. It was found that for large spacings the strong buoyant flow due to the upstream components may actually provide a marginal cooling effect.

The experiments reported above provide important insights into the heat transfer from discrete heat sources during passive liquid cooling. In order to study experimentally the

Figure 3.

Flow pattern adjacent to a vertical plate containing a column of eight simulated electronic components in de-ionized water. Visualization is performed in the vertical midplane through the test surface using a laser sheet. Each of the components dissipates 0.5W. The exposure time is 20 s.

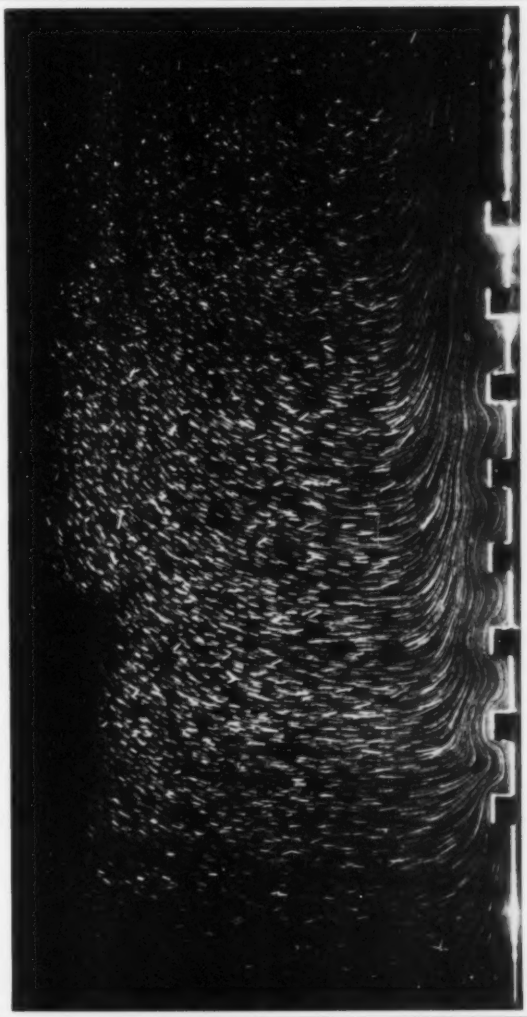

Figure 4.

Computations of natural convection liquid cooling of a simulated electronic component mounted on a substrate. The isotherms in (a) and streamlines in (b) are displayed in a non-dimensional form.

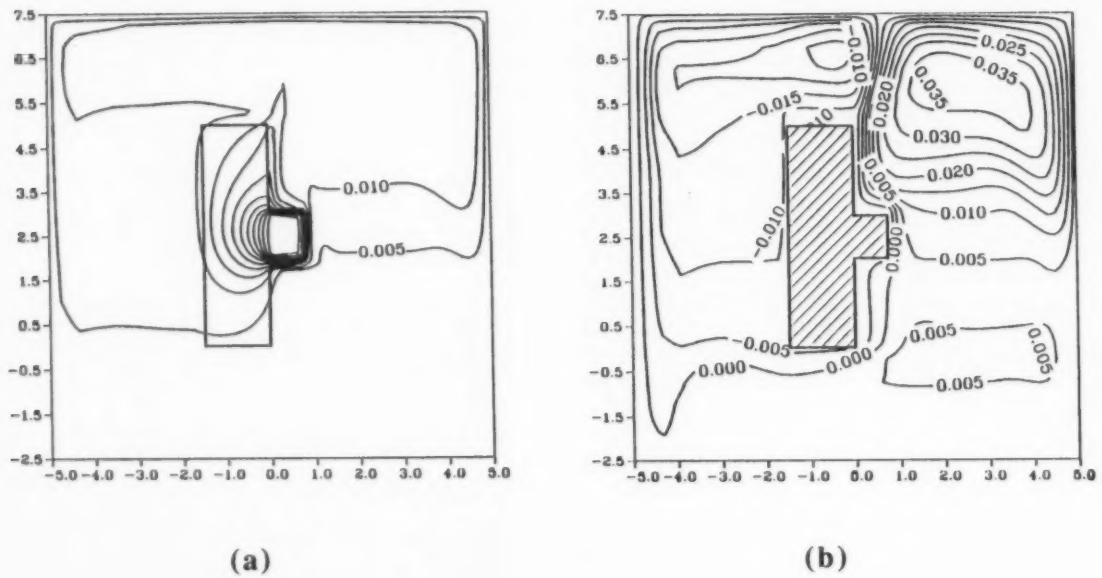

effects of various geometric parameters and material properties on these trends, a multitude of test surfaces would be required. Computational modeling provides an alternative for such studies. The validation of the computer models against experimental data is, however, essential in order to acquire a predictive capability for design.

Computational modeling requires the numerical solution of the relevant equations of fluid flow and heat transfer. These equations describe the conservation principles for mass, momentum and thermal energy. They are strongly non-linear partial differential equations, which for natural convection are interlinked, requiring a simultaneous solution. In order to have a well posed problem, appropriate conditions at the boundaries must be prescribed for the behavior of the velocity and temperature fields. Simulations so far have assumed laminar flow, due to the relative simplicity of such computations. Also, a two-dimensional analysis may sometimes be appropriate.

Sample results of the two-dimensional flow and temperature field computations for a single substrate-mounted heated protrusion in a liquid filled enclosure are seen in Figure 4[8]. These computations are for a power input of approximately 2 W, for a protrusion of the size shown in Figure 3 with water as the coolant. The temperatures are almost uniform within the protrusion due to its high thermal conductivity (100 times that of the coolant). They show a sharp drop in the adjacent liquid,

Figure 5.

Increase in the average surface temperatures of the simulated components in a three by three array for several power levels in FC-75. The increases are over the heat sink wall temperature of 19°C.

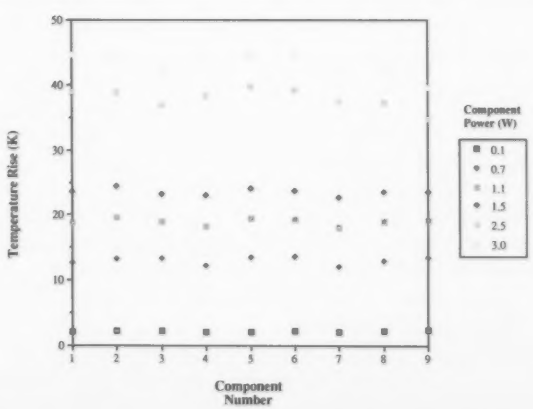

Figure 6.

Leadless chip carrier (LCC) packages. Photograph at left shows a ceramic substrate mounted 20 pin LCC similar to the one used in experiments. On the right a 64 pin LCC is shown without its lid. The heat generating chip is seen at the package center.

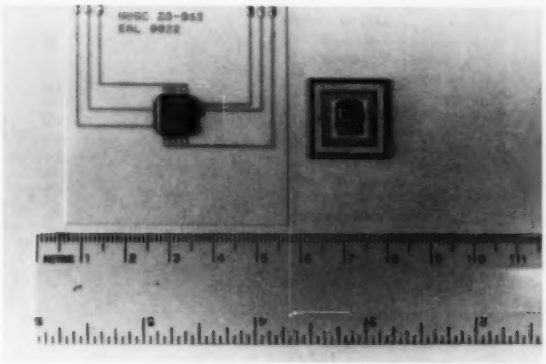

evidenced by the extreme crowding of the isotherms in Figure 4(a). Heat is also transferred into the substrate whose thermal conductivity is assumed the same as that of the liquid (a value characteristic of epoxy-fiberglass with water as coolant). The flow patterns in Figure 4(b) show the formation of two large cells within the enclosure-a faster moving clockwise cell on the right and a slower counterclockwise one on the left. Calculations of this type are useful in studying the temperature response of the bottom protrusion in the column shown in Figure 3, since for this configuration the upper heaters have almost no upstream influence[6].

Simulated Components in a Vertical Channel

When several circuit boards are stacked parallel to each other, the cooling configuration of interest is a channel with arrays of heat sources, as seen in Figure 2(b). The resulting transport has been experimentally studied in de-ionized water for a single column of protruding[5] and flush[7] heaters. The channel was formed with the placement of a parallel unheated shroud adjacent to a test surface as in Figure 3. It was found that for coolants with Prandtl number significantly above one, as for water, the shroud had almost no effect on the heated component temperatures until it was placed within 2-3 mm of the heater surface. It is well known that for liquids with Prandtl number above one, the thermal gradients are confined well within the region of fluid motion. As a result, while the flow patterns showed significant changes in the presence of shroud, the thermal boundary layer was largely unaffected. For very small channel spacings the large reduction in the fluid velocities caused a significant rise in component temperatures. These experiments suggest that the channel spacings in passive liquid immersion cooled designs can be reduced substantially without paying a penalty in heat transfer.

Simulated Components in Enclosures

In many electronic packaging applications such as high dissipation power supplies, the electronic components may be arranged within hermetically sealed enclosures. The heat is removed from the components by the dielectric liquid and is transferred to the enclosure boundaries. The eventual heat rejection from the enclosure boundary may be with the use of finned heat sinks or cold plates.

Studies have been undertaken[9,10] to investigate the natural convection heat transfer from an array of heated protrusions mounted on one wall of a dielectric liquid filled rectangular enclosure, as in Figure 2(c). The protrusions in these studies are of the same size as in Figure 3. Three dielectric liquids of the fluorinert family have been used in order to cover a range of Prandtl numbers from 25 to 1400. A number of different enclosure widths (spacing between the substrate and the vertical enclosure wall facing it) have been studied. Effects of the orientation of the protrusions on the heat transfer and the location of the heat removal enclosure surface(s) have also been examined. Representative average component temperature increases in FC 75 are seen in Figure 5. The top and bottom walls of the 203 mm by 152 mm high and 13 mm wide enclosure were maintained uniformly at 19°C by water cooled heat exchanger plates. All other enclosure boundaries were insulated. The configuration used in these studies is currently being modeled computationally[11].

Cooling of Actual Electronic Packages in Enclosures

The studies described above have used simulated electronic components in order to simplify the heat transfer and flow features to some extent. The pinouts for electrical connections in actual packages can result in additional geometrical complexity. Also, a typical package consists of different materials: the heat generating chip is typically silicon; the substrate is a ceramic or plastic; and regions of the package often have ceramic or plastic encapsulation and metal platings. In order to see if the natural convection liquid immersion transport from an actual electronic package could be accurately modeled, a series of experiments[12] and computations[13] were performed.

The electronic packages were provided by the Naval Surface Warfare Center (NSWC), Crane Division, Indiana. These were leadless chip carriers (LCCs) mounted on 5.08 cm square and 0.71 mm thick ceramic substrates (see Figure 6). The test chip at the center of these packages contained a bank

of resistors for power dissipation and a diode type temperature sensor for the measurement of junction temperature. Two different cooling configurations were studied in[12] using three liquids of the fluorinert family. In the first set, the substrate containing the package was the horizontal bottom boundary of a cubical enclosure, while the upper horizontal surface of the enclosure was the uniform temperature heat sink.

The entire enclosure was rotated 90° clockwise in the second series. Measurements revealed a maximum chip power dissipation of about 1.8 W in FC 75 for an allowable junction temperature of 80°C for both orientations. The heat sink was maintained at 15°C in these experiments. A three-dimensional computational code developed at NPS was used to simulate the second set of experiments[13]. Resulting contours of the non-dimensional temperature along the substrate are seen in Figure 7 for a chip power input of 1.84 W. They show the prominent role of the ceramic substrate in the heat removal from the package. Almost 80% of the generated power was found to be conducted into the substrate, prior to being lost by convection to the surrounding liquid. The non-symmetric thermal spreading around the package is caused by the warm plume shed above the package.

Liquid Immersion Cooling by Boiling

Boiling offers the potential for significant increase in the heat transfer capability in liquid immersion cooling. These increases are due to several effects among which the most significant are latent heat due to the phase change and induced convection due to the motion of the vapor bubbles generated by the boiling. From a heat transfer standpoint the most efficient boiling process is in the nucleate boiling regime. This occurs when the temperature and heat flux at the boiling surface are high enough to generate bubbles of vapor of the fluid and for these bubbles to grow to sufficient size that buoyancy forces will cause them to leave the boiling surface and rise through the fluid. This bubble nucleation and generation process involves a complex interaction of the surface tension and other thermophysical properties of the fluid and the surface finish and surface chemistry of the boiling surface. Bubbles usually are generated at so called nucleation sites on the surface which are naturally occurring surface pits of very small size in the boiling surface. The generation of vapor bubble requires that the surface temperature exceed the equilibrium saturation temperature of the liquid by some amount called the nucleation superheat. This excess temperature is required to generate pressures in the bubble which exceed the equilibrium saturation pressure by an amount sufficient enough to overcome the membrane pressure associated with the surface tension film at the liquid vapor interface of the bubble. The amount of this pressure difference across the liquid vapor interface is strongly dependent on the surface tension properties of the liquid. FC-72, one of the Fluorinerts, has a normal saturation temperature of 56°C, and is therefore a seemingly attractive candidate for use as a boiling heat transfer medium in electronic cooling applications. Unfortunately FC-72, as with the Fluorinerts in general, has a very low surface tension and a correspondingly small wetting angle. The consequence of the surface tension characteristics is that a nucleation superheat in excess of 30°C may be required to initiate the bubble generation process. This means that at the beginning of the boiling process the temperature of the electronic device upon which the boiling is taking place may exceed 90°C! This is an unacceptably high temperature.

At NPS experiments are being conducted[14] to investigate the possible use of auxiliary heaters to help initiate the nucleation process and thereby eliminate the temperature overshoot which characterizes the start up of nucleate boiling. The typical boiling scenario is illustrated in the right hand curve of Figure 8. The data in this figure was generated by using a thin, horizontal, platinum wire (wire 2) as a heating surface. In this experiment an electric current is passed through the wire and the power generation causes the wire temperature to rise. By measuring the resistance of the wire its temperature may be determined and the corresponding heat transfer rate may be determined by measuring the electric power dissipated. The figure shows the heat flux plotted against the temperature

Figure 7.

Non-dimensional temperature contours along the substrate during the natural convection liquid cooling of a 20 pin LCC in FC-75.

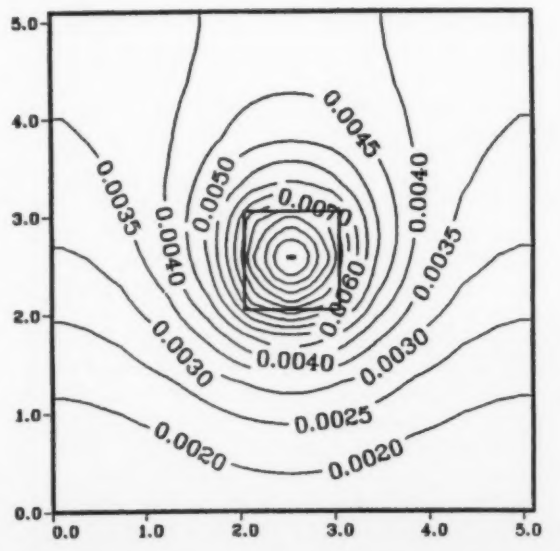

excess above saturation for increasing wire currents. As the right hand curve indicates, the temperature of the wire increases to about 38°C above saturation (this is a wire temperature of 94°C) when the wire heat flux is about 66,000 W/m^2. At this point nucleate boiling has not yet begun and the wire is being cooled by natural convection. An increase in the heat flux to 75,000 W/m^2 causes the superheat to drop to 14°C! This is an indication that nucleate boiling has been initiated and a much more efficient heat transfer process is taking place. As the heat flux to the wire is further increased, the wire temperature continues to increase until the eventual occurrence of film boiling.

The left hand curve in Figure 8, illustrates the results of the use of an auxiliary heater. In this case an auxiliary wire (number 1) has been placed a small distance below the original wire (number 2). The auxiliary wire is heated until vigorous boiling takes place on it and a constant stream of bubbles is rising from it and impinging on the original wire. When the original wire is again heated in the same manner as before, the heat flux-superheat variation appears as in the left hand curve of Figure 8. Here the superheat overshoot has been completely eliminated. The bubbles being released from the lower auxiliary wire serve to initiate the nucleation process on the upper wire without the necessity of excessively high temperatures.

This use of an auxiliary heater to generate bubbles which can trigger the formation and release of bubbles on adjacent heat transfer surfaces placed in the bubble stream holds great promise as a means to efficiently implement boiling heat transfer as an electronics cooling scheme without the danger of component burnout due to excess nucleation superheat temperatures.

Figure 8.

Right hand curve is boiling data for Wire #2 showing the temperature overshoot at the onset of nucleate boiling. Left hand curve is boiling data for Wire #2 in the wake of bubbles from Wire #1 showing the elimination of the temperature overshoot.

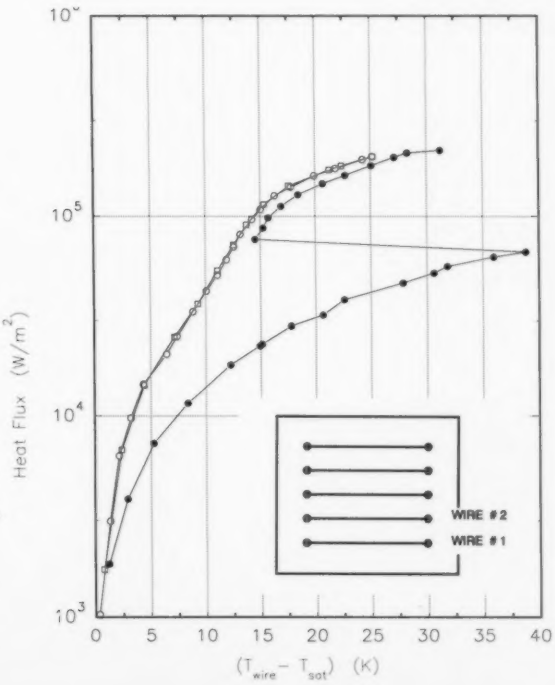

Conclusions

In this article the Naval Postgraduate School research on passive liquid immersion cooling of electronic equipment is described. This activity is motivated by the large projected increases in the power dissipation levels in the currently used Standard Electronic Modules in the Navy. A number of experimental and computational studies of natural convection liquid cooling are discussed for three configurations of interest in applications. The computations have been found to be in reasonable agreement with experiments when the heat transfer within the electronic packages and the substrate is appropriately accounted for. These comparisons provide confidence in the use of the computational code in the design of liquid cooled electronic packages. Recent studies on cooling by boiling are also discussed. The use of auxiliary heaters to initiate the boiling process at reduced superheats is demonstrated for the achievement of very high heat removal capabilities.

Acknowledgements

The authors gratefully acknowledge the collaboration with the Naval Surface Warfare Center (NSWC), Crane Division and their support of our research over the past four years through the SHARP program.

Biographies

Dr. Yogendra K. Joshi is Associate Professor in the Department of Mechanical Engineering at the Naval Postgraduate School. His research activities are in the area of convective heat transfer and its applications to technology and the environment. He teaches courses in heat transfer, fluid mechanics and measurements.

Dr. Matthew D. Kelleher is Professor and Chairman of the Department of Mechanical Engineering at the Naval Postgraduate School. His research interests are in the areas of convective and radiative heat transfer and the applications to

electronics cooling and the modeling of fire propagation. He teaches heat transfer, fluid mechanics and thermodynamics.

References:

1. Kraus, A.D. and Bar-Cohen, A., "Thermal Analysis and Control of Electronic Equipment," Hemisphere Publishing Corporation, Inc., Washington, D.C., 1983, pp.3.
2. Antonetti, V.W., Oktay, S. and Simons, R.E., "Heat Transfer in Electronic Packages," *Microelectronics Packaging Handbook*, Tummala, R.R. and Rymaszewski, E.J. (Eds.), Van Nostrand Reinhold, New York, 1989, pp. 167.
3. Fluorinert Liquids, Product Manual, 3M Corporation, Minneapolis, MN, 1985.
4. Joshi, Y., Willson, T. and Hazard, S.J., "An Experimental Study of Natural Convection From an Array of Heated Protrusions on a Vertical Surface in Water," *Journal of Electronic Packaging*, Transactions of ASME, Vol. 111, pp. 121-128, 1989.
5. Joshi, Y., Willson, T. and Hazard S.J., "An Experimental Study of Natural Convection Cooling of an Array of Heated Protrusions in a Vertical Channel in Water," *Journal of Electronic Packaging*, Transactions of ASME, Vol. 111, pp. 33-40, 1989.
6. Willson, T., "A Study of Natural Convection Cooling of Multiple Discrete Heat Sources in a Vertical Channel," M.S. Thesis, Naval Postgraduate School, Monterey, CA, 1988.
7. Joshi, Y. and Knight, D.L., "Natural Convection From A Column of Flush Heat Sources in a Vertical Channel in Water," *Journal of Electronic Packaging*, Transactions of ASME, Vol. 112, pp. 367-374, 1990.
8. Sathe, S.B. and Joshi, Y., "Natural Convection From A Heat Generating Substrate-Mounted Protrusion in a Liquid Filled Two-Dimensional Enclosure," *International Journal of Heat and Mass Transfer*, Vol. 34, pp. 2149-2163, 1991.
9. Joshi, Y., Kelleher, M.D. and Benedict, T.J., "Natural Convection Immersion Cooling of an Array of Simulated Chips in an Enclosure Filled with Dielectric Fluid," *Heat Transfer in Electronic and Microelectronic Equipment*, A.E. Bergles, Ed., pp. 445-468, 1990.
10. Joshi, Y., Kelleher, M.D., Powell, M. and Torres, E.I., "Natural Convection Heat Transfer From an Array of Rectangular Protrusions in an Enclosure Filled With Dielectric Liquid". Presented at the ASME Winter Annual Meeting, Atlanta, December 1991. Also published in *Heat Transfer Enhancement in Electronics Cooling*, HTD Vol. 183, pp. 9-18, 1991.
11. Mukutmoni, D., Kelleher, M.D. and Joshi, Y., "Computations of Liquid Immersion Cooling for a Three by Three Array of Chips in a Rectangular Enclosure". Presented at the National Electronics Packaging Conference, Anaheim, CA, February 1992.
12. Joshi, Y. and Paje, R.A., "Natural Convection Cooling of a Ceramic Substrate Mounted Leadless Chip Carrier in Dielectric Liquids," *International Communications in Heat and Mass Transfer*, Vol. 18, pp. 39-47, 1991.
13. Wroblewski, D. and Joshi, Y., "Transient Natural Convection From a Leadless Chip Carrier in a Liquid Filled Enclosure: A Numerical Study". Presented at the ASME/JSME Joint Electronics Packaging Conference, Milpitas, CA, April 1992.
14. R.A. Egger, "Enhancement of Boiling Heat Transfer in Dielectric Liquids," M.S. Thesis, Naval Postgraduate School, Monterey, CA, Sept. 1991.

Research on Autonomous Underwater Vehicles at the Naval Postgraduate School

A.J. Healey, R.B. McGhee, R. Cristi, F.A. Papoulias, S.H. Kwak, Y. Kanayama, Y. Lee, S. Shukla, A. Zaky,
Department of Mechanical Engineering

Abstract

This article describes the past accomplishments, presents status, and future areas of concern for research at NPS in mission planning, mission execution, and post mission data analysis to meet the needs of future Naval Autonomous Underwater Vehicles. These vehicles are unmanned, untethered, free swimming, robotic submarines to be used for Naval missions including search, mapping, surveillance, and intervention activity. This project is joint between the Mechanical Engineering, Computer Science and Electrical and Computer Engineering Departments at the Naval Postgraduate School and is focused on a long range program to develop **control technology** for these vehicles. The approach taken combines computer simulation, real time robust control theory, computer architecture and code development, vehicle and component design, sonar data analysis and data visualization.

Started in 1987, the major thrusts are in the areas of **mission planning**, both off-line and on-line, **mission execution** including navigation, collision avoidance, replanning, object recognition, vehicle dynamic response and motion control, real time control software architecture and implementation, and the issues of **post mission data analysis.**

Introduction

This article focuses on systems having to do with the Navy's use of Autonomous Underwater Vehicles (AUVs). AUVs are a class of underwater vehicles that are independent from mother ship support with respect to power and control. AUVs are – **untethered-free swimmers** – with sufficient on-board intelligence to perceive uncharted and unplanned situations and take action in response. We are interested in these vehicles for a variety of military and/or commercial missions where direct human intervention is difficult or dangerous, and where the use of power cables and fibre optic data links are cumbersome. These vehicles will be used to gather data, provide surveillance, and possibly perform tasks in hostile areas. Research at NPS is focused on the issues of advanced controls for mission execution, and the post mission analysis.

Interest in intelligent **untethered underwater vehicles** has been growing recently. University groups include Texas A&M University, (Mayer et. al., 1987) who have developed a knowledge based real time controller, hosted on SUN 4 computers with particular attention paid to hardware and software reliability; University of New Hampshire, who under the

guidance of D. Blidberg (Chappell, (1987)), have built and operated EAVE East vehicles since 1977 with ever increasingly complex computer architectures. EAVE III has a modular, hierarchical architecture using Motorola 68000 series computers running separate PSOS operating systems allowing for multi-processing operation. Lower level tasks are run in "C" while upper level tasks have been run in LISP, with the NIST RCS-3 real time control system (Albus, 1988). At MIT the Sea Grant Program has funded work conducted by Bellingham (1990a), who is exploring the demonstration of intelligent behaviors with a vehicle running on a GESPAC computer having a 68020 CPU with the OS-9 operating system and control code written in "C". Their behaviors are hierarchically prioritized using the "Layered Control" concept (Brooks, 1988), although more recently, (Bellingham, 1990b) has seen fit to introduce a state based layered control to coordinate mission specific behavior. The University of Tokyo has recently developed an underwater vehicle for bottom contour following using neural network techniques, (Ura, 1990). At the Naval Postgraduate School, we have developed an underwater testbed vehicle that is specifically designed to test and verify developments in control technology. It is run in the NPS swimming pool as an environment for experimental mission demonstration using a GESPAC computer with a Motorola 68030 CPU a 2MByte RAM card with control code written in "C". The mission planning interface with the vehicle control computer is embodied in a GRiDCASE laptop MS-DOS machine containing mission details in the form of way points and run times that are obtained from an external pre-mission planning analysis. The NPS AUV II, shown as a sketch in Figure 1, is 84" long displacing about 380 lbs. having 2 propellers, 8 control surfaces, 4 thrusters and, at present, 4 single beam sonar channels (Healey and Good, 1992). Many

Figure 1.

Sketch of the NPS AUV II

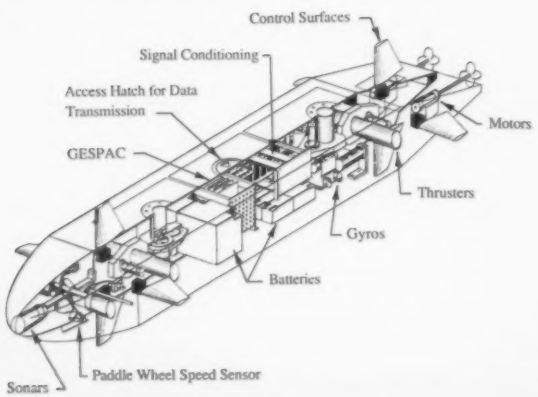

Figure 2.

Mission Planning Expert System

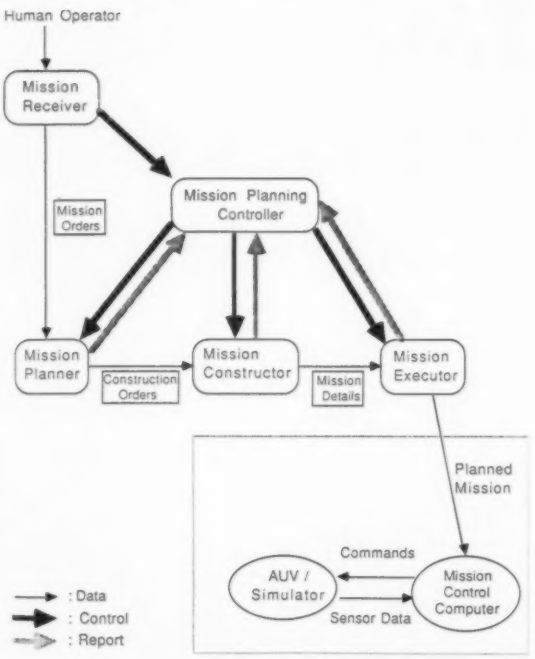

industry groups as well as Navy Laboratories, DARPA and the DRAPER Laboratory have work ongoing in this area.

While no formal control system structure has been adopted by all – in fact there are as many as there are investigators – our opinion is that a structure will be necessary that includes the ability to first perform extensive (if time permits) simulations to verify that the predictable aspects of any mission will be executed in a feasible way. This would be regardless of the mission details. In our structure, this is done with the **Mission Planning Expert System** as shown conceptually in Figure 2. The output is a planned series of geographic way points that avoid charted problem areas and lead the vehicle to its operational site(s) with task descriptors at each target point. This plan encompasses launch, transit to the area, operating in the area, returning to home and recovery.

The **Mission Execution** phase is shown by the structure of activity in Figure 3. **Mission Execution** after launch is conducted between the **Mission Executor** and the **Guidance System** by breaking down the planned mission into a sequence of intermediate way points defined on a finer grid possibly having an adjustable spacing. In more critical areas the spacing would be suitably refined. The **Guidance System** thus interpolates the baseline grid to provide a refined series of way

Figure 3.

Mission Execution System Diagram

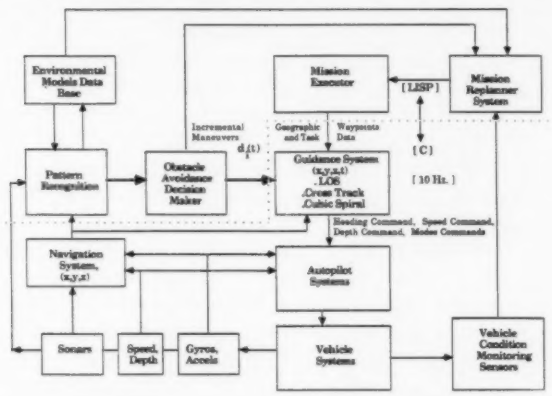

Figure 4.

Line of Sight and PD Steering Autopilot: Experimental Results

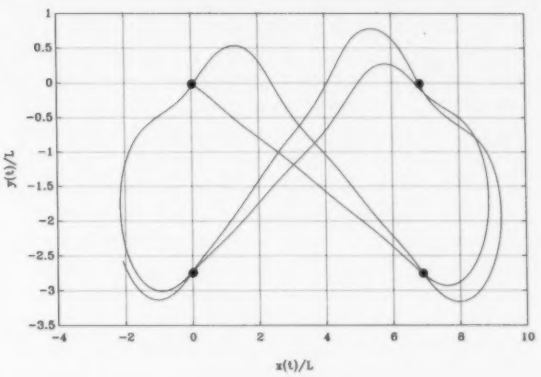

points which are passed to the vehicle **guidance law** and selected according to the degree of precision in path tracking desired by the mission plan. The **guidance law** generates the commands for vehicle's heading, speed, and depth. These commands are then sent to the vehicle **autopilot systems**. Three autopilots are installed for control over the vehicle's speed, heading, and depth. The servo levels of the vehicle's controller then provide final commands to the vehicle's propulsion plant, control surfaces, and thrusters to drive the vehicle to its planned path.

Obstacle avoidance and reflexive maneuvering logic are to be built into the vehicle's guidance system as a command override structure to respond to signals from the **Obstacle Avoidance Decision Maker (OADM).** The **OADM** receives input from **Pattern Recognition** software which correlates information from the sonars and estimates of present location and attitude from the **Navigation System** with an **Environmental Data Base** within the **Mission Executor**. The impending presence of an obstacle is thus flagged. At that time, status as to whether the object is stationary or moving, is to be reflexively avoided, or gradually outmaneuvered (either slow down, speed up, change course, which direction, etc.) is computed. Incremental modifications, $d_i(t)$, to the planned way points and time are then made. Note that for all $d_i(t)$ moves, $d_i(t)$ will be said to tend to zero as t tends to infinity so that the originally planned path will be finally joined. Status signals are sent to the Mission Replanner from internal sensors concerning the condition of the internal equipment such as motor and battery status, motor controller system status, servo power and signal conditioning equipment, and power and internal temperature of the main CPU/Data Acquisition/Data Storage hardware.

Post mission data analysis is accomplished by down loading data that is stored in onboard RAM storage and displaying it on the data post processing computer. The post processor at this time resides in an IRIS graphics workstation containing graphics modules that replicate the environment in which the vehicle is operating together with models for analysis of the vehicle motion data and the sonar sensory data obtained from the mission run (Brutzman et. al., 1992). The results of the planned mission are both simulated prior to mission approval using an IRIS workstation as the environment and vehicle simulator, and then displayed at mission completion. Details of the sonar imagery, or the bottom contour, or other mission specific results would be output in a user-friendly format.

Mission Planning Expert System

The details of our Mission Planning Expert System were given recently by Kwak (1990) and in more detail in Ong, (1990). Basically the system shown in Figure 2 is hosted on a stand alone Symbolics 3675 Lisp Machine. Conceptually it resides off-line from the vehicle where only the results of the planning process (in terms of geographic way points and task level instructions) are to be downloaded to the vehicle's on-board computer. The Mission Planner has been developed entirely within the KEE expert system shell with a corresponding knowledge base detailed by Ong. The mission planner is essentially hierarchical, patterned after the progressive phases of a mission, namely, the initiation by the human operator, the planning, construction, and the mission execution. In this software architecture, the planning operation is supervised by a mission planning controller which is a system devised to oversee the entire process and enforce orderly transition to each phase. There are four role players, the Mission Receiver, the Mission Planner, the Mission Constructor, and the Mission Executor. The Receiver is the human interface and is

embodied in the workstation screens with which the user defines the nature of the mission to be planned. Details such as mission type, location parameters, and planning horizon are entered. The information received is then given to the mission planning controller which initiates all subsequent actions. The mission planner decides on the basis of the data given and its internal knowledge base, which planning algorithm to use. A system of **voters, knowledge processors** and **decision makers** operating on three different rule sets interact with the planner until an acceptable choice is made. The mission constructor then solves the path planning problem with the selected constraints and algorithm. Part of the problem is to select a grid of coordinates on which the plan is based. It should also be noted that the knowledge base will in fact be extensive and contain all necessary known features concerning the mission arena. Maps, bottom contours, current data, charted objects such as subsea wells and offshore platforms, and harbor profiles if needed, must all be represented. Three algorithms are presently active; A*, best first, and a heuristic search. The mission constructor then sends the plan to the mission executor which acts as the interface between the planning system and the vehicle on-board system. The plan is embodied in a sequence of way points with target points and work task parameters identified.

Mission Execution Systems and Results for the NPS AUV

The execution of the mission begins with downloading the mission plan to the on-board **Mission Executor** followed by the vehicle launch. A time delay must be built into the executor to allow for the launching delay. It has been found important that during this launch phase, and especially with a fully autonomous vehicle, some indicator that the internal systems are functional is desirable-we have used a small movement of one of the control surfaces as this indicator. Upon program initiation, the mission execution plans (defined in terms of a series of way points with instructions at target points), are contained in an MS-DOS GRiDCASE laptop computer which is connected via serial link to the vehicle onboard GESPAC MPU30HF single board computer (based on the Motorola 68030 CPU, at 25 Mhz. with 2 Mb of RAM and a 68882 math coprocessor) running with the OS-9 multitasking operating system and 2 GESDAC-2B 8 channel 12 bit DA/AD converter cards. Control code is written in "C" language. The GESPAC system is the interface between the mission planning phase and the vehicle hardware, and it houses the **Guidance System**, the **Navigation System**, and the speed, diving, and steering **Autopilot Systems**, each of which operates under robust Sliding Mode Control. Figure 3 shows a diagram of the execution functions. Details of the theory and design of Sliding Mode Controllers are available in Healey, Papoulias, and Lienard, (1990) and Papoulias and Healey, (1990) and in Healey and Marco, (1992). The major interfacing in the execution phase is between the **Mission Executor** and the **Guidance System** and some interplay with the **OADM**. These systems, (in their future embodiment) are to be hosted in Prolog or C++ language on an Intel 80386 processor based single board computer running MS-DOS within the GESPAC card cage while the **Guidance System** runs in "C" on the current 68030 processor board.

Guidance, Control, and Navigation

The fundamental breakdown of the motion control functions between guidance and autopilot relies on the notion that

Figure 5.

Experimental Results for Speed, Steering, and Depth Control Autopilots

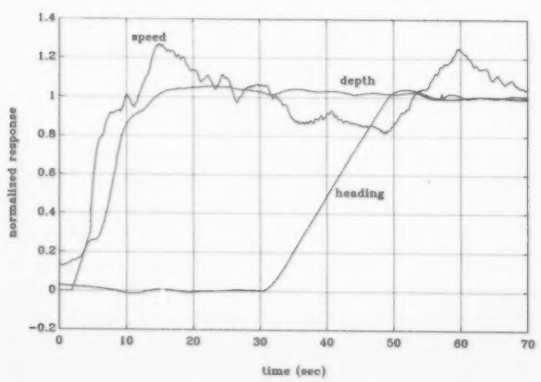

Figure 6.

Obstacle Avoidance Sonar Range and Vehicle Steering Response

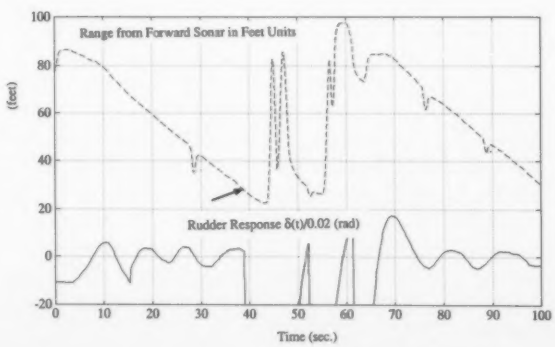

an autopilot is responsible for stabilizing the motion dynamics of the vehicle in terms of its speed, heading, and depth. The guidance law combines commands for the path and position to be followed and other attitude requirements with navigational estimates of true position and orientation, to generate the speed, heading, and depth commands for the autopilot. In this manner, **Guidance** is responsible for dealing with **geometrically and/or kinematically** based relationships, while the **Autopilot** is responsible for control of the vehicle **dynamics**. Such a distinction between guidance and control offers the advantage of analyzing the behavior of different schemes and allows for great flexibility in the design and final selection. An example of a line of sight guidance law with a proportional-derivative heading autopilot is shown in Figure 4, from experimental results in the NPS swimming pool. The commanded path, a figure eight maneuver, was discretized into 4 way points and it can be seen that the results are repeatable after two loops. More way points, provided they are appropriately selected, would result in improved accuracy and a smoother path. Questions pertaining to dynamic interactions between guidance and autopilot laws for accurate path keeping are very important for AUV's for the following reason: due to the fact that an AUV suffers from significant dynamical lags, satisfactory response characteristics of a combined guidance and control law are not guaranteed unless proper care is given in their design. Analysis of this problem revealed regions of stability loss and the emergence of self sustained oscillatory modes. Experimental validation of the theoretical results is scheduled.

Stabilization of the vehicle dynamics was achieved by the independent design of three Sliding Mode autopilots for propulsion, diving, and steering. The added robustness that Sliding Mode Control laws provide was proven sufficient to stabilize the vehicle when operated in full coupled fashion under all six degrees of freedom. An experimental verification is presented in Figure 5, where the response of the vehicle is evaluated under simultaneous speed, heading, and depth change commands. The guidance law in this case was selected to simulate a basic obstacle avoidance maneuver; heading change commands were issued based on the distance from the front wall of the swimming pool as recorded from sonars.

As a result of the vehicle's enhanced maneuverability, in particular the existence of independently controlled bow and stern rudders and dive planes as well as plans for four vertical and horizontal thrusters, considerable effort has been devoted to issues surrounding precise motion control in transition from cruise to hover and dynamic position modes. This was achieved in simulation by means of multiple sliding mode control combined with linear quadratic regulator techniques. Appropriate functional relationships of the weighting factors on different system states in terms of the vehicle forward speed enables smooth transitions between cruise and hove modes and efficient use of the various vehicle actuators.

Figure 7.

Sonar Signature from Pool Maneuvering Run

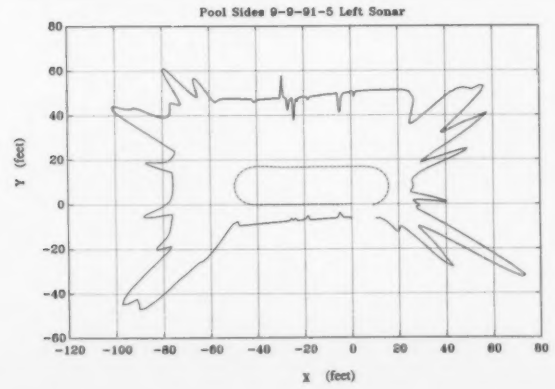

Figure 8.

Segment Identification Result from Post Processing

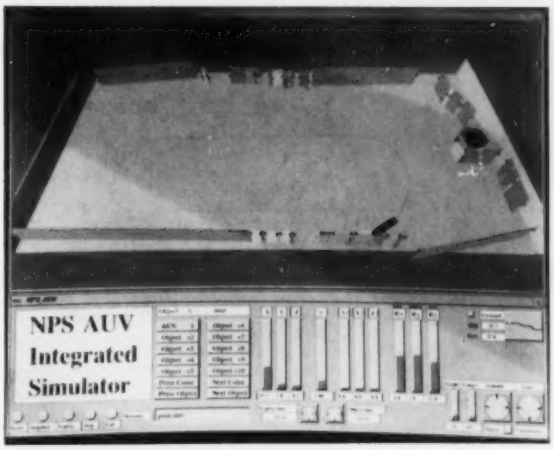

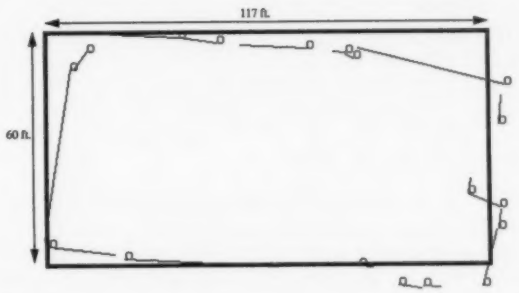

Figure 9.

System for Neural Network Failure Detection and Diagnostics Neural Diagnostic Decision Surface

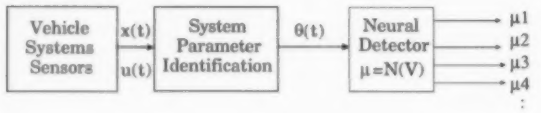

N : Feedforward Neural Networks

μ = Status of Each Failure Mode: Network Output [0 ,..., 1]

θ(t) = System Parameters

Naturally, vehicle guidance and control cannot be accomplished unless reasonably frequent updates are provided by the **Navigation System** which is responsible for estimating where the vehicle is located. This is accomplished by an enhanced dead-reckoning system that takes into consideration vehicle forward speed over the water, heading angle, and heading rate; and provides through the use of an observer an estimate of the side slip velocity. The system has been calibrated based on sonar information from the swimming pool walls as discussed later in the next section.

Obstacle Avoidance

While the **Obstacle Avoidance Decision Maker** is a system that has yet to be defined to its fullest extent at the time of this writing, the vehicle has four sonar ranging systems on board that have been providing mapping data to the pool sidewalls. One of the most important obstacle avoidance issues is to prevent the vehicle from running into a solid object in its path. The use of a forward looking sonar to provide range to such an object has been demonstrated in pool tests where a limit of 25 feet has been set after which a hard turn to the starboard is triggered. The quality of the range signals from the Datasonics PSA 900 200 KHz. is shown in Figure 6 where it has been clearly shown that an obstacle avoidance maneuver was triggered at the correct time to turn the vehicle away from the pool end wall. Working with sonar signals in the underwater environment for autonomous control is not easy and will be the subject of future research.

Underwater Object Recognition using Sonars

Object recognition for the AUV is an important task for its intelligent behavior. We used sonar range data interpretation for this task. Especially, regression analysis was adopted to extract linear features from sonar signature. This linear feature extraction enables the system to perform pattern matching with the environmental database to allow navigational position updating, or, unknown obstacles can be added to the environmental database if they are not previously registered.

The method we have investigated is able to represent line segments in the most general form. That is, even lines which are perpendicular to the X-axis are uniformly representable. Figure 7 shows an example of sonar signature taken by a mission in the NPS pool. Figure 8 is the result of a regression analysis. Another advantage of this method is that the end points of each segment are explicitly obtained. These segments are matched to the environmental model to identify the AUV's position and orientation which in turn corrects possible dead-reckoning errors, (Floyd, Kanayama, and Magrino, 1991).

The terrain-following altitude controlling algorithm using a down-looking sonar was also tested in the NPS pool. Using a filtered signal from the bottom sonar, the controller maintained the AUV at a height of 3.0 feet from the pool bottom.

This sonar interpretation technique has been proven to be extremely effective both for real-time underwater object recognition and for post mission data analysis. An expert system which combines geometric analysis with sonar classification heuristics is successfully able to classify walls and objects in the NPS pool (Brutzman, Compton and Kanayama, 1992).

Further work on sonar detection of objects in the pool and the problems of dealing with noisy sonar data is ongoing. It is planned to investigate the use of a 750 KHz. 1 by 30 degree sector scanning sonar together with a 1 degree conical beam profiling sonar to provide higher resolution images and enhance the development of obstacle avoidance controls.

Figure 10.

Motor 'Failure Decision Surface' as a Function of Rotation Speed and Current; μ_1 = 1 Indicates Shaft Friction Too High; μ_2 = 1 Indicates Normal Operation; μ_3 = 1 Indicates Loss of Loading

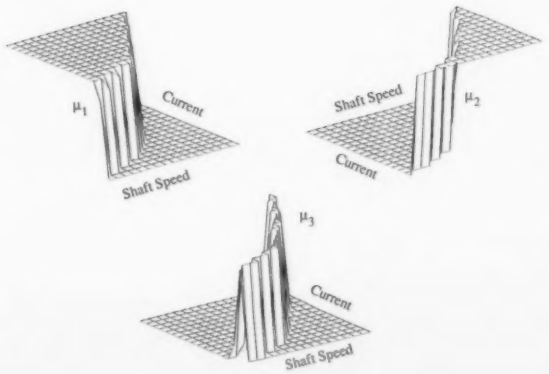

Vehicle Condition Monitoring

Vehicle component reliability is a major issue for any operational AUV system. This problem is being addressed at the time of this writing by NPS, the Naval Coastal Systems Station and the Draper Laboratory. It has to do with monitoring the health status of equipment so that intelligent decisions may be made in software to at least continue the mission in a partial way if failure occurs. Additional sensors dealing with the monitoring of motor currents and voltages, computer systems temperature and cooling needs, servo controller card status, battery voltages, and servo motor currents are now planned to provide input to computer based models of the internal components so the anomalous operating data can be sensed and either corrected or mission adjustments can be made by the mission executor software. The basis of the failure diagnostics system is a Kalman filter system parameter identifier coupled to a neural network diagnoser that is trained to determine the operating mode of the vehicle sub systems. (illustrated in Figure 9). The design of systems of this type is complicated by the need to recognize discrepancies in the inner correlations between system variables, and to link those changes to particular failure modes. Research is needed to define the performance possible from these systems. A neural network has been designed to identify whether a propulsion motor is operating in normal, under or overload conditions with the decision surface shown in Figure 10. More details are given in Healey, (1991).

AUV Integrated Simulation and Post Mission Visualization

The developments and testing of AUV hardware and software is greatly complicated by vehicle inaccessibility during operation. Integrated simulation remotely links vehicle components and support equipment with graphics simulation workstations, allowing complete real-time, pre-mission, pseudo-mission and particularly, post-mission visualization and analysis in the lab environment.

High resolution three-dimensional Silicon Graphics Inc. graphics workstations can provide real-time representations of vehicle dynamics, control system behavior, mission execution, sonar processing and object classification. Use of well-defined, user-readable mission log files as the data transfer mechanism allows consistent and repeatable simulation of all AUV operations.

The flexibility, connectivity and versatility provided by this approach enables sophisticated visualization and analysis of all aspects of AUV development (Brutzman, 1992, Compton, 1992, and Brutzman, Kanayama, and Zyda, 1992). Figure 11 shows an example visualization of an extended minefield search. The bright track is at shallow depth, the grey track is at intermediate depth and the dark track shows commencement of a deep-water minefield search.

Figure 11.

Minefield Search Pattern From The Integrated Simulator

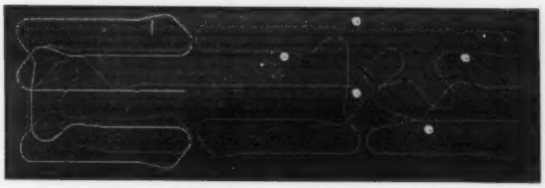

Conclusion

Much more work needs to be done in this community to continue, with appropriate overlap from sufficiently diverse points of view, to illuminate the range and trade-offs of possible structures and technology, hardware and software, needed for precise, reliable control of AUV's in the future. In particular, during the next few years, we plan to

1. Develop techniques for design of mission planning software using a simulator that has realistic run times and vehicle motion dynamics constraints,
2. Develop technology for understanding multiprocessor real time computation with transputers for mission control execution,
3. Understand the precision to which slow speed control can be accomplished in the presence of ocean currents,
4. Understand how to incorporate high resolution imaging sonar into vehicle guidance and control functions to enhance the ability of vehicles in gaining acoustic imagery of potential targets,
5. Understand how to integrate a GPS/INS suite into the vehicle's mission planner and navigation systems,
6. Further the understanding of the design of system diagnostic reasoners using neural networks to increase vehicle operational reliability.

Biographies

Dr. Healey was graduated from London and Sheffield Universities with the degrees B.Sc. (Eng.) and Ph.D. in mechanical Engineering in 1961 and 1966 respectively. He has taught at The Pennsylvania State University, MIT, The University of Texas at Austin, and in 1986, he assumed his present position as Professor and Chairman of Mechanical Engineering at the Naval Postgraduate School. His areas of specialty include Mechanical System Dynamics, Vibration, and Control Systems, and he is presently the leader of the multidisciplinary project in Autonomous Underwater Vehicles at NPS.

Dr. Robert B. McGhee received his Ph.D. in Electrical Engineering at the University of Southern California in 1963 and taught at Ohio State University until 1986 when he joined the Computer Science Department at the naval Postgraduate School. He currently serves as Chairman of that Department. His specialty areas are in Robotics, Walking Machines and Artificial Intelligence.

Dr. Yutaka Kanayama received his Ph.D. degree from University of Tokyo in 1965 and has taught at the University of Electro-Communications in Tokyo and the University of Tsukuba in the areas of Robotics and Computer Science. He was an Adjunct Professor at the University of California at Santa Barbara 1986-1988 and since 1988 has been a professor in the Computer Science Department at the Naval Postgraduate School holding the Grace Murray Hopper Chair 1989-1990. His specialties are in Mobile Robotics and Algorithm Theory.

Dr. Roberto Cristi received his Ph.D. degree in Electrical Engineering at the University of Massachusetts in 1988 and is currently associate Professor of Electrical and Computer Engineering at the Naval Postgraduate School. His specialty is in Adaptive Control, Signal, and Image Processing.

Dr. Fotis A. Papoulias received his Ph.D. degree from the University of Michigan in 1987 and is currently an Assistant Professor of Mechanical Engineering at the Naval Postgraduate School. His research interests are in Dynamics and Control of Mechanical Systems, Guidance and Autopilots for Marine Vehicles, Bifurcation and Chaos.

Dr. Shridar Shukla received his Ph.D. in Electrical and Computer Engineering from the North Carolina State University in 1990. He is currently an Assistant Professor in Electrical and Computer Engineering at the Naval Postgraduate School. His current research interests are in parallel real time computing and fault tolerant distributed computing.

Se-Hung Kwak received his Ph.D. degree in Electrical Engineering from Ohio State University in 1986. He worked as a Post Doctoral Fellow in Electrical Engineering at Ohio State University and since 1987 has been an adjunct Professor in the Computer Science Department at the Naval Postgraduate School. His research interests are in robotics, artificial intelligence, real-time systems, and computer architecture.

Yuh-jeng Lee received a Ph.D. (1988) in Computer Science (Artificial Intelligence) from the University of Illinois at Urbana-Champaign. He is currently an Assistant Professor of Computer Science at the Naval Postgraduate School. His research interests include automatic programming, intelligent systems, real-time systems, and model-based reasoning.

Amr Zaky received his Ph.D. in Computer Science in 1989 from The Ohio State University. Since September 1989, Dr. Zaky has been an Assistant Professor with the Department of Computer Science at the Naval Postgraduate School. Dr. Zaky's research interests are in the areas of Parallel Computing, Computer Architecture, and Real Time Systems.

Acknowledgement

The authors wish to acknowledge the financial support of the Naval Postgraduate School Direct Funded Research Program with the technical sponsorship of Mr. D. Steiger at Office of Naval Technology and partial support from Naval Coastal Systems Center and Naval Ocean Systems Center, Hi.

References

1. Albus, J. S., (1988) "System Description and Design Architecture for Multiple Autonomous Undersea Vehicles" *NIST Technical Note No. 1251*, U.S. Department of Commerce National Institute of Standards and Technology, Sept. 1988

2. Bellingham, J., Consi, T., Beaton, R., (1990a) "Keeping Layered Control Simple", *Proc. Symposium on Autonomous Underwater Vehicle Technology* June 5-6 1990 Washington DC. Published as IEEE Catalog No. 90CH2856-3, pp 3-9

3. Bellingham, J., Consi, T., (1990b) "State Configured Layered Control" *Mobile Robots for Subsea Environments*, Proceedings of the 1st NSF IARP Workshop, Monterey Bay Aquarium Research Institute, California, October 23-26, 1990, pp 75-80

4. Brooks, R., (1986) "A Robust Layered Control System for a Mobile Robot" *IEEE Journal of Robotics and Automation*, Vol. 2, 1986

5. Brutzman, D. P., Compton, M. A., Kanayama, Y., (1992) "Autonomous Sonar Classification Using Expert Systems" to be presented at OCEANS 92, Newport Rhode Island, October 26-29, 1992

6. Brutzman, D. P., Kanayama, Y. and Zyda, M. J., (1992) "Integrated Simulation for Rapid Development of Autonomous Underwater Vehicles," to be presented at IEEE Oceanic Engineering Society

7. Symposium on Autonomous Underwater Vehicles, AUV-92Washington D.C., June 2-3, 1992.

8. Brutzman, D. P., (1992) "NPS AUV Integrated Simulator", *Master's Thesis, Naval Postgraduate School*,Monterey, California, March 1992.

9. Chappell, S. G., (1987) "A Blackboard Based System for Context Sensitive Mission Planning in an Autonomous Vehicle" *Proceedings of the 5th International Symposium on Unmanned Untethered Submersible Technology*, University of New Hampshire, June 1987 Vol. 2 pp 467-476

10. Compton, Mark A., (1992) "Minefield Search and Object Recognition for Autonomous Underwater Vehicles", *Master's Thesis, Naval Postgraduate School*,Monterey, California, March 1992.

11. Floyd, C. A., Kanayama, Y., and Magrino, C., (1991) "Underwater Obstacle Recognition using a Low-Resolution Sonar," *Proceedings of the Seventh International Symposium on Unmanned Untethered Submersible Technology*, University of New Hampshire, Durham, New Hampshire, September 1991, pp 309-327.

12. Healey, A. J., Papoulias, F. A. Lienard, D., (1990) "Multivariable Sliding Mode Control for Autonomous Diving and Steering of Unmanned Underwater Vehicles" *Modeling and Control of Marine Craft*, Elsevier Publications, 1990

13. Healey, A. J., (1991) "Neural Network Based Approach to Failure Diagnostics for Underwater Vehicles" Report No. NPS-ME-91-006, under Contract No. N6133191WR10119, Naval Postgraduate School, Monterey, Calif. September 30, 1991

14. Healey, A. J., Good, M., (1992) "The NPS AUV II Autonomous Underwater Vehicle Testbed: Design and Experimental Verification" *Naval Engineers Journal*, ASNE, May 1992 issue

15. Healey, A. J., Marco, D. B., (1992) "Slow Speed Flight Control of Autonomous Underwater Vehicles: Experimental Results with NPS AUV II" Proceedings of the 2nd International Offshore and Polar Engineering Conference, San Francisco, June 14-19, 1992

16. Hutchison, B. L., Skov, B. E., Bradley, S. E., Rowe, F. D., (1990) "A System Approach to Navigating and Piloting Small UUV's" *Proc. Symposium on Autonomous Underwater Vehicle Technology*June 5-6, 1990 Washington DC. Published as IEEE Catalog No. 90CH2856-3, pp 129-136

17. Kanayama, Y., Hartman, B. I., (1989) "Smooth Local Path Planning for Autonomous Vehicles" *Proceedings of the 1989 IEEE International Conference on Robotics and Automation*, May 14-19, 1989

18. Kwak, S. H., Ong, S. M., McGhee, R. B., (1990) "A Mission Planning Expert System for an Autonomous Underwater Vehicle" *Proceedings of the Symposium on Autonomous Underwater Vehicle Technology*, IEEE Oceanic Engineering Society, June 4-6, 1990 Washington DC., pp 123-128

19. Mayer, R., et. al. (1987) "Situation based Control Architecture for an AUV" *Proceedings of the 5th International Symposium on Unmanned Untethered Submersible Technology*, University of New Hampshire, June 1987, Vol. 2 pp 430-443

20. Ong, S. M., (1990) "A Mission Planning Expert System with 3-D Path Optimization for the NPS Model 2 Autonomous Underwater Vehicle" *MS Thesis Naval Postgraduate School*June 1990

21. Papoulias, F. A., Healey, A. J. (1990) "Path Tracking of Surface Ships Using Multivariable Sliding Mode Control" *Proceedings of the 9th Ship Control Systems Symposium*,Washington DC Sept 10-14, 1990

22. Ura, T., (1990) "Development of AUV'PTEROA'" *Mobile Robots for Subsea Environments*, Proceedings of the 1st NSF IARP Workshop, Monterey Bay Aquarium Research Institute, California, October 23-26, 1990, pp 195-200

Research Notes

NPS-Developed Logistics Support System Evaluated

Commander Second Fleet has four questions to which the battle watch is to know the answers at all times. The questions are: where's the enemy, who's got him engaged, how are we doing, and what's our sustainability. The afloat tactical command and control system, JOTS, provides information on the first three questions but nothing on the fourth. Sustainability is logistics and the logisticians had only pencil and paper for tracking of things which happened one or two days before. To comment on sustainability, one must be able to predict where the force will be logistically several days or a week into the future.

A project directed by Professor David Schrady was begun at the Naval Postgraduate School in 1989 to model the usage and replenishment of fuels and ordnance in a battle group. The models, algorithms, and voluminous data were incorporated in a microcomputer-based program to plan, track, and predict individual ship and battle group logistics states. The resulting system, Battle Group Logistics Coordinator Support System (BGLCSS) was evaluated in Second Fleet exercise 3-90 in June 1990 and subsequently used by the Fleet Logistics Coordinator in Second Fleet exercises 1-91/2-91, 4-91, 1-92, and 2-92. Commander Second Fleet, VADM Kalleres said of his Fleet Logistics Coordinator after the 1-91/2-91 exercises; "You have set a standard in logistic support planning and execution that has enhanced not only fleet exercises but also battle group planning." The Fleet Logistics Coordinator said; "BGLCSS enabled us to schedule logistics evolutions in a timely and effective manner and was a break-through in allowing VADM Kalleres to aggressively pursue tactical logistics."

Interest in logistics has been rising and the Gulf War has created even more interest. BGLCSS in its present form is stand-alone and labor intensive. Commander Third Fleet in August 1991 requested OP-094 to incorporate BGLCSS in JOTS II, then being introduced in the fleet. The OP-094 Fleet Requirements Working Group meeting in October acted favorably on this request and the restructuring of BGLCSS to operate in the JOTS environment is ongoing at the Postgraduate School with DTC-2 hardware and JOTS II software provided by PMW 162.

Professor Schrady discusses battle group rearming with Commander Atlantic Fleet, ADM Paul David Miller, in the afloat flag command center in USS Mount Whitney (LCC-20) during Second Fleet exercise 4-91 in August 1991.

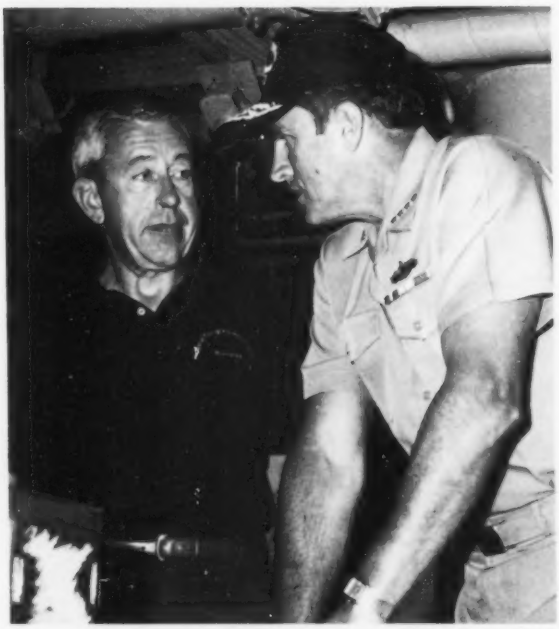

Experiment To Investigate Polar Front In Barents Sea

Coastal ocean acoustics will play a more important role in future Navy anti-submarine warfare (ASW) operations. The following is an excerpt from the Navy's 1992 Posture Statement: "To meet future needs, Naval forces will focus on the challenges of littoral (coastal) and shallow-water operations where anti-submarine warfare, counter-mine warfare, and near-land/over-land anti-air warfare pose special technical problems." For instance, the complex oceanography and bathymetry of a coastal region can seriously affect the performance of Navy sonar systems. At the Naval Postgraduate School (NPS), Professors Ching-Sang Chiu, James H. Miller, and Robert Bourke have been working on coastal and shallow water acoustic problems important for ASW.

In the summer of 1992, NPS and Woods Hole Oceanographic Institution (WHOI) will conduct an acoustic and oceanographic investigation of the Barents Sea Polar Front using acoustic tomography and traditional hydrographic techniques. This work is being funded in part by ONR's Arctic Sciences program (1125AR) and also by the Naval Postgraduate School Direct Funded Research Program.

NPS participation will include the deployment of a shallow water vertical hydrophone array. This array will be used to monitor the WHOI 224 and 400 Hz tomography transmissions at ranges of 50-75 km on cross-frontal and along-front tracks.

Our objectives for this experiment are:

(1) to study the geoacoustic parameters and oceanographic processes that control the acoustic wavefields and their space-time coherence in the Barents Sea, and

(2) to investigate the dynamics of the ocean circulation in the Barents Sea, particularly in the vicinity of the Polar Front.

To meet the first objective, we have been modeling acoustic pulse propagation in the Barents Sea using time-domain ray tracing and parabolic equation codes. The acoustic signature of the frontal oscillations has been simulated using historical environmental data. These simulations will be compared to the collected data.

An assessment will be made on whether the use of vertical hydrophone arrays in a shallow-water tomographic monitoring system can significantly improve the quality of estimates of the ocean structure. Both ray and mode sound propagation models will be used for identification of the observed arrivals, and both ray and mode travel time data will be used in the inverse analyses. Three types of data inversions will be performed: purely acoustic, integrated, and dynamically constrained.

The validation of tomography requires comparison of the purely acoustic inverse results to the hydrographic, temperature sensor and current meter data. Once confidence in tomography is built, all data types will be integrated to produce time series of temperature and current maps having resolution and accuracy not attainable by tomography or conventional measurements alone. (High temporal resolution salinity maps are possible if there is a tight T-S relation.) These "optimal" maps will be useful for the study of frontal dynamics. Assimilation of the data into a nonlinear Quasigeostrophic (QG) ocean model using an Extended Kalman Filter (developed recently by Chiu) will also be performed. Imposing QG constraints in the data inversions will allow for an examination of the degree to which frontal dynamics are ageostrophic.

Figure 1.

Ultraviolet spectrum obtained from the NPS MUSTANG ultraviolet instrument at an altitude of 155 km on March 30, 1990, at 1000 hrs. The intensity is in units of Rayleighs per Angstrom (R/A) where one Rayleigh is equal to 10^6 photons cm^{-2} sec^{-1}.

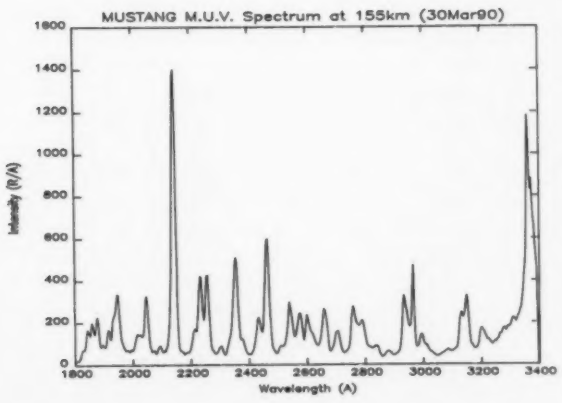

NPS-NRL Experiment Probes Ionosphere Electron Density

Professors D. Cleary and S. Gnanalingam of The Ionospheric Physics group at the Naval Postgraduate School (NPS) are currently involved in developing a technique for global remote sensing of the Earth's ionosphere. This work is motivated by a DoD requirement for global ionospheric electron densities as stated in a 1986 memorandum from the Joint Chiefs of Staff. Knowledge of these densities is essential for a number of defense systems such as over-the-horizon (OTH) radar and emergency communication networks.

It is believed that the distribution of electron densities can be inferred from passive measurements of the ultraviolet radiation emitted by the ionosphere. In order to test this, the Naval Postgraduate School (NPS), in collaboration with the Naval Research Lab (NRL), conducted a NASA suborbital rocket experiment on March 30, 1990. The rocket was launched from the White Sands Missile Range, NM., and reached an apogee altitude of 320 km. The payload consisted of two ultraviolet (UV) spectrographs. The NRL instrument was the High Resolution Airglow and Aurora Spectrograph (HIRAAS) and it observed the wavelength range 500 Å to 1500 Å. The NPS instrument was the Middle Ultraviolet Spectrograph (MUSTANG) which covered the wavelength range 1800 Å to 3400 Å.

The primary objective of the HIRAAS/MUSTANG experiment was to investigate the ion photochemistry which leads to the formation of the Earth's ionosphere. The ultraviolet spectra obtained from the HIRAAS and MUSTANG instruments provides the altitude distributions of molecular

nitrogen, molecular oxygen, nitric oxide, and neutral and singly-ionized atomic oxygen. These species play an important role in the formation of the ionospheric E- and F- regions. It is believed that numerical models of the ionosphere using the above densities as inputs will accurately predict electron density profiles.

The group is currently analyzing the UV spectra obtained from this rocket experiment. Figure 1 shows a sample spectrum obtained from the MUSTANG instrument at an altitude of 155 km. At this altitude the payload was viewing the atmosphere horizontally in an azimuth direction of 40°. This spectrum shows an abundance of molecular and atomic emission features from N_2, NO, O, and O^+. By measuring the intensity of each of these emissions one can infer not only the density of the individual species but also information about the dynamics of the atmosphere such as temperature and energetic electron flux. While analysis of these data continued the scientists planned two more NASA sounding rocket experiments. In late March, 1992, they again launched from the White Sands Missile Range, NM. In August, 1993, they plan to launch from Poker Flat Missile Range in Alaska. The latitude of the Poker Flat range will enable them to investigate the effects of auroral electron precipitation on ionospheric photochemistry. After completing these suborbital rocket experiments, the HIRAAS/MUSTANG instrument package will be flown on the Advanced Research and Global Observation Satellite (ARGOS) in late 1995.

Parallel Computing May Improve Space Surveillance

The U.S. Naval Space Surveillance Center (NAVSPASUR) as well as the Air Force Space Command (AFSPACECOM) each keep track of over 6,000 orbiting objects of various sizes. The theories used to predict the orbits are based on approximate analytical solutions to Newton's equations of motion obtained in the late 1950's and 1960's. The Navy code, PPT2, has been the mainstay of orbit prediction for the fleet. The Air Force code, SGP4, is at the heart of the nation's space defense system. Moderately accurate predictions, on the order of several kilometers (depending on time from epoch), are being achieved with these codes on serial computers.

NAVSPASUR is now responsible as alternate Space Defense Operations Center and must be able to exchange information with AFSPACECOM. Thus an effort is presently being undertaken to standardize the astrodynamic codes and constants. Furthermore, within the next few years the military expects to increase the number of objects cataloged and to require more accurate predictions. One of the reasons for this is to ensure the safety of future astronauts. The accuracy of the predictions could be improved by the use of semi-analytical theories or by completely numerical solutions to Newton's equations. With a commensurate improvement in sensor data, the accuracy of the predictions could be improved to the order of tens of meters with a semi-analytical theory or to meters with a completely numerical solution. However, these improvements would be obtained at the expense of a great increase in computation time on a serial computer.

The most cost effective way to get more accurate predictions for more orbiting objects in a short amount of time would seem to require the use of parallel computers. There are essentially two possible ways in which parallel computers can be used to advantage. If one is to use a massively parallel computer, such as a Connection Machine having 64,000 processors, one can assign a single object to each processor. Such an idea is now under investigation at the NRL. One difficulty here is to assign the data collected to the processors.

Professors B. Neta and D. Danielson at the Naval Postgraduate School are looking at the other possibility. They are developing parallel algorithms which can use many processors to calculate a single orbit. They have already developed a parallel algorithm to numerically solve Newton's law to a very high accuracy and implemented it on an INTEL iPSC/2 hypercube using tens of processor. Their students are currently working on the parallelization of the analytic codes PPT2 and SGP4. They are also planning to develop a parallel version of the semi-analytic code DSST developed at Draper Lab. The challenge is to develop a parallel algorithm which uses the most processors in the most efficient manner.

Recursive Ray Acoustics For Three-Dimensional Sound-Speed Profiles

Prof. Lawrence J. Ziomek of the Department of Electrical and Computer Engineering at the Naval Postgraduate School has recently begun research work on the development of a recursive ray acoustics (RRA) algorithm for *three-dimensional* sound-speed profiles. The RRA algorithm is theoretically simple and because it is recursive, it is fast. And based on *preliminary* test results from computer simulation studies, it is also very accurate. The RRA algorithm uses arc length as the independent variable and at present, it can be used to compute the position, angles of propagation, travel time, and path length along a ray path and to draw ray trace plots for speeds of sound that are functions of all three spatial variables.

Because of the simplicity, speed, and apparent accuracy of the RRA algorithm, the Naval Sea Systems Command (NAVSEA) is supporting Prof. Ziomek to further investigate and enhance the basic RRA algorithm. Prof. Ziomek has already started work on enhancing the RRA algorithm by giving it the capability to process measured, environmental

data, such as sound speed versus depth and bathymetric data. Various curve fitting techniques are being investigated that produce not only accurate curve fits of *noise corrupted data*, but accurate first and second-order derivatives as well. The RRA algorithm depends, in part, on having available accurate values for the gradient of the three-dimensional sound-speed profile. In addition, work has also started on further enhancing the RRA algorithm by giving it the capability to perform sound-pressure level (SPL) calculations that are fast, accurate, and valid (i.e., finite) at both turning points and focal points when the speed of sound is an arbitrary function of depth. The SPL calculations depend, in part, on having available accurate first and second-order derivatives of the depth-dependent sound-speed profile.

In agreement with NAVSEA, Prof. Ziomek will be involved in a technology transfer arrangement with the Applied Research Laboratory (ARL) of The Pennsylvania State University (PSU), which is one of four not-for-profit, university based, research centers of the Department of the Navy. Engineers and scientists at ARL – PSU will independently evaluate the RRA algorithm in order to determine if it is capable of real time operation in Naval weapon systems.

Oceanographic Research Probes Nearshore Dynamics

Prof. Ed Thornton, NPS Oceanography Department, has participated in all the comprehensive nearshore experiments conducted in the U.S. over the last two decades, with the objective to predict the wave-induced three-dimensional velocity field over arbitrary bathymetry. The most recent field experiment was the comprehensive nearshore dynamics experiment DELILAH during October 1990 conducted at the U.S. Army Field Research Facility, Duck, North Carolina. Coupled with the simultaneous experiment SAMSON, 26 electromagnetic current meters and 50 pressure sensors were deployed to measure the directional wave spectra in 13 and 8-m depths and the wave and velocity field in the nearshore. Variable wave conditions were due to hurricanes Josephine, Klaus and Lilly and a "northeaster". Longshore currents were measured up to 2m/s.

Together with students, post-docs and collaborating scientists, Prof. Thornton has developed a number of models to describe the wave and current data acquired. Random wave models describing transformations from offshore to the beach have been developed, which are then used as input to describe longshore current generation across the surf zone. Concerning recent works, it has been demonstrated by model comparison with data that the strong low frequency motions (O(1m/s)) observed at Duck, NC were due to shear instabilities on the longshore current. A shear instability model was extended to include the effects of dissipation in the form of bottom friction. Observed frequency-cyclic wavenumber (f-k) spectra were examined and compared with theoretical predictions. Good qualitative agreement was found between observation and theory at this barred beach, where these motions dominate the observed f-k spectra and where theoretical growth rates of the temporal instability tend to be large. This comparison supports the shear instability hypothesis. Results from an almost planar beach were less conclusive. It was shown that the "typical" longshore current profiles over a plane and barred beach give rise to significantly different stability properties. This suggests that shear instabilities may be a more common feature on barred beaches.

A shallow water, nonlinear spectral wave transformation model was developed for conditions of a mild sloping bottom and small amplitude effects. The evolution equation of the wave action was prescribed by the wave Boltzmann equation, whereby resonant collinear triad interactions transfer energy among Fourier components. Combined shoaling and refraction effects are taken into account through the geometrical optics approximation. A numerical solution of the three wave collision integral was developed, and the steady state wave Boltzmann equation integrated using a piecewise ray method. The model was compared with high-resolution frequency- directional wave measurements, which show nonlinear transfers of energy between both harmonic and non-harmonic frequencies. Good comparisons were obtained with the measured frequency-directional spectra evolving from 10 meter to 4 meter depth.

There is continual effort to transition these research efforts to applications. The wave transformation and longshore current models developed under this research are the basis for the TESS-2 surf model used by the U.S. Navy. Prof. Thornton has been funded by the Office of Naval Research since 1972.

Researchers Simulate The Global Ocean

Oceanographers at the Naval Postgraduate School (NPS) have constructed an eddy-resolving model of the world ocean. It includes the important instabilities of ocean currents and can be used to investigate global climatic change. The model was developed jointly by Professor Albert Semtner of NPS and Dr. Robert Chervin of the National Center for Atmospheric Research (NCAR).

The global ocean model has already been used to simulate the three dimensional ocean circulation of the present day. When coupled to an atmospheric model, it will be able to simulate climates of the future, such as those related to the buildup of greenhouse gases in the atmosphere.

Modeling the ocean with a high degree of accuracy requires one thousand times as much computer power as in a comparable atmospheric situation. With this in mind, the ocean model was constructed to use all the processors of

parallel vector supercomputers. So far the model has been run on CRAY X-MP and Y-MP computers at NCAR.

The ocean simulations to date have provided a baseline estimate of global ocean statistics that can be compared with satellite observations. Mr. Michael McCann and Dr. Tom Murphree of NPS are comparing model output with surface temperature data from NOAA satellites and with surface height data from the Navy Geosat mission.

The ocean simulations have also revealed how the ocean thermohaline circulation provides a 'conveyor belt' for transport of heat and fresh water from the Tropical Pacific to the North Atlantic. Many features of the simulated flow patterns agree well with new subsurface measurements along the preferred path of this transport.

Ocean acousticians such as Profs. Ching-Sang Chiu and James Miller of NPS are using output from the global ocean model to help understand long-range acoustic propagation. They are examining acoustic propagation from Heard Island to Ascension Island, prior to developing strategies for monitoring global ocean temperature trends using acoustic arrays.

The model is now being adapted to run effectively on massively parallel computers, which are expected to attain speeds of up to a trillion operations per second. The adaptation is part of the CHAMMP program on climate modeling, which is sponsored by the US Department of Energy.

Network Interdiction Research Aids Anti-Drug Effort

U.S. Anti-drug efforts have provided new impetus for studying interdiction models. The U.S. Army's SOUTHCOM, which directs U.S. anti-drug efforts in South America, would like to best allocate its limited resources to interdicting cocoa, partially processed cocaine and precursor chemicals in producing areas. Most of the traffic in these commodities is carried along a network of rivers and roads and, consequently, the interdiction problem can be viewed as a network interdiction problem.

Precious research on network interdiction had not treated even the simplest problems adequately. Therefore, Prof. Kevin Wood of the NPS Operations Research Department defined and investigated a simple abstract model:

> An enemy wishes to move as much of a simple commodity from a source node s to a sink node t in a directed network. Each link between nodes i and j has a capacity of τ_{ij} units of commodity and requires of the interdictor an expenditure of τ_{ij} units of resource to break the link. Partially breaking a link is not allowed. The interdictor is to minimize the maximum amount of flow the enemy can push through the network along unbroken links where the enemy is constrained by the link capacities and the interdictor is constrained to use no more than R units of resource.

We think of τ_{ij} as the number of interdiction teams needed to search all traffic along link (i, j) while the capacity τ_{ij} is the amount of drugs or chemicals which could be moved across the link without arousing suspicion.

The basic problem statement is limited but, unlike earlier work, our mathematical programming approach makes generalizations easy. To describe a formulation for the problem, consider the well-known Max-Flow Min-Cut Theorem: The maximum flow from s to t in a capacitated directed network is equal to the capacity of a minimum capacity s-t cut. An s-t cut simply slices the network in two with s on one side and t on the other. The capacity of the cut is the sum of link capacities on the links directed across the cut from the s side to the t side. We hypothesized that the solution to the network interdiction problem was to create a model which identifies a cut, breaks some links in the cut using the available resource and which leaves behind unbroken links in the cut whose total capacity is minimum. This model was developed and then proved to be correct by transformations from a formal min-max statement of the problem.

Computational experiments have shown that reasonable large network interdiction problems can be solved effectively by standard mathematical programming algorithms. The basic formulation has been generalized to handle multiple sources and sinks, multiple resources (e.g., land-based interdiction teams and water-based teams), multiple commodities (e.g., precursor chemicals and coca leaves), and others. However, we have also proved that even a simpler version of the network interdiction problem is "NP-compete", i.e., it belongs to the same theoretically difficult-to-solve class of problems containing the well-known traveling salesman problem.

Future research on this topic will consider using the basic static model in a dynamic framework or look at game-theoretic models in which both the enemy and the Interdictor act probalistically.

A research vessel is an essential laboratory for any naval university. The R/V Pt. Sur, built in 1981, provides an excellent platform for NPS instruction and faculty and student research projects.

Owned by the National Science Foundation, The Pt. Sur is used by NPS under a consortium agreement with other universities and government agencies. Ship time supports coursework in descriptive physical oceanography and operational oceanography. Research projects include: FLIR (forward looking infrared imaging systems) development; acoustic tomography measurements, including successful detection of Heard Island signals in January 1991; measurements of the atmospheric and oceanic planetary boundary layers; and, measurements of ocean circulation and mixing.

The Pt. Sur is 135 feet long with a beam of 32 feet and draft of 9 feet. When fully loaded, the ship displaces 539 tons. The Pt. Sur is equipped with three winches, two frames and two cranes. Two winches have conducting cable for use with CTDs and other electronic packages. There are three laboratory areas on board: wet lab, dry lab and electronics lab. The Pt. Sur has a crew of nine and accommodations for 12 scientists.

The Oceanographer of the Navy has supported shiptime for NPS instruction and research since the inception of the Postgraduate School's oceanography department in 1968. For projects distant from central California, the Oceanographer also provides support for shiptime aboard the USNS DeSteiguer and USNS Bartlett.

DEPARTMENT OF THE NAVY
OFFICE OF NAVAL RESEARCH
ARLINGTON, VA 22217

OFFICIAL BUSINESS
PENALTY FOR PRIVATE USE, $300